National Library of Canada
Bibliothèque nationale du Canada

Canadian Theses Service
Service des thèses canadiennes

Ottawa, Canada
K1A 0N4

## NOTICE

The quality of this microform is heavily dependent upon the quality of the original thesis submitted for microfilming. Every effort has been made to ensure the highest quality of reproduction possible.

If pages are missing, contact the university which granted the degree.

Some pages may have indistinct print especially if the original pages were typed with a poor typewriter ribbon or if the university sent us an inferior photocopy.

Reproduction in full or in part of this microform is governed by the Canadian Copyright Act, R.S.C. 1970, c. C-30, and subsequent amendments.

## AVIS

La qualité de cette microforme dépend grandement de la qualité de la thèse soumise au microfilmage. Nous avons tout fait pour assurer une qualité supérieure de reproduction.

S'il manque des pages, veuillez communiquer avec l'université qui a conféré le grade.

La qualité d'impression de certaines pages peut laisser à désirer, surtout si les pages originales ont été dactylographiées à l'aide d'un ruban usé ou si l'université nous a fait parvenir une photocopie de qualité inférieure.

La reproduction, même partielle, de cette microforme est soumise à la Loi canadienne sur le droit d'auteur, SRC 1970, c. C-30, et ses amendements subséquents.

NL-339 (r. 88/04) c

Canada

THE UNIVERSITY OF ALBERTA

# BLACK HOLES: THE INSIDE STORY

BY

© ERIC POISSON

A THESIS

SUBMITTED TO THE FACULTY OF GRADUATE STUDIES AND RESEARCH IN PARTIAL FULFILMENT OF THE REQUIREMENTS FOR THE DEGREE OF

Master of Science

IN

Theoretical Physics

Department of Physics

Edmonton, Alberta

Spring 1989

National Library of Canada
Canadian Theses Service
Ottawa, Canada
K1A 0N4

Bibliothèque nationale du Canada
Service des thèses canadiennes

The author has granted an irrevocable non-exclusive licence allowing the National Library of Canada to reproduce, loan, distribute or sell copies of his/her thesis by any means and in any form or format, making this thesis available to interested persons.

The author retains ownership of the copyright in his/her thesis. Neither the thesis nor substantial extracts from it may be printed or otherwise reproduced without his/her permission.

L'auteur a accordé une licence irrévocable et non exclusive permettant à la Bibliothèque nationale du Canada de reproduire, prêter, distribuer ou vendre des copies de sa thèse de quelque manière et sous quelque forme que ce soit pour mettre des exemplaires de cette thèse à la disposition des personnes intéressées.

L'auteur conserve la propriété du droit d'auteur qui protège sa thèse. Ni la thèse ni des extraits substantiels de celle-ci ne doivent être imprimés ou autrement reproduits sans son autorisation.

ISBN 0-315-53024-3

Canada

THE UNIVERSITY OF ALBERTA

RELEASE FORM

NAME OF AUTHOR Eric Poisson

TITLE OF THESIS Black holes: the inside story

DEGREE Master of Science

YEAR THIS DEGREE GRANTED 1989

Permission is hereby granted to THE UNIVERSITY OF ALBERTA LIBRARY to reproduce single copies of this thesis and to lend or sell such copies for private, scholarly or scientific research purposes only.

The author reserves other publication rights, and neither the thesis nor extensive extracts from it may be printed or otherwise reproduced without the author's written permission.

Eric Poisson
Department of Physics
University of Alberta
Edmonton, Alberta
T6G 2J1

Date: March 21, 1989

THE UNIVERSITY OF ALBERTA

FACULTY OF GRADUATE STUDIES AND RESEARCH

The undersigned certify that they have read, and recommended to the Faculty of Graduate Studies and Research for acceptance, a thesis entitled "Black holes: the inside story" submitted by Eric Poisson in partial fulfilment of the requirements for the degree of Master's of Science in Theoretical Physics.

Werner Israel

Prof. W. Israel, Supervisor

Prof. D.P. Hube

B A Campbell

Dr. B.A. Campbell

Martin Légaré

Dr. M. Légaré

Date: March 21, 1989

# ABSTRACT

We study in this thesis some aspects of the physics of black hole interiors. In particular, we consider the effects on the interior geometry of non rotating black holes of gravitational collapses presenting small departures from spherical symmetry. For the Schwarzschild black hole, it is shown that aspherical perturbations do not reach the asymptotic portion (for late advanced times) of the singularity. Spherical symmetry hence holds down to very small radii. For the Reissner-Nordstrøm case, these perturbations have more dramatic effects: they produce a separation between the inner and Cauchy horizons. We also verify that, as in the static situation, there exists a singular surface of infinite blueshift on the dynamic Cauchy horizon.

Quantum effects near the black hole singularity are also investigated. A schematic analysis shows that the infinite rise of the curvature can be slowed down if the stress induced by the quantum vacuum polarization is a tension along the axes of the 3-cylinders of constant time $r$ = constant. If the stress is instead a pressure, the singularity occurs sooner than in the classical picture.

# ACKNOWLEDGEMENTS

I cannot even try to express my great indebtedness towards my supervisor Werner Israel. His immense patience, his constant attention and help have made the completion of this thesis possible. His perfectionism and his enthusiasm serve as a model for me. To work with him was the best thing that could happen to me.

I wish to warmly thank my supervisory committee: Douglas P. Hube, Bruce A. Campbell, Martin Légaré and Werner Israel for carefully reading this very long text and helping me to correct the numerous spelling mistakes and bad constructions.

I learned a lot from numerous conversations with numerous people. I want to thank Des McManus, Geoff Hayward, Esteban Calzetta, Claude Barrabès and Diego Pavón for sharing their thoughts with me and making this last year and a half so interesting.

The staff of the Physics Department has been very supportive; I would like to thank everyone concerned, especially John A. Kernahan for being such a caring Associate Chairman.

There are now two gentlemen whom I cannot leave aside. I wish to deeply thank Serge Pineault for being the good friend he is. Among a very long list of things he gladly did for me, Serge introduced me to my present supervisor; I am very thankful he did so. My interest in general relativity grew without bounds after

hearing a talk by Raymond Laflamme. He soon after became a friend and I want to thank him for being such a nice chap.

Finally, there are a few people that helped me to take the big step of leaving home and coming to Edmonton. It was well worth it and I wish to thank Jean-René Roy, Pierre Mathieu and Claude-André Laberge for their good advice.

# TABLE OF CONTENTS


Chapter Page

1- THE INTERIOR OF A SCHWARZSCHILD BLACK HOLE ..... 1

**1.1: Introduction** ..... 1

**1.2: The Schwarzschild geometry** ..... 14
a) The general metric for a static, spherically symmetric geometry. ... 14
b) The Schwarzschild solution. ..... 17

**1.3: The González-Díaz model** ..... 23

**1.4: The semiclassical model** ..... 30
a) Quantum effects in curved spacetime. ..... 30
b) Spherical symmetry holds near the singularity. ..... 34
c) Solving the semiclassical equation. ..... 37

2- THE POWER-LAW METRIC ..... 44

**2.1: Introducing the power-law metric** ..... 44

**2.2: Solving the semiclassical equation** ..... 50
a) Isotropic case (conformally invariant fields). ..... 50
b) General case (conformally invariant scalar fields). ..... 57

**2.3: Stability of the power-law geometries** ..... 68
a) The differential equation. ..... 70
b) The solutions of the differential equation. ..... 73
c) The stress-energy of the test field. ..... 79
d) The stability test. ..... 80

**2.4: Accessibility of the origin** ..... 85

3- THE INTERIOR OF A REISSNER-NORDSTRØM BLACK HOLE ..... 90

**3.1: The Reissner-Nordstrøm solution** ..... 90

**3.2: The static model** ..... 98

**3.3: The dynamic model** ..... 106
a) The dynamic spacetime. ..... 108
b) Infalling radiation crossing the inner horizon. ..... 115
c) Infalling radiation at the Cauchy horizon. ..... 119

**3.4: Conclusion** ..... 126

BIBLIOGRAPHY ..... 132

APPENDIX: FIGURES AND TABLES ..... 137

# LIST OF TABLES


| Table | Page |
|---|---|
| 2.1: Solving the semiclassical equation, case $n = 2$ | 141 |
| 2.2: Solving the semiclassical equation, general case | 142 |
| 2.3: Scalar field in the power-law spacetimes | 144 |
| 2.4: The stability test | 145 |

# LIST OF FIGURES


Figure — Page

1.1: The Schwarzschild spacetime ..... 138

1.2: The join of the González-Díaz model ..... 139

1.3: The gravitational collapse of a spherical star ..... 140

2.1: The graph of $\Gamma(n)$ ..... 143

2.2: The plane $(m, n)$ ..... 146

3.1: The Reissner-Nordstrøm spacetime ..... 147

3.2: Infalling radiation near the inner event horizon ..... 148

3.3: The dynamic model ..... 149

3.4: The "sliced" dynamic model ..... 150

# CHAPTER ONE

# THE INTERIOR OF A SCHWARZSCHILD BLACK HOLE

## 1.1: Introduction

Although the idea of a star having an escape velocity larger than that of light is more than two hundred years old, it was not until the discovery of galactic X-ray sources and of quasars in the early sixties that the idea of complete gravitational collapse, and of black holes, became generally accepted by the physics community [1]. J. Michell in 1783, and later P.S. Laplace in 1796, proposed that if light were composed of particles and, as any other body in the universe, submitted to the force of gravity, then it could be possible that a star be so large that even light could not escape from its surface. This remarkable idea, however, did not survive the discovery, early in the nineteenth century, of the wave theory of light. The idea quickly resurfaced after the results of the eclipse expedition of 1919 became known, but because of the absence of any motivation from astrophysics to introduce such a peculiar object amongst the celestial bodies, it had to wait a while longer before being seriously considered.

In 1930, S. Chandrasekhar, and independently L. Landau, discovered that the electron degeneracy pressure was not sufficient to support a white dwarf from its own gravitational collapse, should the mass of the star be larger than a certain limit.

The existence of such a limit was not understood at that time. A few years later, in 1939, J.R. Oppenheimer and his students realized that a neutron star also could undergo a gravitational collapse, if it was too massive. This result remained almost unnoticed, until the discovery in the early sixties of very powerful energy sources in the universe. It then became clear that accretion of matter onto very compact objects would explain in a very satisfying way the kind of energy that was observed from these sources. The presence of neutron stars hence became established, and since the complete gravitational collapse of a massive enough star could not be prevented by any known mechanism, the idea of a black hole as a real astronomical object finally appeared.

What followed probably were the most fruitful years of gravitation theory since the invention of the general theory of relativity, completed in 1915. In less than fifteen years, the complete nature of black holes was revealed; from the entire description of the geometry outside black holes, to S. Hawking's famous result of 1974 stating that a hole would act as a black body with temperature inversely proportional to its mass. One of the most beautiful results discovered in those years is the realization that black holes are by far the simplest objects in the universe. The works of Israel, Carter, Hawking and Robinson between the years 1967 and 1975 [2] brought the proof that the geometry (i.e. the gravitational field) around the most general black hole (in isolation) is completely determined by three parameters: the mass of the hole, its charge and its angular momentum. This remarkable result, usually referred to with Wheeler's characteristic phrase "a black hole has no hair"[3], is, at first sight, very surprising. Indeed, the gravitational field of a typical star contains virtually an infinite amount of information, since each term in the

multipole expansion of the field can play a rôle. What is the mechanism by which a collapsing star loses all this information, to settle down to a state where only three parameters survive? The complete answer to this question is still unknown, because the general description of a gravitational collapse involving arbitrarily large angular momentum is beyond reach. However, it is possible to study a simpler collapse, where the departure from spherical symmetry is small. Such a perturbative treatment was carried out by R. Price in 1972 [4]. His results show that all the superfluous information is radiated away; part of it (the short wavelength modes) reaching infinity, part of it (the long wavelength modes) being backscattered by the spacetime curvature, which acts as a potential barrier, towards the interior of the hole. This scattering is, moreover, found to happen soon after the initial radiation is emitted from the star: the amplitude of the backscattered waves dies out like $t^{-q}$ for late times ($t \gg 2M$). The parameter $q$ depends on the multipole order of the perturbating field (section 1.4b)). Only three parameters survive when the geometry has settled down: the mass, charge and angular momentum.

What is also remarkable is the fact that the expression for the metric of this most general black hole is explicitly known. It is called the Kerr-Newman solution [5]. In what follows, we will consider two limiting cases of this solution. The simplest black hole is described by the Schwarzschild line element (section 1.2b)); the only non vanishing parameter is here the mass of the hole. Accordingly, the Schwarzschild solution is the unique static, spherically symmetric, vacuum solution to the Einstein field equations describing the exterior geometry of a black hole. The other case that we will consider is the static, spherically symmetric, electrovac (vacuum plus electric field) solution, known as the Reissner-Nordstrøm solution

(section 3.2). It represents the exterior geometry of a non rotating, charged black hole. These two solutions are two special cases of the Kerr-Newman solution: the latter reduces to the Reissner-Nordstrøm solution when the angular momentum of the hole is taken to be zero; the Reissner-Nordstrøm solution then reduces to the Schwarzschild solution when the charge of the hole is put equal to zero. These two solutions are also simpler than the Kerr-Newman solution, since they both possess spherical symmetry.

The physics outside black holes is therefore well known. In fact, detailed calculations of the interaction of holes with their surroundings can be very complicated [6], but it is believed that the basic physics is well understood. The comprehension of the physics *inside* black holes, however, is much more limited. Since the physics of a general gravitational collapse is very difficult to analyse, it is difficult to predict what the interior of a Kerr-Newman black hole should look like, so we are left with the easier problem of determining the interior geometry of a spherical black hole, produced by a spherical gravitational collapse. The situation is here, by contrast, incredibly simple. Birkoff's theorem [7] states that if the geometry of spacetime is spherically symmetric and a vacuum (electrovac) solution to the Einstein field equations, then that geometry is necessarily a piece of the Schwarzschild (Reissner-Nordstrøm) geometry. Therefore, as long as the collapse is spherically symmetric, the geometry outside the star, *even inside the hole*, is everywhere given by the Schwarzschild, or Reissner-Nordstrøm solutions. We are then led to the surprisingly simple picture for a purely spherical black hole: both the interior and the exterior regions of the hole (as long as we are outside the collapsing star) possess the same geometry, described by the appropriate solution of the field equations.

A purely spherical collapse, however, is not a very realistic model. To obtain a more satisfying picture, we should allow the collapse to present at least small departures from sphericity. This model is relatively easy to analyse, and we can hope that it will succeed in showing the qualitative behavior of a general non-spherical collapse. What effect can this have on the interior geometry of a non rotating black hole? We have mentioned earlier that such a collapsing star emits outgoing radiation, in trying to get rid of all its useless information; we might expect that this radiation can play a rôle on the interior geometry of the black hole. In fact, we will see below that while for the Schwarzschild case this outgoing radiation does not play an essential rôle on the interior geometry, it can play a very determining one in the Reissner-Nordstrøm case.

Let us now have a closer look at the interior region of a Schwarzschild black hole, in the purely spherically symmetric picture. This region, as we saw earlier, is also described by the Schwarzschild solution, but this solution presents a very peculiar behavior at the origin of the coordinates $r = 0$: there is a curvature singularity there. Indeed, it can be shown (section 1.2b)) that the spacetime curvature blows up like $r^{-3}$ when $r$ goes to zero. Also, when one considers the endpoints of the gravitational collapse of an uncharged star, one finds quite generally that the collapse only stops when all the mass gets infinitely concentrated at the origin. All this indicates that there is a *physical singularity* at the centre of the Schwarzschild black hole. It is worth noting that singularities appear in other solutions of Einstein's field equations. A very good example is the initial singularity of the Friedmann-Robertson-Walker cosmological solution [8].

How can we interpret the presence of this singularity? At first sight, it is not very surprising: in the Newtonian theory, if one lets a spherical ball of pressureless matter collapse spherically, a singularity will develop since all the mass elements are attracted towards the centre of the ball. But it is clear that in this example, the singularity is simply a consequence of our idealizations; a realistic collapse would present at least small departures from sphericity, and these departures will prevent the singularity from developing. Could it be then, that the general relativistic singularity of the Schwarzschild solution is a mere consequence of too idealized a gravitational collapse model? This was the question considered in the early works of Khalatnikov, Lifshitz and collaborators [9]. They attempted to show that singularities are not a generic feature of general relativity, but rather the consequence of the imposed symmetries of the idealized problems.

Although very appealing, this viewpoint was shown to be incorrect when the *singularity theorems* [10] of Penrose, Hawking and Geroch were developed. These theorems tell us, when applied to the case of black holes, that a singularity always comes with the presence of a ***trapped surface***. A trapped surface is a surface such that a beam of photons sent out perpendicularly from it, both inwards and outwards, will converge. This is precisely the kind of behavior that one observes inside black holes: even if a photon is emitted towards the exterior of the hole, it cannot escape and will start converging towards a photon that was emitted inwards. We can therefore conclude that, according to the singularity theorems, a singularity is truly an essential feature of every black hole. It has to be noted that the theorems possess a certain number of underlying assumptions; one of them (the most restrictive one) roughly states that the energy density of the matter present in the hole, added to

the sum of its principal pressures, should be greater than, or equal to, zero. If this condition, called the ***strong energy condition***, holds for all known classical matter distributions, it is possible that it be violated by quantum matter distributions; a good example of such a distribution being false vacuum (section 1.3), which obeys the equation of state $P = -\rho$, where $\rho$ is positive. However, in the Schwarzschild spacetime, the strong energy condition is satisfied, and we find that a singularity must necessarily exist.

The singularity theorems show that singularities are not only the consequence of the symmetries of a given solution, but are a true generic feature of general relativity. We are therefore back to our question: how can we interpret the presence of those singularities? There are numerous examples showing how the prediction of singularities can be removed when a given theory is replaced by a more complete one. For instance, classical mechanics predicts that a proton-electron system should radiate an infinite amount of energy in a finite time, as the electron spirals towards the proton. The introduction of quantum mechanics showed otherwise. When a better theory is not available, one can always introduce *ad hoc* rules to prevent singular behavior. In our example: Bohr's postulate, according to which electrons in circular orbits should not radiate.

In the case of general relativity, *ad hoc* rules were also introduced, for example, Markov's new law of nature [11] where curvature is always subject to an upper limit of Planckian magnitude. Another example is González-Díaz' interior model for the Schwarzschild black hole (section 1.3). Although *ad hoc* rules can sometimes bring hints towards a better understanding, it is generally expected that

a more complete theory will be needed in order to satisfyingly rule out singular behaviors. It is therefore reasonable to expect that the singularities in general relativity should disappear when a better theory, namely, a quantum theory of gravitation, is discovered. In this view, singularities signal the breakdown of general relativity: the theory becomes invalid in the vicinity of a singularity.

A complete quantum theory of gravitation is still missing, so it is hopeless for the moment to try to directly probe the singularity. However, if we remain far enough from it, such that quantum effects in the geometry can be neglected, it may be possible to apply the ideas of quantum physics to all the other fields, but still treating gravity classically. This is called the semiclassical approach. It is then interesting to evaluate the effects that the quantum fields can have on the geometry; it can be hoped that these effects would succeed in slowing down the infinite rise of the curvature, in the spirit of Le Châtelier's principle [12] (section 1.4c)).

We will devote most of Chapter One, and a part of Chapter Two of this thesis to this question. We will begin with a brief review of the classical Schwarzschild black hole, and proceed with the discussion of an interior black hole model introduced by González-Díaz in 1981 [13]. This model, as we mentioned above, is an example of an *ad hoc* model designed explicitly to remove the black hole singularity. Following this, we will consider the effects of small departures from spherical symmetry in the gravitational collapse, on the interior geometry of the Schwarzschild black hole. We will show that for a significant portion of the spacetime near the singularity, these aspherical perturbations play no rôle; spherical symmetry is therefore expected to hold to a high degree of precision, near this portion of the singularity.

With this result established, we will try to probe the effects due to the vacuum polarization of the quantized fields on the geometry in the vicinity of the singularity. We will show that there are two possibilities: either the infinite rise in the curvature appears *sooner* than in the classical picture (if the stress induced by the vacuum polarization is a pressure), or the curvature remains bounded (if the stress is a tension, rather than a pressure), even for arbitrary small values of $r$, as long as the semiclassical approach remains valid. If the latter picture happens to be the correct one, the singularity of the hole would be better described as a nucleus of finite extent where the mass of the black hole is concentrated.

---

Motivated by the results of section 1.4c), we will introduce at the beginning of Chapter Two a line element where the two relevant metric elements are given by undetermined powers of $r$. The semiclassical problem will then be reconsidered with this "power-law" metric, and new pieces of information will be gathered. The remaining part of Chapter Two will consist in a study of the power-law metric; we will consider the stability of the geometries, as well as the accessibility of the origin.

The interior of a Reissner-Nordstrøm black hole is very different from the interior of a Schwarzschild one (compare Fig. 1.1 and 1.3 with Fig. 3.1). The presence of the inner apparent horizon, which lies on the Cauchy horizon of the spacetime, brings interesting new features to this black hole interior. The Reissner-Nordstrøm solution also presents a curvature singularity at the coordinate value $r = 0$. This was expected on general grounds from the singularity theorems. There is a major difference, however, between this singularity and that of the Schwarzschild solution: the singularity is here timelike. In the Schwarzschild case, an observer

is forced to hit the singularity after he has crossed the horizon of the hole; the situation is completely different for the Reissner-Nordstrøm case: an observer can avoid hitting the singularity, and can end up in an entirely different universe. A consequence is that while in the Schwarzschild case the star is forced to collapse to a single point, in the Reissner-Nordstrøm case the star may bounce and begin a new life in the other universe [14]. Even if the curvature singularity of the Reissner-Nordstrøm solution is timelike, it is still possible that quantum effects will have to play a rôle similar to the rôle they were playing in the Schwarzschild case, but we shall not pursue this question further.

But there is another kind of singularity present in the Reissner-Nordstrøm spacetime. It has been shown [15] (section 3.3) that if one slightly perturbs the geometry, and allows the perturbating field to propagate along the inner apparent horizon (Fig. 3.2) (as it would be the case for the backscattered part of the radiation initially coming from the collapsing star, if the scattering occurs at very late times), then the energy density of the field, when measured by a free falling observer crossing this horizon, blows up to infinity. (The amount of radiation is very small, but its effects can be quite catastrophic!) It is possible to give a heuristic argument explaining this result. Consider in Fig. 3.2 the sequence of light rays approaching the line $v = \infty$. In the exterior region, this line represents future null infinity and these rays therefore represent the radiation backscattered at very late times towards the interior of the hole. There is an *infinite lapse of time* between the first ray and the last one coinciding with $\mathcal{J}^+$. However, inside the hole, the line $v = \infty$ represents the inner apparent horizon, and the lapse of time between the first ray and the last becomes *finite*. There is therefore an infinite accumulation of light rays on the

inner horizon: an observer crossing this horizon would receive an infinite amount of information (the amount of total energy is however finite) in a finite proper time. For this reason, the inner apparent horizon of the Reissner-Nordstrøm spacetime is sometimes referred to as a singular surface of *infinite blueshift*.

We have mentioned above that in the Schwarzschild spacetime, the curvature of spacetime acts on radiation as a potential barrier; since the spacetime outside the hole is static, the barrier simply scatters the waves, without any amplification. There is also such a barrier inside the Reissner-Nordstrøm black hole, but here, the spacetime is dynamic ($r$ is now a time variable). It is the time dependence of the potential barrier which produces the amplification of the waves. This amplification is furthermore found to be infinite when the waves propagate along the inner horizon. Although this result is based on first order perturbation theory where it is assumed that the effects of the perturbation on the geometry remain small, it suggests that perhaps a (perturbation) singularity could develop at the inner apparent horizon. How can we interpret the presence of this new singularity? If the curvature singularity was a necessary consequence of the singularity theorems, what of this one? Could it be that this time, the singularity appears because of our idealizations, because our model for the gravitational collapse is too simplistic? Indeed, we have mentioned that the Reissner-Nordstrøm solution describes the exterior of a charged star undergoing a perfectly spherical collapse; it would then be interesting to consider the consequences of small departures from spherical symmetry. Chapter Three, after a brief review of the Reissner-Nordstrøm solution, will be devoted to this problem. We will show that the radiation emitted

from the surface of the collapsing star plays an essential rôle on the interior geometry of the Reissner-Nordstrøm black hole: it produces a separation of the inner apparent horizon from the Cauchy horizon of the spacetime (section 3.1, Fig. 3.3). The question is now: do we still have in this dynamic situation a singular surface of infinite blueshift? If the answer is yes, where does it arise? At the Cauchy horizon, or at the inner apparent horizon? From our heuristic picture described above, it can be expected that a surface of infinite blueshift will arise at the Cauchy horizon, but that everything should be regular at the inner horizon. We will verify this explicitly in section 3.3 and we will conclude that the singular surface of infinite blueshift is an essential feature of a spacetime possessing a Cauchy horizon, and not a product of simplistic models.

This was the plan of the thesis. Before we close this section, let us say a few words about the notations and conventions. It was not possible, nor a good idea, to try to use a consistent convention throughout the thesis. The reason is that the literature does not, and it appears to be better to follow as much as possible the generally accepted conventions. In most of the thesis, where it is not explicitly stated otherwise, we will use the conventions of Misner Thorne and Wheeler [3]. That is, we will use geometrized units, where $c = G = 1$. In those units, mass and charge have units of length; curvature, energy density and pressure have units of inverse length squared. We will use the spacelike convention $(- + ++)$ for the metric, and the sign convention for the Riemann and Ricci tensors is such that the field equations are written $G_{\mu\nu} = 8\pi T_{\mu\nu}$. In the sections where quantum effects are discussed, and where explicitly stated, Planck units where $c = G = \hbar = 1$ will be used. In section 2.2 (and only there), where we deal with quantum field theory in

curved spacetime, we will take the timelike convention $(+---)$ for the metric. Also in this section, we will use the opposite sign convention for the curvature tensor, such that the field equations will there be written as $G_{\mu\nu} = -8\pi T_{\mu\nu}$. To avoid any confusion, the reader will be warned whenever we depart from the standard MTW conventions.

## 1.2: The Schwarzschild geometry

The objective of this section is twofold. First, a brief description of the Schwarzschild solution is a good starting point to the thesis. Second, we will take the opportunity to derive a few results that will be used later on.

*a) The general metric for a static, spherically symmetric geometry.*

The Schwarzschild geometry is a vacuum solution of the Einstein field equations which is static (the geometry does not depend on time) and spherically symmetric. To derive this solution, we have to consider the most general metric that possesses those symmetries. It is given by the form [16]

$$ds^2 = -A(r)\, dt^2 + B(r)\, dr^2 + r^2 d\Omega^2, \tag{1.1}$$

where

$$d\Omega^2 = d\theta^2 + \sin^2\theta\, d\phi^2 \tag{1.2}$$

is the metric on a 2-sphere. $\theta$ and $\phi$ are the usual spherical coordinates; $r$ is a radial coordinate such that the area of the 2-sphere $r$ = constant, $t$ = constant, is equal to $4\pi r^2$, and $t$ is a time coordinate. Spherical symmetry is reflected by the presence of the last term in the metric, and also by the fact that two arbitrary functions of $r$ are needed. Instead of the form (1.1) , we shall use a more convenient form given by

$$ds^2 = e^{\psi}(-\Phi\, dt^2 + \Phi^{-1} dr^2) + r^2 d\Omega^2, \tag{1.3}$$

where $\psi \equiv \psi(r)$ and $\Phi \equiv \Phi(r)$ are our two arbitrary functions of $r$. We introduce now another function of $r$ derived from $\psi$ and $\Phi$:

$$1 - \frac{2m(r)}{r} \equiv e^{-\psi}\Phi. \tag{1.4}$$

$m(r)$ is called the *mass function* and we will see a bit later why it is called this way.

To write down the field equations for this metric, we need to know the form of the stress-energy tensor [17]. We first assume that the material is a *fluid* characterized by its energy density $\rho$, its radial pressure $P_r$ and its tangential pressure $P_\perp$. We then introduce the orthonormalized tetrad:

$$\begin{aligned}
\vec{e}^{\,\alpha}_{(t)} &= \frac{1}{\sqrt{e^{\psi}\Phi}}\,\partial^\alpha t, \\
\vec{e}^{\,\alpha}_{(r)} &= \frac{1}{\sqrt{e^{\psi}\Phi^{-1}}}\,\partial^\alpha r, \\
\vec{e}^{\,\alpha}_{(\theta)} &= \frac{1}{r}\,\partial^\alpha \theta, \\
\vec{e}^{\,\alpha}_{(\phi)} &= \frac{1}{r\sin\theta}\,\partial^\alpha \phi.
\end{aligned} \tag{1.5}$$

This tetrad forms the proper reference frame of static observers. Hence, it is the proper reference frame of our fluid. This means that we can write its stress-energy tensor as

$$T^{\alpha\beta} = \rho\,\vec{e}^{\,\alpha}_{(t)}\vec{e}^{\,\beta}_{(t)} + P_r\,\vec{e}^{\,\alpha}_{(r)}\vec{e}^{\,\beta}_{(r)} + P_\perp\left(\vec{e}^{\,\alpha}_{(\theta)}\vec{e}^{\,\beta}_{(\theta)} + \vec{e}^{\,\alpha}_{(\phi)}\vec{e}^{\,\beta}_{(\phi)}\right), \tag{1.6}$$

or, since $\vec{e}_{(a)} \cdot \vec{e}_{(b)} = g_{\alpha\beta}\,\vec{e}^{\,\alpha}_{(a)}\vec{e}^{\,\beta}_{(b)} = \eta_{(a)(b)}$ the Minkowski metric, we also have:

$$T^{\alpha}_{\ \beta} = \mathrm{diag}(-\rho, P_r, P_\perp, P_\perp). \tag{1.6'}$$

The fact that the $\theta$ and $\phi$ components of the stress-energy tensor are equal ($= P_\perp$) follows from spherical symmetry. If the fluid is further assumed to be *isotropic*, then we have $P_r = P_\perp$.

It is an elementary exercise in general relativity to derive the field equations for the metric (1.3), (1.4) with stress-energy tensor (1.6). The easy way is to use the results for the field equations obtained in ref. [16] for the form (1.1) and then to translate them into our form. The results are:

$$m' = 4\pi r^2 \rho \tag{1.7}$$

$$\psi' = \frac{4\pi r(\rho + P_r)}{1 - \dfrac{2m}{r}} \tag{1.8}$$

where a prime denotes a derivation with respect to $r$. From the energy conservation equation ${T^{\mu\nu}}_{|\nu} = 0$ we obtain

$$P_r{}' + \frac{2}{r}(P_r - P_\perp) + \frac{m + 4\pi r^3 P_r}{r^2\left(1 - \dfrac{2m}{r}\right)}(\rho + P_r) = 0. \tag{1.9}$$

These are all the equations we need to specify the solution. The fact that we call $m(r)$ the mass function is suggested by eq. (1.7) which is exactly like its Newtonian counterpart.

A simplification occurs when $\psi$ is a constant. From eq. (1.8) we find that this happens when $\rho + P_r = 0$, that is, either when $\rho = P_r = 0$ or when $P_r = -\rho$. Those two cases will both be important later. Eqs. (1.3) and (1.4) then give

$$ds^2 = -e^{2\psi}\left(1 - \frac{2m(r)}{r}\right)dt^2 + \left(1 - \frac{2m(r)}{r}\right)^{-1} dr^2 + r^2 d\Omega^2.$$

Since $\psi$ = constant, we can define a new time coordinate $t_{NEW} = e^{\psi} t_{OLD}$ and the metric becomes

$$ds^2 = -\left(1 - \frac{2m(r)}{r}\right) dt^2 + \left(1 - \frac{2m(r)}{r}\right)^{-1} dr^2 + r^2 d\Omega^2, \qquad \rho + P_r = 0. \quad (1.10)$$

Moreover, eq. (1.9) then reads

$$P_\perp = P_r + \tfrac{1}{2}\, r\, P_r', \qquad \rho + P_r = 0. \quad (1.11)$$

We are now ready to derive the Schwarzschild solution.

*b) The Schwarzschild solution.*

The stress-energy tensor for vacuum is simply $T_{\mu\nu} = 0$ so we take

$$\rho = P_r = P_\perp = 0. \quad (1.12)$$

Eq. (1.7) gives $m$ = constant $\equiv M$. Eq. (1.11) is trivially satisfied and from eq. (1.10) the metric becomes

$$ds^2 = -\left(1 - \frac{2M}{r}\right) dt^2 + \left(1 - \frac{2M}{r}\right)^{-1} dr^2 + r^2 d\Omega^2. \quad (1.13)$$

This is the so-called *Schwarzschild solution*. For test particles far from the hole, the equations of motion in this spacetime reduce to the Newtonian equations with a potential of the form $-M/r$. This property permits us to identify the constant of integration $M$ with the mass of the black hole.

A singularity develops in the metric coefficients at $r = 2M$. This singularity is not a true physical singularity but merely a consequence of the misbehavior of

the coordinates at this radius [18]. To see this, consider a typical non vanishing element of the curvature tensor measured by a free falling (timelike) observer. This is a measure of the tidal forces felt by the observer as he falls towards the hole [19]. This typical element is of order [18]

$$R_{....} \sim \frac{M}{r^3}. \tag{1.14}$$

Also, we have for the curvature invariant:

$$R_{\alpha\beta\gamma\delta}R^{\alpha\beta\gamma\delta} = \frac{48M^2}{r^6}. \tag{1.15}$$

Those two equations, both meaningful physically and independent of any system of coordinates, do not show any bad behavior at $r = 2M$. However, we see that infinite curvature occurs at $r = 0$: this a true physical singularity. Another sign of misbehavior of the coordinates is that when $r < 2M$, $g_{tt}$ is positive and $g_{rr}$ is negative. This means that $r$ and $t$ interchange their rôles as spacelike and timelike coordinates! It is worth noting, however, that $r$ always conserves its geometrical meaning of being a measure of the area of the 2-sphere labelled by $r =$ constant, as we mentioned in the previous subsection.

To remove those difficulties, it is possible to construct a system of well behaved coordinates [18],[20] such that the metric is regular at the horizon radius $r = 2M$. We will now proceed with this construction. Consider a line element of the form

$$ds^2 = -\Phi\, dt^2 + \Phi^{-1}dr^2 + r^2 d\Omega^2, \tag{1.16}$$

where $\Phi \equiv \Phi(r)$ changes its sign at $r = r_0$. We introduce first a new radial coordinate $r^*$ defined by

$$r^* = \int \frac{dr}{\Phi(r)}, \tag{1.17}$$

and then the null coordinates

$$u = t - r^*, \qquad v = t + r^*. \tag{1.18}$$

$u$ and $v$ are respectively called retarded and advanced time. The line element (1.16) then becomes

$$ds^2 = -\Phi \, du dv + r^2 d\Omega^2,$$

where $r$ is now considered to be an implicit function of $u$ and $v$. As always, $r$ keeps its geometrical meaning of being a measure of the area of the 2-sphere $u, v =$ constant. From the last equations, it is clear that radial lightlike geodesics (= path of radial photons) are described by the equations $u =$ constant for outgoing geodesics, and $v =$ constant for ingoing geodesics.

We have not removed the coordinate singularity yet. It is possible to do so by simply relabelling the surfaces $u =$ constant, $v =$ constant. So introduce the constant $\kappa$ called the *surface gravity* [21] and defined by

$$\kappa \equiv \tfrac{1}{2} \, \Phi'(r_0), \tag{1.19}$$

and consider a new set of null coordinates defined by

$$U = -e^{-\kappa u}, \qquad V = e^{\kappa v}. \tag{1.20}$$

With those coordinates, called the *Kruskal-Szekeres coordinates*, the line element becomes:

$$ds^2 = \frac{\Phi}{\kappa^2 UV}\, dU\, dV + r^2 d\Omega^2. \tag{1.21}$$

What we want to verify is that the ratio $\Phi/UV$ is regular at $r = r_0$. To do this, we need to find the relation between $UV$ and $r$. Eqs. (1.18) and (1.20) yield:

$$UV = -e^{2\kappa r^*}. \tag{1.22}$$

We now want to evaluate $\Phi/UV$ at $r = r_0$; it is then sufficient to evaluate the numerator and the denominator in the vicinity of $r = r_0$. Expanding $\Phi(r)$ as a Taylor series and using eq. (1.19) we find that $\Phi(r) \simeq 2\kappa(r - r_0)$. Using this in eq. (1.17) yields: $r^* \simeq \ln|r/r_0 - 1|/2\kappa$. Substituting this result into eq. (1.22) finally gives $UV \simeq -|r - r_0|/r_0$. This shows that, indeed, the ratio $\Phi/UV$ is regular at $r = r_0$. We therefore have found our set of well behaved coordinates for the general line element (1.16).

Let us now apply this formalism to the case of the Schwarzschild solution. $\Phi(r)$ is given by eq. (1.13) : $\Phi(r) = 1 - 2M/r$, so eqs. (1.17) and (1.19) give

$$\begin{aligned} r^* &= r + 2M \ln\left|\frac{r}{2M} - 1\right|, \\ \kappa &= \frac{1}{4M}. \end{aligned} \tag{1.23}$$

With the help of this last equation, eq. (1.22) yields

$$UV = -\left|\frac{r}{2M} - 1\right| e^{r/2M}.$$

From eq. (1.20), it is clear that $U$ is defined only in the range $-\infty < U < 0$, whereas $V$ is defined for $0 < V < \infty$. This region of the $U, V$ plane represents the ***exterior*** of the Schwarzschild black hole. To recover the interior region, we ***analytically continue*** our spacetime such that both $U$ and $V$ are allowed to cover the whole line, from $-\infty$ to $\infty$. This means that we have to replace the last equation by

$$UV = \left(1 - \frac{r}{2M}\right) e^{r/2M}, \tag{1.24}$$

and the line element (1.21) finally becomes

$$ds^2 = -\frac{32M^3}{r} e^{-r/2M} \, dU dV + r^2 d\Omega^2, \tag{1.25}$$

which is manifestly regular at $r = 2M$.

One important feature of the metric in the $U, V$ coordinates is that, from eq. (1.24), we discover that there exist two different horizons: one for $U = 0$, one for $V = 0$. This also means that the horizons are null surfaces. We also discover that there exist two singularities given by $UV = 1$; one for $U$ and $V$ both positive, the other for $U$ and $V$ both negative (see Fig. 1.1). So half of the spacetime is hidden when we use the Schwarzschild coordinates [18]. This doubling of the spacetime is, of course, a consequence of the analytical continuation.

In what we have done so far, there is one tacit assumption that we made and which is important to underline. We have tacitly assumed that the interior of the Schwarzschild black hole is also filled with vacuum. Only in this case can we consider the Schwarzschild solution (1.13) to be valid for $r < 2M$. And only in this case can the double-null form (1.25) be a good description of the spacetime. In the

next section we will consider another model for the Schwarzschild black hole where, while the exterior is described in the same way as we have seen here, the interior is treated in a different manner.

### 1.3: The González-Díaz model

We will consider in this section an *ad hoc* model explicitly designed to remove the singularity at the centre of a Schwarzschild black hole. In 1981, González-Díaz [13] proposed that the equation of state $\rho = P_r = P_\perp = 0$ should not be used to describe the interior of a Schwarzschild black hole and that the solution (1.13) should not be valid there. Instead, he made the simple assumption that $\rho$ be a (positive) constant inside. Using this assumption in eq. (1.7) yields

$$m = \frac{4\pi}{3}\rho r^3. \tag{1.26}$$

Since the *interior* solution must be joined to the *exterior* solution (1.13), it is necessary that $g_{tt}(r \to 2M) \to 0$ and that $g_{rr}(r \to 2M) \to \infty$ when $r = 2M$ is approached from the inside. The easiest way to achieve this is to assume that $g_{tt} = -{g_{rr}}^{-1}$ and then impose that $g_{tt}(r = 2M) = 0$. This assumption, from eq. (1.3), is equivalent to assuming that $\psi = 0$. Again, as we have seen in section 1.2a), this is equivalent to assuming that $\rho + P_r = 0$. So $P_r$ is also a constant inside the hole. Furthermore, eq. (1.11) implies that $P_\perp = P_r \equiv P$. Therefore, the equation of state inside the hole is

$$\rho = -P = \text{constant}, \qquad r < 2M. \tag{1.27}$$

This equation describes "inflationary" material which is often called *false-vacuum*. An important point is that this equation of state violates the energy conditions needed in the proof of the singularity theorems [10]. This means that the singularity theorems do not hold in this black hole interior.

Eqs. (1.10) and (1.26) now give the metric inside the hole:

$$ds^2 = -\left[1-\left(\frac{r}{r_0}\right)^2\right]dt^2 + \left[1-\left(\frac{r}{r_0}\right)^2\right]^{-1} dr^2 + r^2 d\Omega^2, \qquad r < 2M \tag{1.28}$$

where

$$r_0{}^{-2} \equiv \frac{8\pi}{3}\rho. \tag{1.29}$$

This solution of the Einstein field equations has a name: it is called the *static de Sitter* solution. $r_0$ has now to be identified with $2M$:

$$r_0 = 2M. \tag{1.30}$$

Eqs. (1.29) and (1.30) then give

$$\rho = \frac{M}{\frac{4\pi}{3}(2M)^3} \tag{1.31}$$

which could lead to a nice interpretation since the denominator is the volume formula for a sphere of radius $2M$. However, the denominator of eq. (1.31) is not the *proper* volume of the black hole. This last equation must then be seen as a convenient way of expressing the relationship between $\rho$ and the mass of the black hole.

Combining the results that we have, we find that in this model the metric of the Schwarzschild black hole is given by

$$ds^2 = -\Phi\, dt^2 + \Phi^{-1} dr^2 + r^2 d\Omega^2 \tag{1.32}$$

where

$$\Phi(r) = \begin{cases} 1-(r/r_0)^2 & r \leq r_0 \\ 1-(r_0/r) & r \geq r_0, \end{cases} \tag{1.33}$$

and where $r_0 = 2M$ . The material inside the hole is described by the equation of state $\rho = -P =$ constant and we have $\rho = P = 0$ outside.

The striking difference between this interior model and the one of the last section is that here we have a constant curvature tensor. So we have a regular spacetime everywhere inside the black hole. We have got rid of the singularity! This is the reason why this black hole model is worth spending some time to study.

But there is still some work to be done in order to decide whether this model can work, even before trying to justify the interior equation of state. We still have to prove that the interior and exterior solutions can be joined continuously. (The criterion for a continuous join is that the metric and its first derivatives should be continuous at the horizon.) We mentioned earlier the necessary condition that the interior solution should develop a (coordinate) singularity at $r = 2M$. This condition is of course satisfied by our solution but it is not a sufficient condition to have a continuous join. We also need continuity in the first derivatives of the metric.

In fact, it can be expected that the join is not continuous directly from the presence of the discontinuity in the stress-energy tensor [22]. We can however imagine that this discontinuity is only a product of our idealizations and that, in fact, the jump takes place within a finite distance (see Fig. 1.2). This is entirely equivalent to superposing to the sharp jump a shell of material with finite thickness

which plays the rôle of smoothing the jump. Then, we can go back to the idealized problem by formally letting the shell thickness go to zero. The stress-energy tensor will, in this picture, have a term proportional to the Dirac $\delta$ function, evaluated at the horizon, which will represent the thin shell. The coefficient of the $\delta$ function term will therefore represent the stress-energy of the thin shell. The problem of the junction conditions then reduces to the study of the stress-energy tensor of the thin shell [23].

To apply those ideas to our case, consider the following: for the entire spacetime in the González-Díaz model, the radial pressure is $P_r = -\rho\ \theta(r_0 - r)$ where $\rho$ is the positive constant of eq. (1.31) and $\theta$ the Heaviside step function. Eq. (1.11) then gives $P_\perp = P_r + (1/2)r\rho\ \delta(r - r_0)$ . The last term is obviously the contribution from the shell. But to have a meaningful description of $P_\perp^{\rm shell}$, the $\delta$ function must be expressed as an invariant, independently of any coordinate system. This means that we have to replace the argument of the $\delta$ function by the proper distance from the horizon: $s = \sqrt{g_{rr}(r = r_0)}(r - r_0)$. This yields

$$P_\perp = P_r + \tfrac{1}{2} r_0 \rho \sqrt{g_{rr}(r = r_0)}\ \delta(s).$$

Using eq. (1.31) to express $\rho$ as a function of $r_0$, we finally obtain

$$P_\perp^{\rm shell} = \frac{1}{8\pi}\frac{3}{r_0}\sqrt{g_{rr}(r = r_0)}. \tag{1.34}$$

Since $g_{rr}(r \to r_0) \to \infty$, we have that $P_\perp^{\rm shell} = \infty$. Hence the shell would have to supply infinite tangential pressures to support the interior material against its own collapse. We can therefore conclude that the González-Díaz model is dynamically

unstable. This result can be recovered by a direct application of the theory of singular surface layers in general relativity [23]. Such an analysis was carried out by Ø. Grøn in 1985 [24]. An important point to notice is that there is no objection, at least in principle, to the González-Díaz model if the join is put elsewhere than at the horizon.

This section on the González-Díaz model comes as an answer to a paper by Shen and Zhu published early in 1988 [25]. In this paper, the authors constructed Kruskal-Szekeres coordinates for the González-Díaz spacetime and then examined the junction conditions. They concluded that the join at the horizon was continuous and that the model was stable. This must come as a surprise after our previous discussion! There are two major problems with Shen and Zhu's paper. The first one is the way they constructed their Kruskal-Szekeres coordinates. What they did was to construct one set for the exterior region (as we did in the previous section) and another set for the interior region. It can be shown that *the two sets have no relation whatsoever*. There is therefore no meaning to studying the junction conditions with those coordinates. The second problem is that, even if there was a meaning to this study, *a discontinuity in the first derivatives of the metric nevertheless appears*. Unfortunately, Shen and Zhu did not find it. We hope that this section of the thesis will help to clarify the situation regarding this black hole model.

More importantly, I do not think that this model should be taken too seriously, even if it was proven dynamically stable. The reason is that its underlying assumptions are far too simplistic to be realistic. The principal assumption is that the energy density should be constant inside the hole. There is no reason why it

should be so. Indeed, to justify this assumption, one would have to find a way to explain the creation of matter out of nothing, and to explain why this matter has to fill the black hole interior in such a way. Also, inspired by this approach, one could invent any black hole interior model that one likes, and there would be no way to tell which model is the "good one". It is my opinion that a black hole interior model should come from a more fundamental approach.

There is probably nothing wrong in seeing the black hole interior as being filled with vacuum, at least in a spherically symmetric situation. Indeed, in this case, a collapsing star does not emit any gravitational radiation and therefore leaves nothing "behind" but vacuum. When the collapse departs from spherical symmetry, however, gravitational radiation is emitted and it could be that, in this case, the interior be filled with radiation; but this radiation would nevertheless propagate in vacuum. We will see in the next section that, at least when the departure is small, there is a region in the black hole interior where the influence of this radiation is negligible. In this region, then, both spherical symmetry and the vacuum remain a good description.

Again in the next section, we will see that near the singularity, in this vacuum-filled black hole interior, there is a region where vacuum polarization effects of the diverse quantum fields present cannot be neglected. This happens even before quantum effects in the geometry itself have to be considered. In the following pages, we will study the problem of solving the semiclassical Einstein field equations

$$G_{\mu\nu} = 8\pi\langle T_{\mu\nu}\rangle,$$

where $\langle T_{\mu\nu} \rangle$ is the expectation value of the stress-energy tensor, determined by one-loop vacuum polarization effects of the quantized fields.

Before we close this section, let us say a few words about the González-Díaz equation of state

$$\rho = -P = \text{constant}.$$

This equation describes "inflationary" material for which the stress-energy tensor can be written as (see eq. (1.6))

$$T_{\mu\nu} = -\rho \, g_{\mu\nu}.$$

This material is also called *false vacuum* because $T_{\mu\nu}$ is Lorentz invariant (it does not single out any four-velocity). The solution of the field equations for this material is called the *de Sitter* solution and, in a cosmological context, describes the inflationary universe. In the theory of inflation, this equation of state is the consequence of the presence of a Higgs boson field that dominates on the dynamics of the universe [26]. It is also interesting to note that the de Sitter universe of Planckian size plays an important rôle in minisuperspace models of quantum cosmology [27]. This is to say that false vacuum is very likely a genuine quantum effect. The de Sitter spacetime will come back to us when we consider the quantum effects near the singularity.

In conclusion, we will now leave the González-Díaz model and consider from another point of view the problem of determining the metric inside a spherically symmetric black hole.

## 1.4: The semiclassical model

*a) Quantum effects in curved spacetime.*

What we wish to consider in this section is a model for a spherically symmetric, uncharged, black hole where the Schwarzschild solution is valid everywhere except near the singularity. What we expect is that, near the singularity where the curvature is very large, vacuum polarization effects produced by the quantized fields would influence the geometry such that the Schwarzschild solution will not be valid there. It is easy to imagine what could be going on in this region of the black hole. The large curvature near the centre of the hole induces pair creations of all kinds of particles. Each pair will eventually recombine, but on an average, their contribution on the stress-energy tensor will not be zero. Accordingly, this non-vanishing stress-energy will have an effect on the geometry of spacetime and the Schwarzschild solution will not hold in that region. This simple picture can be very helpful to understand what follows.

The problem of determining the quantum effects in a curved spacetime is complicated. To have a complete understanding of those effects, a theory where gravity and all the other interactions are quantized would be needed. But quantum gravity is still not on the market so we have to start from somewhere else. One possibility, in analogy with quantum mechanics where the motion of the electrons is quantized but not the electromagnetic field, is to assume that there is a "regime" where gravity can be treated classically, while all the other fields are quantized. This approach is called "quantum field theory in curved spacetime". In this framework,

one first specifies the background geometry (for example, the Friedmann-Robertson-Walker cosmological solution), then considers a type of field (for example, a massless scalar field), and then quantizes the field on the given background. Interesting quantities can then be calculated (for example, the stress-energy tensor of the quantum field).

An interesting thing happens when the stress-energy of the quantized fields dominates over all the other contributions. The fields then act as a *source* in the Einstein field equations. The problem thus becomes: specify the background geometry, quantize the fields, calculate the stress-energy tensor, and then solve for the background geometry via the semiclassical Einstein field equations

$$G_{\mu\nu} = 8\pi\langle T_{\mu\nu}\rangle. \tag{1.35}$$

This is called the *backreaction* problem and it is somehow analogous to a Hartree-Fock self-consistent treatment of multi-electronic atoms. For example, one can quantize a massless scalar field on a Friedmann-Robertson-Walker background and then solve for the scaling factor $a(t)$.

It is of course difficult to obtain an expression for $\langle T_{\mu\nu}\rangle$ and I do not claim that I am able to do so. What I can do, however, is to use results that others have already obtained! I will do so in Chapter Two of this thesis. For now, let us be more general in the discussion. The principal observation regarding the general expression for the renormalized vacuum expectation value of the stress-energy tensor, when one-loop Feynman diagrams are considered, is that it depends on the curvature tensor squared. This is true for all one-loop contributions from all quantized fields,

including one-loop graviton diagrams. Another way of saying this is that vacuum polarization effects induce terms quadratic in the curvature tensor in the standard Einstein-Hilbert gravitational action [28], and hence in the field equations [29].

Schematically, we can write:

$$S_g = \frac{1}{16\pi} \int d^4x\sqrt{-g}\,(R + c_1 R....^2 l_P^2 + \cdots), \tag{1.36}$$

$$G_{\mu\nu} = 8\pi\langle T_{\mu\nu}\rangle \sim R....^2 l_P^2, \tag{1.37}$$

where $l_P$ is the Planck length (the curvature tensor has units [length]$^{-2}$) and $c_1$ a coefficient of order unity. This coefficient depends on the *effective number of quantized fields*, that is, the number of spin-0 fields times a certain characteristic coefficient; plus the number of spin-1/2 fields times their characteristic coefficient; and so on. The derivations and details can be found in the book by Birrell and Davies (ref. [29]).

Where can the semiclassical equation be applied? Qualitatively, from eq. (1.35), it is clear that if the $T_{\mu\nu}$ eigenvalues in a given quantum state are much different from the averaged value $\langle T_{\mu\nu}\rangle$, then the semiclassical approach becomes a poor approximation. So we expect that eq. (1.35) will be valid when quantum fluctuations are small. On the other hand, it is believed that quantum effects in the geometry itself become important around the Planck length $l_P = \sqrt{G\hbar/c^3} \approx 10^{-33}$cm. Of course, the semiclassical equation cannot work around this length scale. Now, from eq. (1.36), the quantum field effects are expected to become important when

$$R.... \sim R....^2 l_P^2.$$

In the case of a Schwarzschild black hole, a typical element of the curvature tensor is given by eq. (1.14) and the last equation becomes

$$\frac{G}{c^2}\frac{M}{r^3} \sim \left(\frac{G}{c^2}\frac{M}{r^3}\right)^2 \frac{G\hbar}{c^3},$$

or:

$$r \sim r_Q \equiv \left(\frac{G^2\hbar}{c^5}\, M\right)^{1/3}, \tag{1.38}$$

where all the factors of $c$ and $G$ have been reinserted. In Planck units, eq. (1.38) becomes $r \sim r_Q \equiv M^{1/3}$. For a solar mass black hole, $r_Q \approx 10^{-20}$cm, which is much larger than the Planck length. From these results, we can expect that the semiclassical equation (1.35) or (1.37) will be valid in the range:

$$1 \ll r \leq r_Q = M^{1/3}, \tag{1.39}$$

in Planck units. For $r \sim 1$, the effects caused by a fully quantized theory of gravitation become important, whereas for $r \gg r_Q$, quantum effects in general (including one-loop quantum gravity) become negligible and we recover the classical solution.

Before we go further in this direction, we need to answer a very important question: can we expect spherical symmetry to hold at small radii? This is a very important question because, if the answer is yes, the general problem of determining the quantum effects at the centre of the hole will be greatly simplified. We will consider this in the next subsection.

***b) Spherical symmetry holds near the singularity.***

In this subsection we consider the problem of a star undergoing a nearly spherical gravitational collapse. In particular, we will study the effect on the region near the singularity of small departures from spherical symmetry in the gravitational collapse. We will show that at late (advanced) times, non-spherical perturbations have negligible effects on the singularity. This means that at sufficiently late advanced times, spherical symmetry holds, not just externally but also down to very small radii.

The general problem of non-spherical gravitational collapse is very complicated and most of the studies undertaken so far postulated only small departures from spherical symmetry. What is usually considered is the propagation of aspherical perturbations on a spherically symmetric background, as we mentioned in section 1.1. Price [4] showed in 1972 that part of the gravitational radiation emitted by small aspherical "lumps" in the density distribution of the star is backscattered towards the hole by the curvature of the Schwarzschild spacetime. If the initial perturbation is a multipole of order $l$, then the amplitude of the external (backscattered) radiation field falls off as $t^{-(2l+2)}$. This means that external perturbations caused by small departures from spherical collapse die off at times larger than the characteristic timescale $2M$. This decay of external radiation will play an important rôle in what follows.

Fig. 1.3 is a spacetime diagram depicting the collapse of a spherical star. The coordinates used are the same as in section 1.2b). Choose a late advanced time $v_1$, whose world line meets the singularity $r = r^* = 0$ at point C. Let $u_1$ be

the retarded time whose world line also meets point C. From eq. (1.18) it is clear that we have

$$u_1 = v_1, \tag{1.40}$$

and from eqs. (1.20) and (1.23) we obtain for the Kruskal coordinates

$$U_1 = V_1^{-1} = e^{-v_1/4M}. \tag{1.41}$$

(The interior region is the one for which $U, V > 0$; we have used the analytical continuation of eq. (1.20).) Choose now any intermediate time $\bar{v}$ such that

$$2M \ll \bar{v} \ll v_1. \tag{1.42}$$

Perturbations at the region of the singularity for which $v > v_1$ (at the right of point C) come from several contributions. The first contribution is the infalling radiation at times later than $v_1$. But, as we discussed previously, an external perturbation dies off like $v^{-(2l+2)}$ for a multipole of order $l$. This means that this first contribution is very small and can be neglected. The second contribution comes from infalling radiation that passes through segment MD to be scattered by the curvature of spacetime towards segment CD. Since $\bar{v}$ is also a "late time", the argument used above still applies and this contribution too is negligible. Then comes the contribution of the infalling radiation that crosses segment AM and scatters towards segment MN, and that of the outgoing radiation escaping from the star and crossing segment AB to reach segment MN. Those contributions have

little effect since the radial thickness of the slice MN is exponentially small: near the horizon, for $r = 2M - \Delta r$ , $U = U_1$ , $V = \bar{V}$; eq. (1.24) reduces to

$$\begin{aligned} \Delta r &\simeq 2Me^{-1}U_1\bar{V} \\ &\simeq 2M\ e^{(\bar{v}-v_1-4M)/4M} \\ &\simeq 2M\ e^{-v_1/4M}, \end{aligned} \tag{1.43}$$

where eqs. (1.41) and (1.42) have been used. If this were only a statement about the smallness of a *coordinate* difference, it would not mean very much. But we have outlined in section 1.2 that $r$ is a direct measure of the area of the 2-spheres $r =$ constant. The fact that $\Delta r$ is small therefore leads to the fact that the difference in the areas is small. This also means that the region of spacetime corresponding to segment MN is small. The result is that the smallness of $\Delta r$ guarantees that the perturbation reaching segment CD will be very small, since very little of the radiation will be focussed through segment MN. So this contribution too can be neglected.

Since we do not have any other contribution, we arrive at the surprisingly simple conclusion that for regions of the singularity corresponding to late advanced times, aspherical perturbations become very small and can be neglected. We have to remember that inside the black hole, $r$ and $t$ have interchanged their rôles of spacelike and timelike coordinates. The concept of exterior late times then becomes interior large distances. Now, a spacelike hypersurface $r =$ constant, still in the Schwarzschild spacetime, is described by the line element:

$$ds^2 = \text{constant}\ dt^2 + r^2 d\Omega^2,$$

where the constant is positive. This line element describes a "3-cylinder" whose axis is the $t$ axis and where the surfaces of constant $t$ are 2-spheres, all of the same radius $r$. Therefore, $r$ represents the radius of the cylinder; it decreases as time increases. In this geometrical picture, the decay of external aspherical perturbations is reflected near the singularity as a spatial damping with increasing distance along the 3-cylinders $r$ = constant.

It is clear that this result simplifies considerably the problem of determining the geometry of the region near the singularity, since we know that a study using spherical symmetry can be undertaken and be meaningful. Note that the results derived in this subsection were first discovered by Doroshkevich and Novikov in 1978 [30] from an analysis similar to that of Price (ref. [4]). The derivation found here is however simpler.

With the confidence that we now have that spherical symmetry holds (at late times) near the singularity, we can now turn to the problem of the quantum effects near the singularity.

*c) Solving the semiclassical equation.*

[Warning: we will use Planck units in this subsection.]

The results derived in the two previous subsections now allow us to consider the problem of the quantum effects on the geometry near the singularity of a spherical black hole. From the last subsection we know that at sufficiently late times, the spacetime is spherically symmetric near the singularity even if the gravitational

collapse presents small departures from sphericity. From subsection 1.4a) we know that the semiclassical Einstein field equations

$$G_{\mu\nu} = 8\pi\langle T_{\mu\nu}\rangle \tag{1.44}$$

can be applied in the range $1 \ll r \leq r_Q \equiv M^{1/3}$. The way to proceed would then be to start with a spherically symmetric line element given by eq. (1.1):

$$ds^2 = -A(r)\, dr^2 + B(r)\, dt^2 + r^2 d\Omega^2.$$

Since we are *inside* the black hole, $r$ plays the rôle of *time*, whereas $t$ plays the rôle of *space*. The fact that this metric does not depend on $t$ means that the spacetime is *spatially homogeneous*. The next step would be to quantize each type of field (spin-0, spin-1/2, etc.) on this general background; then to compute the vacuum expectation value of the stress-energy tensor induced by the presence of the quantum fields. Using this result in the semiclassical equation, the aim would be to solve for the functions $A(r)$ and $B(r)$ with the constraint that for $r \gg r_Q$, the Schwarzschild solution should be recovered.

This is too difficult a problem for me to handle at this stage, and I will have to learn a few more things before going back to it. For now I will consider only simplified versions of this problem. In Chapter Two of this thesis we will make an ansatz regarding the form of the two functions of $r$, motivated by the results of this subsection. With this simplified form for the line element, the backreaction problem can be handled relatively easily. But for the moment we will take advantage of our previous observation that, for one-loop vacuum polarization effects, $\langle T_{\mu\nu}\rangle$ is proportional to the square of the curvature. The proportionality constant is

expected to be a number of order unity depending somehow on the effective number of quantized fields (see section 1.4a)). For the moment we know nothing about this number, not even its sign. The reason is that it is still uncertain what exactly those quantum fields are. What is needed to gather the information is *the* correct Grand Unified Theory which is not yet singled out. We shall therefore leave this number undetermined, until we go a bit further into this problem in Chapter Two.

So, with all this in mind and recalling from eq. (1.14) that the curvature of a Schwarzschild spacetime goes as $M/r^3$, we make the ansatz of allowing $M$ to become a function of $r$ and of writing the $tt$-component of the vacuum expectation value of the stress-energy tensor schematically as

$$\langle -T^t{}_t \rangle = \frac{3}{4\pi}\, a^2\, \frac{m^2(r)}{r^6}, \tag{1.45}$$

where $a^2$ is our unknown coefficient depending on the effective number of fields, expected to be of order unity. The important point is that the sign of $a^2$ can be either positive or negative ($a$ in itself does not have any meaning, only $a^2$ does). The factor $3/4\pi$ is inserted for convenience. Since $t$ is a spacelike coordinate, $\langle -T^t{}_t \rangle$ is not an energy density but rather a negative pressure, or *tension*, along the axes of the 3-cylinders of constant time $r$ = constant (see section 1.4a)). This is why we write $-T^t{}_t$ instead of $\rho$.

We can now use eq. (1.45) to solve the $tt$-component of eq. (1.44). This is the same thing as solving eq. (1.7):

$$m'(r) = 4\pi r^2 \langle -T^t{}_t \rangle.$$

We easily find that the solution for $m(r)$ is

$$\frac{m(r)}{r^3} = \frac{1}{a^2 + (r/r_Q)^3}, \tag{1.46}$$

where the constant of integration has been identified with $r_Q$. This equation is, of course, our new curvature function taking into consideration the quantum effects. For $r \gg r_Q$, eq. (1.46) reduces to $m(r)/r^3 \simeq (r_Q/r)^3$ which means that $m(r)$ becomes constant and equal to $r_Q^3$. Thus, for $r \gg r_Q$, we recover the Schwarzschild solution.

The behavior of eq. (1.46) for $r \sim r_Q$ depends strongly on the sign of $a^2$. If it is negative, a singularity develops at $r = |a^2|^{1/3} r_Q$. So, if $a^2$ is negative, the physical singularity occurs *sooner* than in the classical solution. However, if $a^2$ is positive, the right hand side of eq. (1.46) goes to the finite limit, for $r \ll r_Q$:

$$\frac{m(r)}{r^3} \to a^{-2}, \tag{1.47}$$

that is, the curvature does not rise above Planckian magnitudes [11]. From this to the conclusion that there is no singularity anymore, is a step that we cannot take. We have to remember that this is just a semiclassical investigation. As we approach the Planck length, those results become invalid. The only conclusion that we can make is that, if the constant $a^2$ is *positive*, or in other words, if the stress induced by vacuum polarization is a tension rather than a pressure; then in the limits of our semiclassical treatment, the curvature does not raise to infinity but stops around the Planckian magnitude. The spacetime is then *self-regulatory*, much in the spirit of Le Châtelier's principle [12] which states that a system responds so as to oppose an

imposed perturbation. This is very encouraging. It can now be seriously suspected that the singularity could be avoided if mother nature were kind enough to provide the right sign for $a^2$! Instead of having an infinite concentration of mass, the black hole would appear to have a nucleus of radius of order $r_Q$ where all its mass would be contained.

Let us now go further in this study of the case where $a^2$ is positive. We however have to remember that it is equally possible that $a^2$ be negative, but since this case is far less interesting than the "positive" one, let us hide it under the carpet for the remaining of the discussion. So, with $a^2$ positive, we want now to use our solution for $m(r)$ to discover the metric in the semiclassical region. We consider the range $a \ll r \ll r_Q$ so eq. (1.46) yields: $m(r) \simeq r^3/a^2$. Eqs. (1.3) and (1.4) give

$$ds^2 = -\left(\frac{2m(r)}{r} - 1\right)^{-1} dr^2 + e^{2\psi(r)} \left(\frac{2m(r)}{r} - 1\right) dt^2 + r^2 d\Omega^2, \qquad (1.48)$$

which reduces to, when applied to our case:

$$ds^2 \simeq -\tfrac{1}{2}a^2 \frac{dr^2}{r^2} + r^2 \left(e^{2\psi(r)}\, d\left(\tfrac{\sqrt{2}}{a}\, t\right)^2 + d\Omega^2\right).$$

We can now rescale our units by making the transformation $t_{NEW} = \sqrt{2}/a\, t_{OLD}$. The last equation then becomes

$$ds^2 \simeq -\tfrac{1}{2}a^2 \frac{dr^2}{r^2} + r^2 \left(e^{2\psi(r)}\, dt^2 + d\Omega^2\right), \qquad a \ll r \ll r_Q. \qquad (1.49)$$

Since $r$ plays the rôle of the time coordinate, and from the form of the line element, it seems a good idea to make this last transformation: $\tau = -\ln r$ (time increases as $r$ decreases), and $z = t$. This finally yields

$$ds^2 \simeq -\tfrac{1}{2}a^2\, d\tau^2 + e^{-2\tau}\left(e^{2\psi(\tau)}\, dz^2 + d\Omega^2\right). \tag{1.50}$$

This line element has a form similar to the cosmological de Sitter solution that we have briefly discussed at the end of section 1.3. The principal feature of this spacetime is the exponentially decreasing "radius" of the 3-cylinders $\tau =$ constant. This suggests the possibility of a "long squeeze picture" replacing the conventional "big crunch picture" of the classical Schwarzschild solution.

We still have an undetermined function $\psi(\tau)$. Eq. (1.8) applied in the range $a \ll r \ll r_Q$ gives

$$\frac{d\psi(r)}{dr} \simeq -\frac{2\pi a^2}{r}\left(\langle T^r{}_r\rangle - \langle T^t{}_t\rangle\right),$$

or, when we use the $\tau$ coordinate

$$\frac{d\psi(\tau)}{d\tau} \simeq -2\pi a^2\left(\langle T^r{}_r\rangle - \langle T^t{}_t\rangle\right); \tag{1.51}$$

so $\psi(\tau)$ can be determined once $\langle T^r{}_r\rangle$ is specified. We shall not go further in this direction.

If we look at the metric when we allow $r$ to approach the neighbourhood of $a$, we find from eq. (1.13) that an inner horizon appears when $r = 2m(r)$, or $\sqrt{2}r \simeq a$. This could yield interesting new features in the geometry, should $a$ be a few

orders of magnitude larger than unity. But if $a$ is smaller than that, this value of $r$ is too close to the Planck length and we are outside the semiclassical limits. Again, we will not go further in this direction.

To conclude this section, and this chapter, let us go back to the semiclassical metric in the form (1.49). We are still assuming that $a^2$ is positive and that we lie in the range $a \ll r \ll r_Q$. The interesting feature that we would like to point out is that *for a value of $r$ much less than the "quantum radius" $r_Q$, $g_{rr}$ is given by a power law*. This simple expression for $g_{rr}$ suggests the study of the backreaction problem from another angle. We could assume *a priori* that both $g_{rr}$ and $g_{tt}$ are given by to-be-determined powers of $r$. It turns out that it is relatively easy to solve the semiclassical equation with such a background, the solutions giving constraints on the power coefficients. So, motivated by the very positive results of this subsection (the discovery of the self-regulatory spacetime), we will attack this problem in the next chapter. We will see that we can add new pieces of information to what we have found so far.

# CHAPTER TWO

# THE POWER-LAW METRIC

## 2.1: Introducing the power-law metric

The last section of Chapter One brought us interesting new information about the structure of a black hole nucleus. It was found that if the stress induced by vacuum polarization effects is a tension, then the spacetime is self-regulatory. By assuming that this was the case, it was then discovered that for $l_P \ll r \ll r_Q$, where $l_P$ is the Planck length and $r_Q$ the radius at which quantum effects become important, the metric element $g_{rr}$ is proportional to $r^{-2}$ (eq. (1.49)). The metric element $g_{tt}$ was left undetermined. It is clear that in order to gather more information, especially on the sign of $a^2$ (eq. (1.45)), the backreaction problem must be attacked from another angle. In this view, we will therefore postulate that, for $r$ much less than the "quantum radius", but much larger that the Planck length, the metric of a spherical black hole can be given by

$$ds^2 = -\frac{dr^2}{(\alpha r)^m} + (\alpha r)^n \, dt'^2 + r^2 d\Omega^2, \tag{2.1}$$

where $m$ and $n$ are two undetermined integers; $t'$ is the ordinary Schwarzschild coordinate (we will use later on a coordinate $t$ *different* from the Schwarzschild coordinate), and $\alpha^{-1}$ is the length scale that tells us that $r$ is small ($\alpha r \ll 1$).

The aim now is to reconsider the backreaction problem starting with the line element (2.1). Solving the semiclassical equation should bring constraints on the powers $m, n$, as well as on $\alpha$. From the results already obtained, we should be able to verify that $m = 2$, and $\alpha^{-1}$ should be identified with $r_Q$. The following sections will be devoted to this calculation. Using previously obtained results from quantum field theory on curved spacetime, we will derive an expression for $\langle T_{\mu\nu} \rangle$ on the background (2.1), and then solve the semiclassical Einstein fields equations. The rest of the chapter will consist of a general study of the line element (2.1) from a purely classical viewpoint. We will consider stability of the solutions for every couple $(m, n)$, as well as the accessibility of the origin $(r = 0)$.

To be able to consider the backreaction problem with our "power-law" background, it is helpful to simplify the form of the line element (2.1). Consider the metric on the 2-spheres $r =$ constant, $t =$ constant, (eq. (1.2)):

$$d\Omega^2 = d\theta^2 + \sin^2\theta \; d\phi^2.$$

If we focus attention around the "North Pole" $\theta = 0$, we can rewrite this equation as

$$d\Omega^2 \simeq d\theta^2 + \theta^2 \; d\phi^2. \tag{2.2}$$

There is no real loss in generality in doing this, since, from spherical symmetry, we can choose the origin of the $\theta$ coordinate wherever we want. We can therefore cover the entire 2-sphere with small coordinate patches such that, for each patch, $\theta$ is always small enough to verify $\sin\theta \simeq \theta$. The result is that we can focus attention on one of these patches, knowing that the situation will be the same for everyone of them; what really matters being the $r$ dependence. We can now look at eq. (2.2)

with new eyes: $\theta$ can be viewed as a (bounded) radial coordinate and we can define the new coordinates

$$x' = \theta \cos\phi, \qquad y' = \theta \sin\phi. \tag{2.3}$$

Eq. (2.2) then becomes

$$d\Omega^2 \simeq dx'^2 + dy'^2, \tag{2.4}$$

the flat metric. This demonstration is just the mathematical way of saying that, for small distances, the surface of a sphere appears to be flat. With this simplification, eq. (2.1) becomes

$$ds^2 = -\frac{dr^2}{(\alpha r)^m} + (\alpha r)^n \, dt'^2 + r^2(dx'^2 + dy'^2).$$

Since $r$ represents a timelike coordinate, it appears to be a good idea to make the coordinate transformation

$$t = \left| \int \frac{dr}{(\alpha r)^{m/2}} \right|, \qquad z = t', \tag{2.5}$$

yielding

$$ds^2 = -dt^2 + [\alpha r(t)]^n \, dz^2 + [r(t)]^2 \, (dx'^2 + dy'^2). \tag{2.6}$$

In order to integrate eq. (2.5), let us first consider the case where $m \neq 2$. We get $\beta t = (\alpha r)^{1-m/2}$, where $\beta \equiv |1 - m/2|\alpha$. If we define:

$$x \equiv \frac{x'}{\alpha}, \qquad y \equiv \frac{y'}{\alpha}, \tag{2.7}$$

it is easy to verify that eq. (2.6) becomes

$$ds^2 = -dt^2 + (\beta t)^{2p}(dx^2 + dy^2) + (\beta t)^{2q} dz^2, \qquad m \neq 2, \tag{2.8}$$

where $p \equiv 2/(2-m)$ and $q \equiv n/(2-m)$. Consider now the case where $m = 2$. Eq. (2.5) yields $\alpha r = e^{-\alpha t}$ so eq. (2.6) becomes

$$ds^2 = -dt^2 + e^{-2\alpha t}(dx^2 + dy^2) + e^{-n\alpha t}dz^2, \qquad m = 2. \tag{2.9}$$

To summarize the results, we can write the line elements (2.8) and (2.9) as

$$ds^2 = -dt^2 + A^2(t)(dx^2 + dy^2) + B^2(t)\, dz^2, \tag{2.10}$$

where

$$A^2(t) = \begin{cases} (\beta t)^{2p} & m \neq 2 \\ e^{-2\alpha t} & m = 2, \end{cases} \tag{2.11}$$

$$B^2(t) = \begin{cases} (\beta t)^{2q} & m \neq 2 \\ e^{-n\alpha t} & m = 2, \end{cases} \tag{2.12}$$

and

$$p = \frac{2}{2-m}, \qquad q = \frac{n}{2-m}, \qquad \beta = \left|1 - \frac{m}{2}\right| \alpha. \tag{2.13}$$

It has to be noted that for $m \geq 2$, $t \to \infty$ when $r \to 0$, whereas for $m < 2$, $t \to 0$ as $r \to 0$.

The line element (2.10) represents an *homogeneous, anisotropic cosmological solution* where the $z$ direction behaves differently from the $x$ and $y$ directions. Since we have a diagonal form for the metric tensor, we recognize in eq. (2.10) a special case of a Bianchi Type I cosmological solution [31]. This type of solution is obtained when one is interested in a non isotropic universe (for example, to study

the evolution of the departures from isotropy as the universe expands). If $n = 2$, then $A^2(t) = B^2(t)$ and eq. (2.10) reduces to

$$ds^2 = -dt^2 + A^2(t)(dx^2 + dy^2 + dz^2), \qquad n = 2. \tag{2.14}$$

This is the well-known Friedmann-Robertson-Walker solution describing a homogeneous, isotropic and spatially flat universe [32]. The case where $n = 2$ therefore represents an isotropic matter distribution inside the black hole.

This transformation from a black hole interior solution, eq. (2.1), to a cosmological solution, eq. (2.10) is very important because it simplifies our problem tremendously. The reason is that quantum field theory in a cosmological background has been extensively studied [33]. The case $n = 2$ is particularly simple because not only the line element (2.14) has flat hypersurfaces of constant time, but it is also *conformally flat* [34]. This means there exists a function $\Omega$ called the *conformal factor* (and not related to the 2-sphere line element) such that our metric tensor can be written as $g_{\mu\nu} = \Omega^2 \eta_{\mu\nu}$ where $\eta_{\mu\nu}$ is the Minkowski metric tensor of flat spacetime. To see this, define the new time coordinate $\eta$ (not related to the Minkowski metric!) as:

$$\eta = \left| \int \frac{dt}{A(t)} \right|. \tag{2.15}$$

Then rewrite eq. (2.14) in terms of this new coordinate:

$$ds^2 = A^2(\eta)(-d\eta^2 + dx^2 + dy^2 + dz^2), \qquad n = 2. \tag{2.16}$$

It becomes clear that the flat Friedmann-Robertson-Walker line element is conformally flat, and that the conformal factor is $A(\eta)$.

Before we can finally explain why the case $n = 2$ is so simple, we need to expand on the topic of conformal transformations [34]. A *conformal transformation* is defined in general as a transformation that maps a metric $g_{\mu\nu}$ into another metric $\tilde{g}_{\mu\nu}$ via $\tilde{g}_{\mu\nu} = \Omega^2 g_{\mu\nu}$ where $\Omega$ is a smooth function of the spacetime. This transformation is equivalent to rescaling the units of measure at every point of the spacetime. Now, a field $\Psi$, solution of its field equation in the metric $g_{\mu\nu}$, is said to be *conformally invariant* if there exists a number $s$ such that $\tilde{\Psi} \equiv \Omega^s \Psi$ is a solution of the field equation in the metric $\tilde{g}_{\mu\nu}$. For example, it can be shown that the electromagnetic field is conformally invariant. The massless scalar field is originally not conformally invariant, but it is possible to modify its wave equation (by adding a term $R\Psi$, where $R$ is the curvature scalar) such that it becomes so. For more information on conformal transformations, see ref. [34].

In quantum field theory on curved spacetime, when one has a conformally invariant field evolving in a conformally flat spacetime, one has the *conformally trivial situation*. The expectation value of the stress-energy tensor becomes easy to calculate since the evaluation of its trace only will give all the different elements [35]. It is then sufficient to calculate the expectation value of the trace of the stress-energy tensor, which is easier than calculating all the components.

This is why the case $n = 2$ is so important: we have a conformally trivial situation. This allows us to quantize *conformally invariant fields of all spins* at once since the expressions for the trace of the stress-energy tensor differ only in the values of a few coefficients called *the coefficients of the trace anomaly* [35]. We will consider this case first in the following section.

## 2.2: Solving the semiclassical equation

[Warning: in this section, we will use Planck units, as well as the timelike convention $(+---)$ for the metric. The field equations will be written $G_{\mu\nu} = -8\pi T_{\mu\nu}$ (opposite sign convention for the curvature tensor).]

We will consider here the backreaction problem for the line element (2.10). First for the isotropic, $n = 2$ case, and then for the general case, we will find the expression for the expectation value of the stress-energy tensor (for all conformally invariant fields in the isotropic case, for conformally invariant scalar fields in the general case). Using this expression as the right hand side of the Einstein field equation, we will find constraints on the values of the powers $(m, n)$, as well as on the scaling factor $\alpha$.

*a) Isotropic case (conformally invariant fields).*

We consider the line element (2.10)–(2.13) in the case where $n = 2$. This corresponds to an isotropic distribution of matter. Eqs. (2.14), (2.11) and (2.13) give the complete expression for this line element, but it is more convenient to work with the conformally flat form (2.15) and (2.16), which we rewrite as

$$ds^2 = C(\eta)(d\eta^2 - dx^2 - dy^2 - dz^2), \tag{2.17}$$

with $C(\eta) \equiv A^2(\eta)$. It will also be useful to introduce a new function $D(\eta)$ defined by

$$D(\eta) = \frac{C'(\eta)}{C(\eta)}, \tag{2.18}$$

where the prime denotes a differentiation with respect to $\eta$.

— To proceed further, we will have to separate the calculations into three different cases. We know from the last section that we already have to separate the value $m = 2$ from all the other values of $m$. A look at eqs. (2.11) and (2.15) then tells us that we also have to separate the value $p = 1$, or $m = 0$, from all the other values of $p$, or $m$. The three cases are therefore the following: first of all we will consider the case $m \neq 2,\ m \neq 0$; then the case $m = 0$, and finally the case $m = 2$. Table 2.1 summarizes the results.

So assume for the moment that $m \neq 2,\ m \neq 0$. Eq. (2.11) gives the expression for $A(t)$ that we can substitute in eq. (2.15) to give

$$\eta = \left| \int \frac{dt}{(\beta t)^p} \right|,$$

which yields, after integration

$$\gamma\eta = (\beta t)^{1-p}, \tag{2.19}$$

where $\gamma \equiv |1 - p|\ \beta$. The assumption that $m \neq 0$ was necessary to avoid the case where $p = 1$. Substituting eq. (2.19) into eq. (2.11) yields

$$C(\eta) \equiv A^2(\eta) = (\gamma\eta)^l, \tag{2.20}$$

where

$$l \equiv \frac{2p}{1-p} = -\frac{4}{m}, \tag{2.21}$$

and where we have used eq. (2.13). After substituting eq. (2.20) into eq. (2.18), we easily find

$$D(\eta) = l\eta^{-1}. \tag{2.22}$$

We are now ready to examine the stress-energy tensor. Birrell & Davies [36] derive an explicit form for $\langle T_{\mu\nu} \rangle$ valid for all conformally invariant fields (see section 2.1). It is given by

$$\langle T^{\mu}_{\ \nu} \rangle = -\frac{1}{16\pi^2} \left( \frac{\tilde{\alpha}}{9} \, {}^{(1)}H^{\mu}_{\ \nu} + 2\tilde{\beta} \, {}^{(3)}H^{\mu}_{\ \nu} \right), \tag{2.23}$$

where $\tilde{\alpha}$ and $\tilde{\beta}$ are the coefficients of the trace anomaly, their values depend on the type of field (see previous section); ${}^{(1)}H^{\mu}_{\ \nu}$ and ${}^{(3)}H^{\mu}_{\ \nu}$ are two tensors depending on the square of the curvature, as well as on the derivatives of the curvature. For the line element (2.17), they have the form

$$\begin{aligned}
{}^{(1)}H^{0}_{\ 0} &= 9C^{-2}(-D''D + \tfrac{1}{2}D'^2 + \tfrac{3}{8}D^4) \\
{}^{(1)}H^{1}_{\ 1} &= -3C^{-2}(2D''' - D''D + \tfrac{1}{2}D'^2 - 3D'D^2 + \tfrac{3}{8}D^4) \\
{}^{(3)}H^{0}_{\ 0} &= \tfrac{3}{16}C^{-2}D^4 \\
{}^{(3)}H^{1}_{\ 1} &= -\tfrac{1}{2}C^{-2}(-D'D^2 + \tfrac{1}{8}D^4).
\end{aligned} \tag{2.24}$$

Isotropy guarantees that ${}^{(1)}H^{1}_{\ 1} = {}^{(1)}H^{2}_{\ 2} = {}^{(1)}H^{3}_{\ 3}$, the same relation holding for ${}^{(3)}H^{\mu}_{\ \nu}$. Eq. (2.24) is easily evaluated with the help of eqs. (2.20) and (2.22). We find that all the elements of the $H$ tensors have the same $\eta$ dependence:

$${}^{(.)}H^{\cdot}_{\ \cdot} = \mathcal{O}\left[(\gamma\eta)^{-2l}\eta^{-4}\right],$$

or, if we translate back to the $t$ coordinate, using eq. (2.19):

$${}^{(.)}H^{\cdot}_{\ \cdot} = \mathcal{O}(t^{-4}). \tag{2.25}$$

(We will see a bit later that it is not necessary to go further into the details of the calculations.) Eq. (2.25) can now be substituted into eq. (2.23) to yield

$$\langle T^{\mu}_{\ \nu} \rangle = \mathcal{O}(t^{-4}), \qquad m \neq 2,\ m \neq 0. \tag{2.26}$$

To use this result in the semiclassical equation, we still have to evaluate the Einstein tensor for the line element (2.17). Again. we can copy the results directly from Birrell & Davies [37] (or any other textbook of general relativity, but watch out for the sign conventions!). The Ricci tensor elements are

$$\begin{aligned} R^{0}_{\ 0} &= \tfrac{3}{2} C^{-1} D' \\ R^{1}_{\ 1} &= \tfrac{1}{2} C^{-1} (D' + D^2), \end{aligned} \tag{2.27}$$

with $R^{1}_{\ 1} = R^{2}_{\ 2} = R^{3}_{\ 3}$. This yields for the Ricci scalar:

$$R = 3C^{-1}(D' + \tfrac{1}{2} D^2). \tag{2.28}$$

The Einstein tensor is then given by $G^{\mu}_{\ \nu} = R^{\mu}_{\ \nu} - 1/2\ \delta^{\mu}_{\ \nu} R$, or, more explicitly:

$$\begin{aligned} G^{0}_{\ 0} &= \tfrac{3}{2} C^{-1} D' - \tfrac{3}{2} C^{-1} (D' + \tfrac{1}{2} D^2) \\ G^{1}_{\ 1} &= \tfrac{1}{2} C{-}1 (D' + D^2) - \tfrac{3}{2} C^{-1} (D' + \tfrac{1}{2} D^2). \end{aligned} \tag{2.29}$$

Eq. (2.29) can then be evaluated, using once again eqs. (2.20) and (2.22). It follows that all the $G^{\mu}_{\ \nu}$ have the same $t$ dependence:

$$G^{\mu}_{\ \nu} = \mathcal{O}(t^{-2}), \qquad m \neq 2,\ m \neq 0. \tag{2.30}$$

We see now why the details of the calculations can be omitted: the $t$ dependence of $\langle T^{\mu}_{\ \nu} \rangle$ and $G^{\mu}_{\ \nu}$ are not the same. This means that the semiclassical

equation $G^{\mu}_{\ \nu} = -8\pi\langle T^{\mu}_{\ \nu}\rangle$ cannot be solved, since we want a solution valid at all times, not only at a single, particular value of $t$. The conclusion is that all the cases where $m \neq 2$, $m \neq 0$ have to be excluded. That limits our choice quite a lot!

Let us now consider the case $m = 0$. We will in fact repeat the same analysis as before: eqs. (2.11) and (2.13) now give $A(t) = \beta t$, so eq. (2.15) yields

$$\beta\eta = \ln \beta t. \tag{2.31}$$

After having used this in eq. (2.20), we find that the conformal factor $C(\eta)$ is now given by

$$C(\eta) = e^{2\beta\eta}, \tag{2.32}$$

yielding for $D(\eta)$:

$$D(\eta) = 2\beta. \tag{2.33}$$

We can go like that exactly like we did previously, using the eqs. (2.23), (2.24) and (2.29). The results are

$$\langle T^{\mu}_{\ \nu}\rangle = \mathcal{O}(t^{-4}), \qquad m = 0, \tag{2.34}$$

$$G^{\mu}_{\ \nu} = \mathcal{O}(t^{-2}), \qquad m = 0, \tag{2.35}$$

as before. So the case $m = 0$ too has to be excluded.

The only remaining case is $m = 2$, the result we wanted to recover in the first place! Let us consider this case now. Going back to eq. (2.11), we find that

now $A(t) = e^{-\alpha t}$. Eq. (2.15) yields $\alpha\eta = e^{-\alpha t}$ so we get $C(\eta) = (\alpha\eta)^{-2}$, and $D(\eta) = -2\eta^{-1}$. Substituting these results in eq. (2.24) yields

$$\begin{aligned} {}^{(1)}H^0{}_0 &= 0 \\ {}^{(1)}H^1{}_1 &= 0 \\ {}^{(3)}H^0{}_0 &= 3\alpha^4 \\ {}^{(3)}H^1{}_1 &= 3\alpha^4. \end{aligned} \tag{2.36}$$

Inserting eq. (2.36) into eq. (2.23) gives

$$\langle T^0{}_0 \rangle = \langle T^1{}_1 \rangle = -\frac{3}{8\pi^2}\,\tilde{\beta}\,\alpha^4, \qquad m = 2. \tag{2.37}$$

The fact that we now have constant values for $\langle T^\mu{}_\nu \rangle$ will allow us to finally solve the semiclassical equation. The elements of the Einstein tensor can also be calculated from eq. (2.29) and we get

$$G^0{}_0 = G^1{}_1 = -3\alpha^2, \qquad m = 2. \tag{2.38}$$

The semiclassical Einstein field equations

$$G^\mu{}_\nu = -8\pi \langle T^\mu{}_\nu \rangle \tag{2.39}$$

are then easy to solve. They give constraints on the value of $\alpha$ when a value for $\tilde{\beta}$ is specified:

$$\alpha^{-1} = \sqrt{\frac{-\tilde{\beta}}{\pi}}. \tag{2.40}$$

What is $\tilde{\beta}$ ? Again, Birrell & Davies provide the answer [38]. For spin-0 conformally invariant fields, $360\tilde{\beta} = -1$; for spin-1/2, $360\tilde{\beta} = -11/2$; and for spin-1, $360\tilde{\beta} = -60$. The general expression for $\tilde{\beta}$ is therefore

$$360\tilde{\beta} = -N_0 - \tfrac{11}{2}N_{1/2} - 60N_1, \tag{2.41}$$

where $N_0$ is the number of scalar fields, and so on. So $\alpha^{-1}$ can be evaluated once the *effective number of fields* $\tilde{\beta}$ (see section 1.4a)) is specified. This piece of information is unfortunately still missing, and will come once the good Grand Unified Theory is singled out. Nevertheless, it is a relief to discover that the value of $\tilde{\beta}$ is necessarily negative. This means, from eq. (2.40) that $\alpha^{-1}$ is real, corresponding to a positive $a^2$, in the language of the last chapter. It has to be remembered that eq. (2.40) is valid only for $n = 2$ (isotropic material), and for conformally invariant fields. We are still far from a complete description of the quantum effects at the black hole centre!

It is interesting to note that eq. (2.37) is the description of a false vacuum $\rho = -P =$ constant, which yields the de Sitter solution of section 1.3 and of eq. (1.28). In return, if we take the limit of line element (1.28) for $r \ll r_0$, we recover line element (2.1) with $(m, n) = (2, 2)$. The González-Díaz model bounces back! But this time, only a small region of the black hole interior is filled with false vacuum.

Summarizing, when we investigate the case $n = 2$, keeping $m$ undetermined, the value $m = 2$ gets to be singled out naturally in solving the semiclassical equation for conformally invariant fields. The solution for $(m, n) = (2, 2)$ is the de Sitter

solution with material in a false vacuum state. The quantum radius $\alpha^{-1}$ can be evaluated once the effective number of fields $\tilde{\beta}$ is specified. These results are in agreement with the analysis of section 1.4c). Our assumption that $n = 2$ would correspond to the assumption that $\psi(\tau) = 0$ in eq. (1.50).

In the next subsection, we will consider the general problem where $n$ is left undetermined. Since we no longer have the conformally trivial situation (the line element (2.10) is not conformally flat), we shall restrict ourselves to the backreaction problem involving only conformally invariant scalar fields.

*b) General case (conformally invariant scalar fields).*

We will now consider the backreaction problem for the line element (2.10)–(2.13), keeping both $m$ and $n$ undetermined. The calculations will involve only conformally invariant scalar fields and will provide a unique value for $m$. As in the last subsection, we will find that $m$ has to be equal to 2. We will also find that $n$ must lie in the range $0 \leq n \leq 6$ in order for $\alpha$ to be real. Unfortunately, to calculate all the elements of $\langle T_{\mu\nu} \rangle$ is a very complicated task, and only expressions for its trace can be found in the literature [39]. So, to simplify the problem a bit further, we will solve not the full semiclassical equation itself, but its *trace*: $G^{\mu}{}_{\mu} = R^{\mu}{}_{\mu} - 1/2\, \delta^{\mu}{}_{\mu} R = -R = -8\pi \langle T^{\mu}{}_{\mu} \rangle$, or

$$R = 8\pi \langle T \rangle, \tag{2.42}$$

where $\langle T \rangle \equiv \langle T^{\mu}{}_{\mu} \rangle$. This does not bring as much information, but we shall see what it can reveal anyway.

To derive an expression for $\langle T \rangle$, we will follow closely the paper written by Hu quoted in ref. [39]. All the hard work is done in this paper, we will merely copy the results. The first step is to define a variable $\eta$, similar to that of the previous subsection, for the line element (2.1) that we rewrite in the form

$$ds^2 = dt^2 - b_1{}^2(t)\,(dx^2 + dy^2) - b_3{}^2(t)\,dz^2, \tag{2.43}$$

with $b_1(t) \equiv A(t)$ and $b_3(t) \equiv B(t)$. To do so we introduce the function $b(t)$ defined as

$$b(t) \equiv \left[b_1{}^2(t) b_3(t)\right]^{1/3}, \tag{2.44}$$

and define our new time variable by

$$\eta \equiv \left| \int \frac{dt}{b(t)} \right|. \tag{2.45}$$

By substituting the two last equations into eq. (2.43), we get

$$ds^2 = b^2(\eta)\,d\eta^2 - b_1{}^2(\eta)\,(dx^2 + dy^2) - b_3{}^2(\eta)\,dz^2, \tag{2.46}$$

It is now necessary to introduce a collection of new functions of $\eta$ that will lighten the expressions of $R$ and $\langle T \rangle$. So let

$$d_1 \equiv \frac{b_1'}{b_1}, \qquad d_3 \equiv \frac{b_3'}{b_3},$$

and:

$$\begin{aligned} D &\equiv \tfrac{2}{3} d_1 + \tfrac{1}{3} d_3, \\ Q &\equiv \tfrac{1}{9}(d_1 - d_3)^2, \\ S &\equiv \tfrac{1}{9}(d_1 - D)(d_1 - d_3)^2, \\ U &\equiv \tfrac{1}{9}(d_1' - d_3')^2, \end{aligned} \tag{2.47}$$

where a prime denotes a differentiation with respect to $\eta$. There is an apparent difference between those equations and the ones found in Hu's paper. The reason is that Hu discusses the more general situation where the line element is written as

$$ds^2 = dt^2 - \sum_{i=1}^{3} b_i{}^2(t)\,(dx^i)^2,$$

whereas we deal with the special case $b_1 = b_2$. So eqs. (2.44) and (2.47) are written in the more general form in Hu's paper.

With the functions defined in eq. (2.47), the curvature scalar for the line element (2.46) takes the form

$$R = 6\,b^{-2}\,(D' + D^2 + Q), \tag{2.48}$$

and the expectation value of the trace of the stress-energy tensor is

$$\begin{aligned}\langle T\rangle = \frac{1}{480\pi^2 b^4}\;&(D''' - 4D'D^2 - 4DQ' - 4QD' \\ &+Q'' - 12Q^2 - 3U + \tfrac{8}{3}S')\,.\end{aligned} \tag{2.49}$$

In the case where $b_1 = b_3$ (or $n = 2$), we get from eq. (2.47) that $Q = S = U = 0$. It is then easy to verify that the eqs. (2.48) and (2.49) agree with the similar equations of the last subsection, when applied to scalar fields.

The procedure to obtain explicit expressions for $\langle T\rangle$ and $R$ and to solve the semiclassical equation (2.42) is now quite straightforward. Eqs. (2.11) and (2.12) give us $b_1$ and $b_3$ as functions of $t$. With the help of eq. (2.44), we can integrate eq. (2.45) to find the new time variable $\eta$. Then $b_1$ and $b_3$, now functions of $\eta$ can

be inserted in eq. (2.47) and finally eqs. (2.48) and (2.49) can be evaluated. In order to integrate eq. (2.45) for $\eta$, we will have to separate the calculations in a few cases, just like we did in the previous subsection. So, even if the procedure is simple, the rest of this subsection will not be very appealing! The cases are listed in Table 2.2, where a summary of the results of this subsection is also given. The only case where we can actually solve the semiclassical equation is when $m = 2$. We begin to discuss this case in the paragraph starting above eq. (2.57).

Consider first the case $m \neq 2$, $n + 3m \neq 2$. Eqs. (2.11) and (2.12) give $b_1 = (\beta t)^p$, $b_3 = (\beta t)^q$, where $\beta$, $p$ and $q$ are defined in eq. (2.13). Eq. (2.44) yields $b = (\beta t)^{(2p+q)/3}$ and we obtain from eq. (2.45) the relation between $\eta$ and $t$:

$$\gamma\eta = (\beta t)^{(3-2p-q)/3}, \tag{2.50}$$

where $\gamma \equiv |(3-2p-q)/3|\ \beta$. The assumption that $n+3m \neq 2$ protects us from the possibility that the exponent in eq. (2.50) is equal to zero. We have now to express $b_1, b_3$ and $b$ as functions of $\eta$. It is easy to show that the are given by

$$\begin{aligned} b_1(\eta) &= (\gamma\eta)^\kappa, \\ b_3(\eta) &= (\gamma\eta)^\lambda, \\ b(\eta) &= (\gamma\eta)^{(2\kappa+\lambda)/3}, \end{aligned} \tag{2.51}$$

with

$$\kappa \equiv \frac{3p}{3-2p-q}, \qquad \lambda \equiv \frac{3q}{3-2p-q}. \tag{2.52}$$

With these results, we can write down the functions (2.47) explicitly. First we have $d_1 = \kappa\eta^{-1}$ and $d_3 = \lambda\eta^{-1}$; and then:

$$\begin{aligned} D &= \tfrac{1}{3}(2\kappa + \lambda)\eta^{-1}, \\ Q &= \tfrac{1}{9}(\kappa - \lambda)^2\eta^{-2}, \\ S &= \tfrac{1}{27}(\kappa - \lambda)^3\eta^{-3}, \\ U &= \tfrac{1}{9}(\kappa - \lambda)^2\eta^{-4}. \end{aligned} \tag{2.53}$$

Eq. (2.53) can finally be substituted into eqs. (2.48) and (2.49) to yield

$$\begin{aligned} R &= \mathcal{O}\left[(\gamma\eta)^{-2(2\kappa+\lambda)/3}\eta^{-2}\right], \\ \langle T\rangle &= \mathcal{O}\left[(\gamma\eta)^{-4(2\kappa+\lambda)/3}\eta^{-4}\right]; \end{aligned}$$

or, when we go back to the $t$ coordinate:

$$\left.\begin{aligned} R &= \mathcal{O}(t^{-2}) \\ \langle T\rangle &= \mathcal{O}(t^{-4}) \end{aligned}\right\} \qquad m \neq 2,\ n + 3m \neq 2. \tag{2.54}$$

This shows, like we found in the previous subsection, that the semiclassical equation cannot be solved, and that we have to rule out this case. We have therefore narrowed down our choices for $m$ and $n$, and we have now to repeat the above analysis for the remaining cases.

This paragraph will then be devoted to the case $m \neq 2, n + 3m = 2$. The expressions for $b_1$ and $b_3$ are the same as above, but $b$ is now simply given by $b = \beta t$.

The integration of eq. (2.45) then gives $\beta\eta = \ln \beta t$, yielding $b_1 = e^{p\beta\eta}$, $b_3 = e^{q\beta\eta}$ and $b = e^{\beta\eta}$. Using these results to evaluate eq. (2.47) gives $d_1 = p\beta$, $d_3 = q\beta$, and:

$$\begin{aligned} D &= \beta, \\ Q &= (p-1)^2\beta^2, \\ S &= (p-1)^3\beta^3, \\ U &= 0. \end{aligned} \tag{2.55}$$

We finally obtain the expressions for $R$ and $\langle T \rangle$ by inserting eq. (2.55) in eqs. (2.48) and (2.49):

$$\left.\begin{aligned} R &= \mathcal{O}(t^{-2}) \\ \langle T \rangle &= \mathcal{O}(t^{-4}) \end{aligned}\right\} \qquad m \neq 2,\ n + 3m = 2. \tag{2.56}$$

So here too, we cannot solve the semiclassical equation and we have to abandon this case as well. But there is a subtle point that we have to discuss. If $p = 1$, or equivalently from eq. (2.13), $m = 0$, which then corresponds to $n = 2$ since $n + 3m = 2$; it is easy to see from eqs. (2.55), (2.48) and (2.49) that $\langle T \rangle = 0$ while $R = 6t^{-2}$. This is a bit different than what eq. (2.56) tells us. But this does not change the fact that we cannot solve the semiclassical equation so the case $p = 1$ is no more special. In fact, the case $m = 0, n = 2$ has already been studied in the last subsection: it was rejected there too. It is interesting to note that the detailed version of eq. (2.34) shows that the elements of the stress-energy tensor are not zero, but are related by $\langle T^0_{\ 0} \rangle = -3\langle T^1_{\ 1} \rangle$ which yields a vanishing trace.

We can now look at the case $m = 2$ which should be more interesting than those we have examined so far! For $m = 2$, eqs. (2.11) and (2.12) give $b_1 = e^{-\alpha t}$

and $b_3 = e^{-n\alpha t/2}$. With this we find that $b = e^{-(4+n)\alpha t/6}$ so we need to consider separately the cases $n \neq -4$ and $n = -4$. Let us begin with the case $n \neq -4$. Eq. (2.45) can be integrated to yield $|\bar{\gamma}|\eta = e^{\bar{\gamma}t}$ where $\bar{\gamma} \equiv (4+n)\alpha/6$. The metric elements then become

$$\begin{aligned} b_1(\eta) &= (|\bar{\gamma}|\eta)^{-6/(4+n)}, \\ b_3(\eta) &= (|\bar{\gamma}|\eta)^{-3n/(4+n)}, \\ b(\eta) &= (|\bar{\gamma}|)^{-1}. \end{aligned} \tag{2.57}$$

Substituting eq. (2.57) into eq. (2.47) yields

$$d_1 = \frac{6}{4+n}\,\eta^{-1}, \qquad d_3 = -\frac{3n}{4+n}\,\eta^{-1},$$

and:

$$\begin{aligned} D &= -\eta^{-1}, \\ Q &= \left(\frac{2-n}{4+n}\right)^2 \eta^{-2}, \\ S &= -\left(\frac{2-n}{4+n}\right)^3 \eta^{-3}, \\ U &= \left(\frac{2-n}{4+n}\right)^2 \eta^{-4}. \end{aligned} \tag{2.58}$$

This yields, when inserted in eqs. (2.48) and (2.49), the following expressions for $R$ and $\langle T \rangle$:

$$\left.\begin{aligned} R &= 12\left[\tfrac{1}{6}(4+n)\right]^2\left(1+\tfrac{1}{2}N^2\right)\,\alpha^2 \\ \langle T\rangle &= \frac{\left[\frac{1}{6}(4+n)\right]^4}{240\pi^2}\,\left(1-\tfrac{5}{2}N^2+4N^3-6N^4\right)\,\alpha^4 \end{aligned}\right\} \quad m=2,\ n\neq -4, \tag{2.59}$$

where

$$N \equiv \frac{2-n}{4+n}. \tag{2.60}$$

Once again we find constant values for those two quantities when $m = 2$. This allows us to solve the semiclassical equation. We find a relation between the value of $\alpha$ and $n$ given by

$$\alpha^{-1} = \sqrt{\frac{\Gamma(n)}{810\pi}}, \qquad m = 2,\ n \neq -4, \tag{2.61}$$

where

$$\Gamma(n) \equiv \frac{(4+n)^2}{1+\frac{1}{2}N^2}\ \left(1 - \tfrac{5}{2}N^2 + 4N^3 - 6N^4\right). \tag{2.62}$$

Before we discuss this result, let us first consider the last case (finally!): the case where $m = 2, n = -4$. For those values of $m$ and $n$ we find that $b_1 = e^{-\alpha t}, b_3 = e^{2\alpha t}$ and $b = 1$. This yields that $\eta$ is simply equal to $t$. So we have $d_1 = -\alpha$, $d_3 = 2\alpha$, which give $D = 0$. We also find $Q = \alpha^2$, $S = -\alpha^3$ and $U = 0$. Using those results in eqs. (2.48) and (2.49) yields

$$\left.\begin{aligned} R &= 6\alpha^2 \\ \langle T \rangle &= -\frac{\alpha^4}{40\pi^2} \end{aligned}\right\} \qquad m = 2,\ n = -4. \tag{2.63}$$

The semiclassical equation then gives the following expression for $\alpha$:

$$\alpha^2 = -30\pi, \qquad m = 2,\ n = -4, \tag{2.64}$$

corresponding to an imaginary $\alpha$.

We have just found an imaginary value for $\alpha^{-1}$. Inspection of eqs. (2.61) and (2.62) reveals that there too, imaginary values can arise. What is the meaning of this? If we go back to our original line element, eq. (2.1), it is clear that an imaginary value for $\alpha^{-1}$ is unacceptable since it represents a scaling factor. So the conclusion would be that we have to reject all values of $n$ for which $\alpha^{-1}$ is found to be imaginary. Unfortunately, this is not the correct interpretation. To find the reason why, we must go further back to section 1.4c). In deriving eq. (1.49), which is the motivation behind the power-law metric of this chapter, we explicitly assumed that $a^2$ was positive. So the assumption that $a$ is real is directly reflected here by our understanding that $\alpha^{-1}$ is a scaling factor. So the rejection of imaginary values for $\alpha^{-1}$ would correspond to the rejection of negative values of $a^2$. This is a step that we cannot take. Eqs. (2.61), (2.62) and (2.64) cannot therefore be viewed as constraints on the values of $n$. But they can be seen as a valuable piece of information telling which values of $n$ lead to a self-regulatory spacetime, with constant curvature, near the center of the black hole. The "true" value of $n$ would then have to come from a more detailed analysis, as discussed at the beginning of section 1.4c).

So what are those values of $n$ which give real values for $\alpha^{-1}$? Fig. 2.1 shows the graph of $\Gamma(n)$, drawn with the help of eq. (2.62). We find that the only values of $n$ for which $\Gamma(n)$ is positive, making $\alpha^{-1}$ real, lie in the range

$$0 \leq n \leq 6. \tag{2.65}$$

But this does not give the complete picture. Eq. (2.65) would be valid only if the only contribution to vacuum polarization would come from scalar fields. We know

from eq. (2.40) that $\alpha^{-1}$ also depends on the effective number of fields. In fact, it is easy to verify that if one puts $\tilde{\beta} = -1/360$ in eq. (2.40) and $n = 2$ in eq. (2.61), the results are the same. The point is that a complete expression for $\alpha^{-1}$ would involve a function of the effective number of fields ***and*** a function of $n$. It is therefore possible that the range (2.65) should be modified. However, what is remarkable is the fact that $m = 2$ is singled out without any doubt. This is important because the line element (2.1) with $m = 2$ leads to constant curvature. This means that the self-regulatory spacetime comes out quite naturally, if the sign of $\alpha^{-2}$, or $a^2$, is positive. On this issue, unfortunately, we will have to wait to know better.

In conclusion we can say that the analysis of this section agrees very well with the simpler (and more direct) one of section 1.4. The crucial point is of course the nature of the stress induced by vacuum polarization. Should it be a tension (positive $\alpha^{-2}$ or $a^2$), then the spacetime is self-regulatory. Should it be a pressure (negative $\alpha^{-2}$ or $a^2$), then things get even worse than in the classical description, a singularity developing *before* $r = 0$. A good sign comes from eqs. (2.40) and (2.41) which show that, when the matter distribution near the black hole centre is *isotropic*, $\alpha^{-2}$ is definitely positive. After all, isotropy seems like a pretty reasonable requirement. An $n$ much different from 2 would means large departure from isotropy, which aesthetically speaking, is not what we would expect. So I consider that this study of the quantum effects near the centre of a black hole shows that it is *likely*, but far from *certain*, that spacetime is self-regulatory there, the infinite rise of the curvature being stopped by vacuum polarization effects caused by the presence of the quantized fields.

This concludes the discussion on the quantum effects near the centre of a spherically symmetric black hole. What follows in this chapter is a study of other aspects of the line element (2.1).

## 2.3: Stability of the power-law geometries

In this section we continue our study of the power-law metric of section 2.1. We will consider here the *stability* of the different geometries corresponding to the different pairs $(m, n)$. In particular, we will be interested in the stability of the geometries (2.1) in the region $\alpha r \ll 1$, where this metric is expected to be valid. The stability of a geometry can be characterized loosely by the property that small perturbations propagating in the background geometry always remain small, if the geometry is stable. That is, perturbations do not become so large that they could modify the geometry itself. As an example, consider the propagation of some perturbation, say a gravitational wave, in a flat spacetime. It is clear that if the perturbation carries energy and momentum, the originally flat spacetime will have to curve to respond to the presence of this energy. The perturbation then appears as ripples on the flat background. So, even if the perturbation can be said to be small in some sense, it still has a non negligible effect on the background spacetime. With this meaning understood, the background spacetime (the flat spacetime in our example) would be *unstable* if its response to a small perturbation is large.

Consider another example: the propagation of perturbations inside a Schwarzschild black hole (described by the classical solution, without the quantum effects). Suppose that the curvature superposed on the Schwarzschild background and induced by the perturbation rises to infinity as $r$ goes to zero. What is the effect on the background geometry? Since the Schwarzschild curvature *also* goes to infinity, as $M/r^3$, we need to know *how fast* the perturbation curvature blows up. If it behaves, say, like $r^{-2}$, it will be negligible compared to the background curvature

and the Schwarzschild geometry would be said to be stable against this type of perturbation. But if instead we find that the perturbation curvature behaves like, say, $r^{-4}$, then we would say that the Schwarzschild geometry is unstable. But we have to be careful. The calculation of the behavior of the perturbation curvature is based on a *perturbative* treatment, which holds only when the perturbation is *small*. When it becomes large, backreaction effects on the background geometry (the perturbation is large enough to act as a source on the geometry) have to be taken into account and the perturbative calculation breaks down. So from this type of analysis, we can say that a given geometry is *stable*, when perturbations remain small; but we can never say that it is *unstable*, even when the perturbation blows up.

We will then consider the curvature induced by a perturbation in our geometries (2.1) in the vicinity of the centre ($\alpha r \ll 1$). The perturbation will be represented by a massless scalar field $\Psi$ propagating in the background spacetimes. The problem then consists in solving the wave equation of the field in the spacetimes (2.1) and in calculating the induced curvature by constructing the stress-energy tensor of the field. This will be done for each pair $(m, n)$. As a criterion for stability, we will adopt the condition that the curvature induced by the perturbation should be at most as large as the background curvature:

$$R_{\text{perturbation}} \leq R_{\text{background}}, \tag{2.66}$$

where $R$ is the curvature scalar. Eq. (2.66) will be called the *stability test* and if it is satisfied for a given pair $(m, n)$, we will say that this geometry passes the test and is stable. If, on the other hand, eq. (2.66) is not satisfied for the pair $(m, n)$, then

we will say that this geometry fails the test. The graph of Fig. 2.2 summarizes the work of the entire section. The stable geometries are represented by dotted points in the $m, n$ plane.

In regard to the results of section 1.4b), it can seem pointless to proceed with this quite complicated analysis. After all, we have shown that external perturbations do not reach the region of spacetime where the line element (2.1) is expected to hold. The spacetime should therefore be automatically stable! This is true and in fact, the analysis of this section has no consequences on the other parts of this thesis. This section is inserted here mainly for completeness, and because the results derived in it will be applicable to any solution that can be modeled by the line element (2.1). For example, a glance at Fig. 2.2 tells us that the geometry corresponding to the pair $(-1, -1)$ is stable. But the Schwarzschild line element, eq. (1.13), for $r \ll 2M$, is exactly of the form (2.1) with $(m, n) = (-1, -1)$. So we get automatically that the Schwarzschild geometry, near the singularity, is stable. The information gathered in Fig. 2.2 can be very useful and this is one of the reason why we will spend some time on this study.

*a) The differential equation.*

We will now derive the differential equation describing the behavior of a ***massless scalar field*** in the spacetimes (2.1). In a general spacetime with metric $g_{\mu\nu}$, such a test field obeys the wave equation [40]

$$g^{\alpha\beta}\Psi_{|\alpha\beta} = 0, \tag{2.67}$$

where the stroke ($_|$) denotes a covariant differentiation. When written out explicitly, the left hand side reads

$$\begin{aligned} g^{\alpha\beta}\Psi_{|\alpha\beta} &= \Psi^{,\alpha}_{\ ,\alpha} + \Gamma^{\mu}_{\mu\alpha}\Psi^{,\alpha} \\ &= \Psi^{,\alpha}_{\ ,\alpha} + \frac{1}{\sqrt{-g}}\left(\sqrt{-g}\right)_{,\alpha}\Psi^{,\alpha} \\ &= \frac{1}{\sqrt{-g}}\left[\sqrt{-g}\Psi^{,\alpha}_{\ ,\alpha} + \left(\sqrt{-g}\right)_{,\alpha}\Psi^{,\alpha}\right] \\ &= \frac{1}{\sqrt{-g}}\left(\sqrt{-g}g^{\alpha\beta}\Psi_{,\beta}\right)_{,\alpha}, \end{aligned}$$

where $g$ is the determinant of the matrix formed by the metric tensor. This yields that the wave equation can now be written as

$$\left(\sqrt{-g}g^{\alpha\beta}\Psi_{,\beta}\right)_{,\alpha} = 0. \tag{2.68}$$

Since we have a diagonal metric, the elements of $g^{\alpha\beta}$ can be evaluated directly. They are: $g^{rr} = -(\alpha r)^m$, $g^{tt} = (\alpha r)^{-n}$, $g^{\theta\theta} = r^{-2}$ and $g^{\phi\phi} = r^{-2}\sin^{-2}\theta$. The determinant $g$ is also easy to read out and we find $\sqrt{-g} = (\alpha r)^{(n-m)/2}r^2\sin\theta$. Eq. (2.68) then yields

$$\begin{aligned} (\alpha r)^{m+n}\Psi_{,rr} + \left(2 + \frac{m+n}{2}\right)(\alpha r)^{m+n}r^{-1}\Psi_{,r} \\ +(\alpha r)^n r^{-2}\hat{L}^2\Psi - \Psi_{,tt} = 0, \end{aligned} \tag{2.69}$$

where $\hat{L}^2$ is the "angular momentum operator":

$$\hat{L}^2 = -\frac{1}{\sin\theta}\frac{\partial}{\partial\theta}\left(\sin\theta\frac{\partial}{\partial\theta}\right) - \frac{1}{\sin^2\theta}\frac{\partial^2}{\partial\phi^2}. \tag{2.70}$$

We can separate the variables in eq. (2.69) by postulating a solution of the form

$$\Psi(t,r,\theta,\phi) = \sum_{l,m} \int d\omega \; \Psi_{lm}^{(\omega)}(t,r,\theta,\phi), \tag{2.71}$$

where

$$\Psi_{lm}^{(\omega)}(t,r,\theta,\phi) = \psi(r) Y_{lm}(\theta,\phi) e^{-i\omega t}, \tag{2.72}$$

and where $Y_{lm}$ are the spherical harmonics. Substituting eqs. (2.71) and (2.72) into eq. (2.69) yields

$$r^2 \frac{d^2\psi}{dr^2} + \left(2 + \frac{n+m}{2}\right) r \frac{d\psi}{dr} + (\alpha r)^{-m} \left[\frac{\omega^2}{\alpha^2}(\alpha r)^{2-n} + l(l+1)\right] \psi = 0,$$

that can be simplified by introducing the following dimensionless quantities:

$$x \equiv \alpha r, \qquad y(x) \equiv \psi(\alpha r), \qquad \Lambda \equiv \frac{\omega^2}{\alpha^2}. \tag{2.73}$$

We finally obtain

$$x^2 y'' + \left(2 + \frac{m+n}{2}\right) x y' + x^{-m} \left[\Lambda x^{2-n} + l(l+1)\right] y = 0. \tag{2.74}$$

The explicit solution of this differential equation cannot be expressed in closed form, but we can use the fact that we are only interested in the behavior of $y$ when $x \ll 1$ to simplify eq. (2.74). For example, if $n > 2$, $\Lambda x^{2-n}$ dominates over $l(l+1)$ and this last term can be neglected, allowing us to find an explicit solution to the differential equation. This is the kind of game we shall play in the next subsection.

*b) The solutions of the differential equation.*

Before we seek for the solutions of eq. (2.74), we shall spend some time gathering a few results from ref. [41]. In what follows, eq. (2.74) will always be reduced to one of the following forms, by some approximation using the fact that $x$ is very small:

$$x^2y'' + axy' + (bx^p + c)y = 0, \tag{2.75}$$

or

$$x^2y'' + axy' + cy = 0. \tag{2.76}$$

We are interested in finding the asymptotic behavior for $x \ll 1$ of the solutions $y$ of eqs. (2.75) and (2.76). Consider first eq. (2.75). Its explicit solution is

$$y = x^{(1+a)/2} Z_\nu \left( \frac{2}{p} \sqrt{b}\, x^{p/2} \right), \tag{2.77}$$

where $Z_\nu$ is the most general linear combination of $J_\nu$ and $Y_\nu$, the Bessel functions of order $\nu$. The argument of $Z_\nu$ in eq. (2.77) for $x \ll 1$ can be either $\gg 1$ or $\ll 1$, depending on the sign of $p$. The parameter $\nu$ is given by

$$\nu = \frac{1}{p}\sqrt{(1-a)^2 - 4c}, \tag{2.78}$$

and can be imaginary as well as real. The asymptotic behaviors of the Bessel functions are well known and given by

$$J_\nu(\xi \ll 1) \approx \frac{\xi^\nu}{2^\nu \nu!},$$

$$Y_\nu(\xi \ll 1) \approx -\frac{(\nu-1)!2^\nu}{\pi}\frac{1}{\xi^\nu};$$

and

$$J_\nu(\xi \gg 1) \approx \sqrt{\frac{2}{\pi\xi}} \cos\left[\xi - (\nu + \tfrac{1}{2})\tfrac{\pi}{2}\right],$$

$$Y_\nu(\xi \gg 1) \approx \sqrt{\frac{2}{\pi\xi}} \sin\left[\xi - (\nu + \tfrac{1}{2})\tfrac{\pi}{2}\right].$$

We can summarize this by writing $Z_\nu(\xi \ll 1) \sim \xi^{\pm\nu}$ and $Z_\nu(\xi \gg 1) \sim \xi^{-1/2} e^{\pm i\xi}$. The phase factor of the solution does not really matter and we will consider only the modulus of $y$ in what follows. It can then be verified that $|Z_\nu(\xi \ll 1)| \sim \xi^{\pm \mathrm{Re}\nu}$ and that $|Z_\nu(\xi \gg 1)| \sim \xi^{-1/2}$. Re$\nu$ is a notation for the real part of $\nu$. Using now these results in eq. (2.77) yields that the asymptotic behavior of $|y|$ for $x \ll 1$ can be written as

$$|y(x \ll 1)| \sim x^Q, \tag{2.79}$$

where

$$Q = \begin{cases} \frac{1}{2}(1 - a \pm p\ \mathrm{Re}\nu) & p > 0 \\ \frac{1}{2}(1 - a - \frac{1}{2}p) & p < 0 \end{cases} \qquad \text{form (2.75);} \tag{2.80}$$

so all the information that we need to obtain about the solution is the power coefficient $Q$. To select the sign in eq. (2.80), we will use the "worst behavior criterion" that stipulates that if we have the choice between two solutions, we should select the larger one. The reason is that if the worst behaved modes pass the stability test, then the other ones will too. By choosing the worst behavior, we make sure that nothing passes through the stability test filter by mistake. So, going back to eq. (2.80), the worst behavior criterion tells us to choose the minus sign since it will give a lower $Q$ than with the plus sign, yielding a larger $|y|$.

Consider now the solution of eq. (2.76). It is simply given by

$$y = C_1 x^{(1-a+\mu)/2} + C_2 x^{(1-a-\mu)/2}, \tag{2.81}$$

where $C_1$ and $C_2$ are two arbitrary constants and where $\mu$ is given by

$$\mu = \sqrt{(1-a)^2 - 4c}. \tag{2.82}$$

By applying again the worst behavior criterion, we find that the asymptotic behavior of $|y|$ for $x \ll 1$ is in the form of eq. (2.79) with $Q$ now given by

$$Q = \tfrac{1}{2}(1 - a - \mathrm{Re}\mu), \qquad \text{form (2.76)}. \tag{2.83}$$

To summarize what we have so far, the original differential equation (2.74) can be reduced, in the region $x \ll 1$, to one of the two forms (2.75) and (2.76). In both cases, the asymptotic behavior of the solution can be written in the form

$$|y(x \ll 1)| \sim x^Q,$$

with $Q$ given by

$$Q = \begin{cases} \frac{1}{2}(1 - a - p\,\mathrm{Re}\nu) & p > 0 \\ \frac{1}{2}(1 - a - \mathrm{Re}\mu) & p = 0 \\ \frac{1}{2}\left(1 - a - \frac{1}{2}p\right) & p < 0. \end{cases} \tag{2.84}$$

We still can simplify this equation a bit further. From eq. (2.78), it is clear that $\mathrm{Re}(\nu) \leq |1-a|/p$, yielding when substituted into eq. (2.84) $Q \geq \frac{1}{2}(1 - a - |1-a|)$ if $p > 0$. Again, if we want to select the worst possible behavior, we can simply rewrite this last equation with an equality sign. This is equivalent to imposing $c = 0$ in eq. (2.78). This is reflected in our initial equation (2.74) by considering a "low

frequency, $s$ wave", that is, by letting $\Lambda \to 0$, $l = 0$. This is to say that this kind of wave will give the worst behavior that we can find. So, to select it for the stability test will give us the most restrictive conditions, which is exactly what we want. Using the same trick with eq. (2.82), we finally obtain:

$$Q = \begin{cases} \frac{1}{2}(1 - a - |1 - a|) & p \geq 0 \\ \frac{1}{2}\left(1 - a - \frac{1}{2}p\right) & p < 0. \end{cases} \tag{2.85}$$

All we have to do now is to apply this result to the differential equation (2.74). We shall do so by separating all the different pairs $(m, n)$ into five cases. These cases, and the corresponding values found for $Q$ are listed in Table 2.3.

Consider first the case $m = 0$. With this value for $m$, eq. (2.74) reduces to

$$x^2 y'' + (2 + \tfrac{1}{2}n)xy' + [\Lambda x^{2-n} + l(l+1)]y = 0,$$

which is of the form of eq. (2.75) with $1 - a = -(1 + n/2)$ and $p = 2 - n$. For $n \leq 2$ we have $p \geq 0$ and we get that $Q = -(2+n)/2$ if $n \geq -2$, and that $Q = 0$ if $n \leq -2$ (we see in eq. (2.85) that the sign of $1 - a$ makes a difference on the value of $Q$). For $n > 2$ we find that $Q = -1$. Summarizing what we have just found:

$$Q = \begin{cases} 0 & n \leq -2 \\ -\frac{1}{2}(2 + n) & -2 \leq n \leq 2 \\ -1 & n > 2 \end{cases} \qquad m = 0. \tag{2.86}$$

Consider now the case $m = 2 - n$. Using this equation in eq. (2.74) yields

$$x^2 y'' + 3xy' + [\Lambda + l(l+1)x^{-m}]y = 0,$$

which is of the form (2.75) with $1 - a = -2$ and $p = -m$. With $m \leq 0$ we get from eq. (2.85) that $Q = -2$. The special case $m = 0$ corresponds to $n = 2$ and our result agrees with eq. (2.86). When $m > 0$, we find that $Q = -1 + m/4$. So we can summarize this paragraph by writing

$$Q = \begin{cases} -2 & m \leq 0 \\ \frac{1}{4}(m-4) & m > 0 \end{cases} \qquad m + n = 2. \tag{2.87}$$

Now comes the turn of the case $n = 2$. Eq. (2.74) here becomes

$$x^2 y'' + (3 + \tfrac{1}{2}m)xy' + [\Lambda + l(l+1)]x^{-m} y = 0,$$

which again is in the form (2.75) with $1 - a = -(2 + m/2)$ and $p = -m$. For $m < 0$, we have $Q = -(2 + m/2)$ if $m \geq -4$, and $Q = 0$ if $m \leq -4$. For $m < 0$ we find $Q = -1$. This leads to the following equation:

$$Q = \begin{cases} 0 & m \leq -4 \\ \frac{1}{2}(4+m) & -4 \leq m \leq 0 \\ -1 & m > 0 \end{cases} \qquad n = 2. \tag{2.88}$$

We still have to examine two more cases. As the first one, consider $n > 2$. Since we assume $x \ll 1$, $l(l+1)$ can be neglected when compared to $\Lambda x^{2-n}$ in eq. (2.74), so this equation becomes

$$x^2 y'' + \left(2 + \frac{m+n}{2}\right) xy' + \Lambda x^{2-m-n} y = 0.$$

We now find $1-a = -(2+m+n)/2$ and $p = 2-m-n$. Assume first that $m+n \leq 2$. If $m+n \geq -2$, we have that $Q = -(2+m+n)/2$, whereas if $m+n \leq -2$, then $Q = 0$. If we now assume that $m+n > 2$, then we find that $Q = -1$. So:

$$Q = \begin{cases} 0 & m+n \leq -2 \\ -\frac{1}{2}(2+m+n) & -2 \leq m+n \leq 2 \\ -1 & m+n > 2 \end{cases} \qquad n > 2. \tag{2.89}$$

The last case is $n < 2$. This time it is $\Lambda x^{2-n}$ that is negligible when compared to $l(l+1)$ in eq. (2.74), which now becomes

$$x^2 y'' + \left(2 + \frac{m+n}{2}\right) x y' + l(l+1) x^{-m} y = 0.$$

For this case we find that $1-a = -(2+m+n)/2$ and that $p = -m$. For $m \leq 0$ we get from eq. (2.85) that $Q = -(2+m+n)/2$ if $m+n \geq -2$, whereas $Q = 0$ if $m+n \leq -2$. For $m > 0$ we get that $Q = -(2+n)/4$. Summarizing:

$$Q = \begin{cases} 0 & m \leq 0,\ m+n \leq -2 \\ -\frac{1}{2}(2+m+n) & m \leq 0,\ m+n \geq -2 \\ -\frac{1}{4}(2+n) & m > 0 \end{cases} \qquad n < 2. \tag{2.90}$$

The equations (2.86)–(2.90) give the asymptotic behavior for $x \ll 1$ of all the solutions of the differential equation (2.74) via eq. (2.79). The results are summarized in Table 2.3. We are now in a position to calculate the curvature induced by the stress-energy of the test field. This is what we will do in the next subsection. After this, we will proceed with the stability test.

*c) The stress-energy of the test field.*

In the last subsection we have found the asymptotic behavior for $\alpha r \ll 1$ of the solutions of the wave equation for a massless scalar field propagating in the "power-law" spacetimes of eq. (2.1). From those solutions, we will construct the stress-energy tensor of the test field and evaluate the curvature induced by its presence.

The stress-energy tensor of a massless scalar field is given by [40] :

$$T_{\mu\nu} = \Psi_{,\mu}\Psi_{,\nu} - \tfrac{1}{2} g_{\mu\nu} \Psi^{,\alpha}\Psi_{,\alpha}. \tag{2.91}$$

We will be interested in the *trace* of this tensor, which we can write as

$$T = -g^{\alpha\beta}\Psi_{,\alpha}\Psi_{,\beta}. \tag{2.92}$$

To find the asymptotic behavior of eq. (2.92), we use the fact that $\Psi \propto y$ and that, from eq. (2.79) $|y(x \ll 1)| \sim x^Q$. This yields that $\Psi_{,t} \sim \Psi_{,\theta} \sim \Psi_{,\phi} \sim x^Q$, and $\Psi_{,r} \sim x^{Q-1}$. We also have that $g^{rr} \sim x^m$, $g^{tt} \sim x^{-n}$, and $g^{\theta\theta} \sim g^{\phi\phi} \sim x^{-2}$. Using those results in eq. (2.92) yields

$$-T \sim x^{2Q}\left[x^{-n} + x^{-2}(x^m + 1)\right].$$

The stress-energy tensor couples to the curvature of spacetime via Einstein's field equations $G_{\mu\nu} = 8\pi T_{\mu\nu}$, that yield, when we take the trace: $R = -8\pi T$. The result is that we can write the curvature induced by the stress-energy of the test field as

$$R_{\text{perturbation}} \sim x^{2Q}\left[x^{-n} + x^{-2}(x^m + 1)\right]. \tag{2.93}$$

There is still a missing ingredient that we have to provide before we can finally enter the stability testroom. We need to compute the curvature scalar for the background geometry of eq. (2.1). To do this calculation, we can apply the results of section 1.1a) to obtain $\rho$, $P_r$ and $P_\perp$. The sum $-\rho + P_r + 2P_\perp$ is then equal to $-R/8\pi$. This is a straightforward calculation and we shall merely give the result. We find that

$$R_{\text{background}} = \frac{1}{r^2}\left\{2 + \left[2(m+1) + n\left(1 + \frac{m+n}{2}\right)\right](\alpha r)^m\right\},$$

which yields, when we consider only the asymptotic behavior for $\alpha r \ll 1$ :

$$R_{\text{background}} \sim x^{-2}(x^m + 1). \tag{2.94}$$

We have now everything in hand to proceed with the stability test.

*d) The stability test.*

At the beginning of the section we have stated the stability test that we shall impose on every one of our spacetimes characterized by the pairs $(m, n)$. In the preceding subsection, we have derived expressions for the background curvature and for the perturbation curvature, the latter depending on the values of $Q$ derived in section 2.3b) and listed in Table 2.3. The stability test can then be obtained by substituting eqs. (2.93) and (2.94) into eq. (2.66). This yields

$$x^{2Q}\left[x^{-n} + x^{-2}(x^m + 1)\right] \leq x^{-2}(x^m + 1). \tag{2.95}$$

This last equation will impose constraints on $Q$ that will have to be satisfied by the actual values in order to have stability. The first step is to extract the condition

equations for $Q$ from eq. (2.95). To do so, just like in the previous subsection, we will have to separate all the possible values of $m$ and $n$ into a few cases. The results of this analysis are summarized in Table 2.4.

Consider first the case $m \geq 0$. This condition makes that 1 dominates over $x^m$ (since $x \ll 1$) and that eq. (2.95) reduces to

$$x^{2Q+2}(x^{-n} + x^{-2}) \leq 1.$$

Assume now that $n \geq 2$. The last equation then simplifies further to $x^{2Q+2-n} \leq 1$, which leads to $2Q + 2 - n \geq 0$. The condition on $Q$ is then $Q \geq (n-2)/2$. If $n \leq 2$, then we get $x^{2Q} \leq 1$, which requires $Q \geq 0$. So for the case $m \geq 0$ we obtain that the conditions that $Q$ must satisfy in order to have stability are

$$Q \geq \begin{cases} \frac{1}{2}(n-2) & n \geq 2 \\ 0 & n \leq 2 \end{cases} \qquad m \geq 0. \tag{2.96}$$

Consider now the case $m \leq 0$. Here, it is $x^m$ that dominates over 1, so eq. (2.95) reduces to

$$x^{2Q}(x^{2-m-n} + 1) \leq 1.$$

Assume first that $m + n \geq 2$. The last equation then becomes $x^{2Q+2-m-n} \leq 1$, or, $2Q + 2 - m - n \geq 0$. The condition on $Q$ is then $Q \geq (m + n - 2)/2$. If we now let $m + n \leq 2$, we find $x^{2Q} \leq 1$, or $Q \geq 0$. So the stability condition for the case $m \leq 0$ is

$$Q \geq \begin{cases} \frac{1}{2}(m+n-2) & m+n \geq 2 \\ 0 & m+n \leq 2 \end{cases} \qquad m \leq 0. \tag{2.97}$$

We now have our stability conditions on $Q$. The next step is to compare the actual values of $Q$, eqs. (2.86)–(2.90), Table 2.3; with the conditions (2.96) and (2.97), Table 2.4, to see which of the pairs $(m, n)$ correspond to stable geometries. To proceed with this verification, we shall again separate the task into a few cases, following the entries of Table 2.3.

The first case is $m = 0$. For $n \leq -2$, we find that $Q = 0$. From eq. (2.96) (bottom), or eq. (2.97) (bottom), we verify that $Q = 0$ satisfies the condition for stability. Those values of $m$ and $n$ therefore pass the test. For $-2 \leq n \leq 2$, we have that $Q = -(2+n)/2$, which satisfies the condition only if $n = -2$. Finally, for $n > 2$, $Q = -1$. Eqs. (2.96) (top) and (2.97) (top) tell us that $Q$ must satisfy $Q \geq (n-2)/2$; so we obviously have a violation of the stability condition. The corresponding values of $m$ and $n$ then fail the test. *The conclusion for the case $m = 0$ is that we have stable solutions only for $n \leq -2$.*

The second case is $m + n = 2$. For $m \leq 0$ we find that $Q = -2$. From eq. (2.97) we discover that $Q$ must satisfy $Q \geq 0$. We therefore fail the test. For $m > 0$ we get from eq. (2.96) (bottom) that the condition is $Q \geq 0$, while eq. (2.87) gives $Q = (m-4)/4$. The condition is then satisfied if $m \geq 4$. *So the conclusion for the case $m + n = 2$ is that we have stable solutions only for $m \geq 4$.*

The next case is $n = 2$. If $m \leq -4$, we have that $Q = 0$. Eq. (2.97) (bottom) then tells us that $Q$ must be equal or greater that zero. We therefore pass the test. For $-4 \leq m \leq 0$, we find that $Q = -(m+4)/2$. This is equal to zero only when $m = -4$ and we pass the test only value of $m$. Finally, if $m > 0$, we find that $Q = -1$, while $Q$ must still be equal or larger that zero. So, here we fail the test.

*The conclusion for the case $n = 2$ is then that we have stable solutions only for $m \leq -4$.*

Now comes the turn of $n > 2$. For $m + n \leq -2$ we have that $Q = 0$. Eq. (2.97) (bottom) then confirms that we pass the test. If $-2 \leq m + n \leq 2$, $Q = -(2 + m + n)/2$. But this value of $Q$ equals zero only if $m + n = -2$, so we pass the test only for this value of $m + n$. Finally, if $m + n > 2$, we have $Q = -1$. Both eqs. (2.96) (top) and (2.97) (top) require non negative values for $Q$, so here we fail the test. *The conclusion for the case $n > 2$ is that we have stable solutions only for $m + n \leq -2$.*

The final case is $n < 2$. For $m \leq 0$, $m + n \leq -2$, we find that $Q = 0$. Eq. (2.97) (bottom) demands $Q \geq 0$, so we pass the test. For $m \leq 0$, $m + n \geq -2$, we have that $Q = -(2 + m + n)/2$. Eq. (2.97) is satisfied only if $m + n = -2$ and we pass the test only for this value of $m + n$. Finally, if $m > 0$ , $Q = -(2 + n)/4$ and we find from eq. (2.96) (bottom) that $Q$ must be at least equal to zero. This is satisfied only if $n \leq -2$. *So the conclusion for the case $n < 2$ is that we have stable solutions for $m \leq 0$, $m + n \leq -2$ and for $m > 0$, $n \leq -2$.*

We have now considered all the possible cases and the complete set of stable solutions can be gathered from the last sentences of the previous five paragraphs. Fig. 2.2 is a picture of the plane $(m, n)$ representing all the possible geometries of eq. (2.1). The stable geometries are indicated by the dotted points of the plane. We see that they are found below the lines $n = -(2 + m)$ (for $m \leq 0$), and $n = -2$ (for $m \geq 0$). This figure is the very economical summary of this whole section!

This completes our study of the stability of the geometries. In the next section we will consider another aspect of the spacetimes: the accessibility of the origin $r = 0$.

## 2.4: Accessibility of the origin

Before we leave the topic of the power-law metric of eq. (2.1), there is another property of those spacetimes that we would like to have a look at. Let us go back for a short moment to eq. (1.50). The interesting thing about that line element is the exponentially decreasing radius of the 3-cylinders $r$ = constant,

$$ds^2 = e^{-2r}(\text{constant}\ dz^2 + d\Omega^2).$$

This suggests the possibility that, even if there were a singularity at $r = 0$ ($\tau = \infty$), it would remain hidden to observers for an infinite amount of time. The problem of the singularity could then be avoided because a singularity that develops only in the remote future is quite harmless. What we want to find then, are the spacetimes $(m, n)$ for which arbitrary observers will reach the origin $r = 0$ only after an infinite amount of proper time. We therefore need to solve the geodesic equation for arbitrary free falling observers, in the spacetimes of eq. (2.1).

The problem of geodesic motion is easy to solve with the help of the "Lagrangian method" [42] similar to that of ordinary classical mechanics. It can be shown that the geodesic equation describing the path of a free falling observer in an arbitrary spacetime is obtained by writing the Euler-Lagrange equation for the Lagrangian

$$L = \tfrac{1}{2}\, g_{\mu\nu}\, \dot{x}^\mu \dot{x}^\nu,$$

where $\dot{x}^\mu \equiv dx^\mu/d\lambda$ and where $\lambda$ is an affine parameter along the geodesic. If the geodesic is a timelike path, then $\lambda$ can be chosen to be the proper time measured

by the observer moving on the geodesic. For the line element (2.1), the Lagrangian is

$$2L = -(\alpha r)^{-m}\dot{r}^2 + (\alpha r)^n \dot{t}^2 + r^2\dot{\phi}^2, \tag{2.98}$$

if we assume that the motion takes place in the equatorial plane $\theta = \pi/2$ (spherical symmetry!). If we choose $\lambda$ to be the proper time along the geodesic, we get that $L$ has the constant value $L = -1/2$. The geodesic equation is then given simply by the Euler-Lagrange equation

$$\frac{d}{d\lambda}\frac{\partial L}{\partial \dot{x}^\alpha} - \frac{\partial L}{\partial x^\alpha} = 0. \tag{2.99}$$

Let us first apply this equation for $x^\alpha = t$. Since the Lagrangian has no $t$ dependence, we get that

$$\frac{\partial L}{\partial \dot{t}} = (\alpha r)^n \dot{t} = \text{constant} \equiv E.$$

Similarly, we have for $x^\alpha = \phi$:

$$\frac{\partial L}{\partial \dot{\phi}} = r^2\dot{\phi} = \text{constant} \equiv J.$$

This is the well known property that a constant of motion always comes with a cyclic variable. If $t$ represented a timelike coordinate, $E$ would be interpreted as the energy per unit mass of the test particle moving on the geodesic. But such an interpretation could be misleading since here $t$ is a spacelike coordinate. Instead, $E$ should be interpreted as a conserved linear momentum. However, $J$ still represents the angular momentum per unit mass of the test particle. We can now substitute

the two last equations into eq. (2.98) and use the fact that the numerical value of the Lagrangian is also constant. This yields

$$-(\alpha r)^{-m}\dot{r}^2 + (\alpha r)^{-n}E^2 + r^{-2}J^2 = -1,$$

or

$$\frac{dr}{(\alpha r)^{m/2}\sqrt{1+(\alpha r)^{-n}E^2 + r^{-2}J^2}} = -d\lambda. \tag{2.100}$$

We want to solve eq. (2.100) in the vicinity of the origin. We can therefore neglect the 1 in the square root, since it is much smaller than $J^2r^{-2}$ (of course, this is true only if $J$ is not zero, but we consider the most general free falling observer). Eq. (2.100) then reduces to

$$\frac{dr}{(\alpha r)^{m/2}\sqrt{E^2(\alpha r)^{-n} + J^2r^{-2}}} = -d\lambda. \tag{2.101}$$

To simplify this equation a bit further, we need to separate the values of $(m,n)$ in the two cases $n \geq 2$, and $n \leq 2$.

Consider first the case $n \geq 2$. The dominant term in the square root is here $E^2(\alpha r)^{-n}$ (if $n = 2$, we have to replace this by $(E^2\alpha^{-2} + J^2)r^{-2}$, but the result would be the same). Eq. (2.101) then reads

$$(\alpha r)^{(n-m)/2}\, dr = E\, d\lambda.$$

To integrate this equation, first assume that $m - n \neq 2$. We then find

$$r^{(2+n-m)/2} \propto \lambda - \lambda_0,$$

and we see that if $m - n > 2$, $\lambda$ goes to infinity when $r$ goes to zero. We then say that the origin is not accessible. On the other hand, if $m - n < 2$, then $r \to 0$ for $\lambda \to \lambda_0$. We now say that the origin is accessible. If $m - n = 2$, we would find that $r$ depends exponentially on $\lambda$ and that $r \to 0$ as $\lambda \to \infty$. *The conclusion for the case $n \geq 2$ is that the origin is inaccessible only for $m - n \geq 2$.*

Consider now the case $n \leq 2$. This time, the dominant term in the square root is $J^2 r^{-2}$, so eq. (2.101) reduces to

$$(\alpha r)^{-m/2}\, r\, dr = -J\, d\lambda.$$

To integrate this equation, assume first that $(m-2) \neq 2$. This leads to

$$r^{(4-m)/2} \propto \lambda - \lambda_0,$$

which tells us that if $m > 4$, then $r \to 0$ for $\lambda \to \infty$. This holds also for $m = 4$ where the dependence on $\lambda$ is now exponential. When $m < 4$, we find that $r \to 0$ for $\lambda \to \lambda_0$. *The conclusion for the case $n \leq 2$ is that the origin is inaccessible only for $m \geq 4$.*

The results of this section are summarized in Fig. 2.2 where the spacetimes for which the origin is inaccessible are represented by circles. An interesting feature is that the spacetimes for which $m$ is equal to 2, "the quantum-effects spacetimes", do have an accessible origin. This seems to be in contradiction with the "long squeeze" effect that we discussed at the beginning of this section. The key to this apparent paradox is that in the spacetime (1.50), only the observers *at rest* meet the origin after an infinite amount of proper time. In this section, on the other

hand, we were dealing with free falling observers. So the time dilatation effects of ordinary special relativity ensure that those observers meet the origin within a finite lapse of proper time.

This completes our study of the power-law metric. In Chapter Three, we will still consider the interior of spherically symmetric black holes, but with new complications: we will then allow the black hole to be charged.

# CHAPTER THREE

# THE INTERIOR OF A REISSNER-NORDSTRØM BLACK HOLE

## 3.1: The Reissner-Nordstrøm solution

We will consider in this Chapter the spacetime inside the Reissner-Nordstrøm black hole. We have briefly mentioned in section 1.1 that our interest is on the effects on the inner apparent horizon (and on the Cauchy horizon) of a gravitational collapse presenting small departures from spherical symmetry. Before we specify the formulation of the problem further, let us recall the main features of the Reissner-Nordstrøm spacetime; to this end, we will first derive the solution, with the help of the machinery of section 1.2a).

The Reissner-Nordstrøm solution [43] is a static, spherically symmetric solution of the Einstein field equation for a stress-energy tensor corresponding to the electromagnetic field of a point charge located at the origin. According to Birkoff's theorem [7] (section 1.1), this solution represents the exterior geometry of a charged star undergoing a spherical gravitational collapse. Since we have staticity and spherical symmetry, the form of the solution must be given by eq. (1.3)

$$ds^2 = e^{\psi}\left(-\Phi\ dt^2 + \Phi^{-1}dr^2\right) + r^2 d\Omega^2, \tag{3.1}$$

where $\psi$ and $\Phi$ are two functions of $r$ to be determined by solving the field equations (1.7)–(1.9). To do this however, one must first find the form of the stress-energy tensor, and this requires the knowledge of the expression for the electromagnetic field tensor, $F^{\alpha\beta}$. To find this, it is necessary to solve Maxwell's equations in the background geometry of eq. (3.1), for a point charge located at the origin.

The strategy to find the solution is then the following: first, some physical considerations will permit us to directly write down an expression for the electromagnetic field tensor, in terms of a yet to-be-determined function of $r$. From this we will be able to find an expression for the stress-energy tensor. A simplification then occurs: the electromagnetic field obeys the equation of state $\rho + P_r = 0$, which means, as we know from eq. (1.10), that the function $\psi$ is constant and can be taken to be zero. After this, it becomes simple to solve Maxwell's equations and to finally obtain the complete solution.

So the first step is to write down an expression for $F^{\alpha\beta}$. Since we have a static situation, it is physically reasonable to expect that a static observer should observe only an electric field, produced by the point charge. And since we consider a point charge located at the origin, this electric field should be radial. Furthermore, we recall that the reference frame of a static observer is given by the orthonormalized tetrad of eq. (1.5). All those considerations allow us to write down the form of the electromagnetic tensor as

$$\begin{aligned} F^{\alpha\beta} &= 2E(r)\ \vec{e}^{\,[\alpha}_{(t)}\vec{e}^{\,\beta]}_{(r)} \\ &\equiv E(r)\left(\vec{e}^{\,\alpha}_{(t)}\vec{e}^{\,\beta}_{(r)} - \vec{e}^{\,\alpha}_{(r)}\vec{e}^{\,\beta}_{(t)}\right), \end{aligned} \tag{3.2}$$

if we also note that $F^{\alpha\beta}$ is by definition an antisymmetric tensor. Using now the eqs. (1.5) and (3.1), we obtain

$$\begin{aligned} F^{\alpha\beta} &= 2E(r)e^{-\psi(r)}\delta^{[\alpha}{}_{t}\delta^{\beta]}{}_{r}, \\ F_{\alpha\beta} &= -2E(r)e^{\psi(r)}\delta^{t}_{[\alpha}\delta^{r}{}_{\beta]}. \end{aligned} \tag{3.3}$$

The stress-energy tensor can now be easily evaluated. It is given in general by the expression [44]

$$T^{\alpha}{}_{\beta} = \frac{1}{4\pi}\left(F^{\alpha\mu}F_{\beta\mu} - \tfrac{1}{4}\delta^{\alpha}{}_{\beta}F^{\mu\nu}F_{\mu\nu}\right), \tag{3.4}$$

which yields, when using eq. (3.3):

$$T^{\alpha}{}_{\beta} = P_{\rm el}\ \mathrm{diag}(-1,-1,1,1), \tag{3.5}$$

where $P_{\rm el} = E^2/8\pi$, a familiar result. By comparing eqs. (3.5) and (1.61), one sees that, as announced, the electromagnetic field obeys the equation of state $\rho + P_r = 0$, which means that $\psi(r) = 0$.

We now have to solve Maxwell's equations in the background geometry of eq. (3.1). The only relevant equation here is [44]

$$F^{\alpha\beta}{}_{|\beta} = 4\pi j^{\alpha}, \tag{3.6}$$

which relates the divergence of the electromagnetic field to the source current. Since, in our case, the spacetime is free of sources, (except at the origin), the right hand

side of eq. (3.6) vanishes. Following the same steps that we used to derive eq. (2.68), we arrive at the following equation:

$$\left(\sqrt{-g}F^{\alpha\beta}\right)_{,\beta} = 0. \tag{3.7}$$

The only non trivial component of this last equation yields, with the use of eq. (3.1) (with $\psi = 0$), and of eq. (3.3):

$$\frac{d}{dr}\, r^2 E(r) = 0,$$

which is easily integrated to give $E(r) = e/r^2$, where $e$ is the constant of integration that can be interpreted as the charge of the black hole. Of course, we have recovered the familiar equation for the electric field of a point charge. Substituting this result into the expression of $P_{\rm el}$ brings

$$P_{\rm el} = \frac{1}{8\pi}\,\left(\frac{e}{r^2}\right)^2. \tag{3.8}$$

We have now an explicit expression for the stress-energy tensor of the electromagnetic field. All we have to do now is to solve Einstein's field equations. It is easy to show that eq. (1.11) is satisfied automatically, whereas eqs. (1.7), (3.5) and (3.8) give $m' = e^2/2r^2$, which yields

$$m(r) = M - \frac{e^2}{2r}, \tag{3.9}$$

where $M \equiv$ constant. Inserting this result in eq. (1.10) finally yields the *Reissner-Nordstrøm* solution:

$$ds^2 = -f\, dt^2 + f^{-1}dr^2 + r^2 d\Omega^2, \tag{3.10}$$

where

$$f(r) \equiv 1 - \frac{2M}{r} + \frac{e^2}{r^2}. \tag{3.11}$$

It is instructive to rewrite eq. (3.11) as

$$f(r) = \frac{(r - r_+)(r - r_-)}{r^2}, \tag{3.11'}$$

where

$$r_\pm = M \pm \sqrt{M^2 - e^2}. \tag{3.12}$$

(We will assume from now on that $e^2 \leq M^2$). The fact that $f(r)$ possesses two zeros means that this spacetime possesses *two* horizons. The *outer* (event) horizon, located at $r = r_+$, forms the boundary of the black hole. The *inner* (apparent) horizon, located at $r = r_-$, lies within the hole.

It is now time to introduce useful new coordinates that will help us do the calculations of the following sections. First, introduce as in eq. (1.23) a new radial coordinate $r^*$, defined by

$$\begin{aligned} r^* &\equiv \int \frac{dr}{f(r)} \\ &= r + c_+ \ln|r - r_+| - c_- \ln|r - r_-|, \end{aligned} \tag{3.13}$$

where

$$c_\pm \equiv \frac{r_\pm^2}{r_+ - r_-}. \tag{3.14}$$

It can be noted that $r^* \to -\infty$ when $r \to r_+$, and that $r^* \to \infty$ when $r \to r_-$. We introduce now the null coordinates

$$u = t - r^*, \qquad v = t + r^*. \tag{3.15}$$

It is then easy to show that the line element (3.10) can be rewritten as

$$ds^2 = -du\,[2\,dr + f(r)\,du] + r^2 d\Omega^2, \tag{3.16}$$

or

$$ds^2 = dv\,[2\,dr - f(r)\,dv] + r^2 d\Omega^2. \tag{3.17}$$

It is also possible to give a double-null form, as in eq. (1.21), but this will not be of any use for us. From the last three equations, it can be inferred that outgoing radial lightlike geodesics follow $u$ = constant lines, whereas ingoing ones follow $v$ = constant lines.

A study of the Reissner-Nordstrøm solution was completed by Graves and Brill in 1960 [20]. The presence of the inner apparent horizon plays an important rôle in the global geometry of the spacetime. Fig. 3.1 is a conformal diagram representing the analytical continuation of the Reissner-Nordstrøm spacetime [45]. Unlike the Schwarzschild spacetime (Fig 1.1), the singularity is here *timelike*, this means that an observer falling into the hole can avoid hitting the singularity, and as the diagram shows, may end up in another universe. This interesting property is even preserved when one considers the collapse of a charged star. In this case, the left side of the conformal diagram must be replaced by the spacetime of the star interior. But the "upper" universe is still there and the star, instead of collapsing to a point, may bounce and start a new life in this other universe [14].

The inner apparent horizon also coincides with what is called the *Cauchy horizon* [46] of the "initial" hypersurface $\Sigma$. Roughly, a Cauchy horizon is the boundary of the spacetime where the initial conditions specified on $\Sigma$ cease to completely determine the future. This is related, of course, to the well known *initial value problem*: suitable initial conditions (say, for a given field), specified at one instant of time should be enough (with an evolution equation) to determine the value of the field at all times. The Cauchy horizon signals the breakdown of the initial value problem: events at "later times" than the Cauchy horizon are not determined uniquely by the initial conditions on $\Sigma$. To understand this better, consider the point P in Fig. 3.1. This point lies before the Cauchy horizon and it is clear that a causal curve reaching P must have previously crossed $\Sigma$. Therefore, the initial conditions specified on the hypersurface $\Sigma$ determine uniquely what goes on at point P. The set of all such points is called the *domain of dependence* of $\Sigma$. On the other hand, consider the point Q, located after the Cauchy horizon. It can be seen that, now, information reaching Q could have come from other regions than $\Sigma$. For example, information can come from the singularity. The point Q is therefore outside the domain of dependence of $\Sigma$. The boundary of the domain of dependence is precisely the Cauchy horizon. As the diagram shows, the Cauchy horizon of the Reissner-Nordstrøm spacetime coincides with the inner apparent horizon.

The presence of the inner-Cauchy horizon brings new problems. The study of the propagation of perturbations inside the Reissner-Nordstrøm black hole shows that something very peculiar happens in the vicinity of this horizon. The energy density of the perturbating field, when measured by a free falling observer crossing the horizon, blows up to infinity [15]. We have given at the end of section 1.1 a

heuristic argument explaining this infinite blueshift in terms of an infinite accumulation of light rays along the Cauchy horizon. This disturbing result has suggested that the interior region of a charged black hole could be in fact different from what the static solution depicts: the inner horizon is perhaps unstable, and it is possible that a singularity would develop there. This new singularity would, in consequence, block off the way to the other universe in a very efficient way! A conclusion could not be reached, however, since the calculations of ref. [15] are based only on a perturbative analysis, which makes sense only if the effects of the perturbation on the background spacetime remain small. This is obviously not the case here, and the backreaction of the geometry must be taken into account before the issue can be settled. We will say more about this in section 3.4.

We will consider in the next section the problem of the propagation of light rays along the line $v = \infty$, showing that we indeed have a singular surface of infinite blueshift located on the inner apparent horizon (Cauchy horizon) of the black hole. In section 3.3, we will try to evaluate the effects of a realistic gravitational collapse by allowing the collapse to present small deviations from spherical symmetry. We will see that the radiation emitted from the surface of the star produces the effect of separating the Cauchy horizon from the inner apparent horizon (Fig. 3.3). We will then show that while everything becomes regular on the apparent horizon, the Cauchy horizon remains a singular surface of infinite blueshift, in accordance with the heuristic picture (an infinite amount of information is received by an observer within a finite proper time).

### 3.2: The static model

We will now proceed in showing that in the static Reissner-Nordstrøm spacetime, the energy density of infalling radiation blows up to infinity at the inner apparent horizon, when measured by a free-falling observer. The problem is easy to formulate. We want to find an expression for the energy density of infalling radiation, measured by a free-falling observer. The stress-energy tensor of the infalling radiation can be written as

$$T_{\text{in}}^{\alpha\beta} = \rho_{\text{in}} l^{\alpha} l^{\beta}, \tag{3.18}$$

where $\rho_{\text{in}}$ is a function of $r$, and where $l^{\alpha}$ is the four-velocity of the infalling photons. Now, the energy density measured by a free-falling observer is

$$\rho_{\text{in}}^{\text{obs}} = T_{\text{in}}^{\alpha\beta} u_{\alpha} u_{\beta}, \tag{3.19}$$

where $u^{\alpha}$ is the four-velocity of the observer. We then get that the quantity we want to evaluate is

$$\rho_{\text{in}}^{\text{obs}} = \rho_{\text{in}} \left(u^{\alpha} l_{\alpha}\right)^2 . \tag{3.20}$$

The problem then separates into three parts. The first part consists in solving the geodesic equation for $l^{\alpha}$. The second part is to solve the energy conservation equation for $T_{\text{in}}^{\alpha\beta}$, and hence to find an expression for $\rho_{\text{in}}$. Finally, we will have to solve the geodesic equation for $u^{\alpha}$. Collecting the results will bring the expression for $\rho_{\text{in}}^{\text{obs}}$ via eq. (3.20).

But first of all, we need to choose the coordinate system that we want to work with. The obvious choice is to use the $r, v$ coordinate system, since the

radially infalling photons follow the $v$ = constant lines. This leads to a very simple expression for $l^\alpha$. It is also a good choice because our surface of interest is the surface $v = \infty$. We can therefore write the line element as

$$ds^2 = dv(2\ dr - f\ dv) + r^2 d\Omega^2, \tag{3.17}$$

with

$$f = -\frac{(r_+ - r)(r - r_-)}{r^2}. \tag{3.11'}$$

We are interested in the interior region $r_- \leq r \leq r_+$, this is why we rewrote eq. (3.11') in this form, showing that $f$ is nonpositive in this region. Fig. 3.2 shows the region of interest and illustrates the problem.

The first step is then to find an expression for the null vector $l^\alpha$. For simplicity, we shall consider only radial four-velocities. This means that the $\theta$ and $\phi$ components of $l^\alpha$ will be set equal to zero. There is no real loss in generality in doing so, and this will greatly simplify the demonstration. With this understood, the equation $g_{\alpha\beta} l^\alpha l^\beta = 0$ reduces to

$$\frac{dv}{d\lambda}\left(2\frac{dr}{d\lambda} - f\frac{dv}{d\lambda}\right) = 0, \tag{3.21}$$

since $l^\alpha \equiv dx^\alpha/d\lambda$, where $\lambda$ is a parameter along the ingoing, radial geodesics. There is a special class of such parameters, called *affine parameters* [47]; when $\lambda$ is an affine parameter, the geodesic equation for a null vector $k^\alpha \equiv dx^\alpha/d\lambda$ is

$$k^\alpha{}_{|\beta} k^\beta = 0, \qquad \lambda : \text{affine parameter.} \tag{3.22}$$

Otherwise, the geodesic equation reads

$$k^{\alpha}{}_{|\beta}k^{\beta} = \Lambda k^{\alpha}, \qquad \lambda : \text{ordinary parameter}, \tag{3.23}$$

where $\Lambda$ is some function of the coordinates. For convenience, let us choose $-r$ to be our parameter $\lambda$. We choose $-r$ since $r$ decreases along the ingoing light rays. Now, ingoing light rays follow the $v$ = constant lines; we can therefore write down the expression for $l^{\alpha}$ as

$$\begin{aligned} l^{\alpha} &= \left(l^{v}, l^{r}, l^{\theta}, l^{\phi}\right) \\ &= (0, -1, 0, 0)\,. \end{aligned} \tag{3.24}$$

To check whether $-r$ is an affine parameter, we need to calculate $l^{\alpha}{}_{|\beta}l^{\beta}$; if the result is zero, then we have an affine parameter. To do this calculation, we would need first to calculate the connection coefficients $\Gamma^{\alpha}{}_{\beta\gamma}$, but there is a quicker way. The trick is to observe that if $l_{\alpha}$ can be written as the gradient of some function $\chi$: $l_{\alpha} = \chi_{,\alpha}$, then the equation $l^{\alpha}{}_{|\beta}l^{\beta} = 0$ holds automatically. To prove this, the first step is to verify that

$$l_{\alpha|\beta} = \chi_{|\alpha\beta} = \chi_{|\beta\alpha} = l_{\beta|\alpha},$$

by observing that the coefficients $\Gamma^{\alpha}{}_{\beta\gamma}$ are symmetric with respect to the lower indices. Then we have that

$$l_{\alpha|\beta}l^{\beta} = l_{\beta|\alpha}l^{\beta} = \tfrac{1}{2}\left(l^{\beta}l_{\beta}\right)_{,\alpha},$$

which is identically zero. Hence, to verify that $-r$ is an affine parameter, we must verify that $l_{\alpha}$ is the gradient of some function. Using eq. (3.17), it is easy to see that

$$l_{\alpha} = (-1, 0, 0, 0)\,, \tag{3.25}$$

so that

$$l_\alpha \, dx^\alpha = -\, dv = -v_{,\alpha} \, dx^\alpha .$$

This shows that $\chi = -v$, and that $-r$ is indeed an affine parameter. This means that our $l^\alpha$ satisfies the geodesic equation

$$l^\alpha{}_{|\beta} l^\beta = 0. \tag{3.26}$$

Now that we have an expression for $l^\alpha$, the second step is to find one for $\rho_{\text{in}}$. This is done by inserting eq. (3.18) in the energy conservation equation: $T^{\alpha\beta}{}_{|\beta} = 0$. This yields

$$\begin{aligned} 0 &= \rho_{\text{in},\beta} l^\alpha l^\beta + \rho_{\text{in}} l^\alpha{}_{|\beta} l^\beta + \rho_{\text{in}} l^\alpha l^\beta{}_{|\beta} \\ &= \left( \rho_{\text{in},\beta} l^\beta + \rho_{\text{in}} l^\beta{}_{|\beta} \right) l^\alpha , \end{aligned}$$

where we have used eq. (3.26). Now, $\rho_{\text{in},\beta} l^\beta$ is simply $d\rho_{\text{in}}/d(-r)$, and using the familiar equation for the divergence of a vector, we get

$$\begin{aligned} \frac{d}{dr} \ln \rho_{\text{in}} &= \frac{1}{\sqrt{-g}} \left( \sqrt{-g} l^\alpha \right)_{,\alpha} \\ &= -\frac{1}{r^2} \frac{d}{dr} r^2 \\ &= -\frac{d}{dr} \ln r^2 ; \end{aligned}$$

which finally yields

$$\rho_{\text{in}} = \frac{k}{r^2}, \tag{3.27}$$

where $k$ is an arbitrary constant for each given ingoing light ray. Since these rays are labelled by $v$, $k$ is effectively an arbitrary function of $v$, since we can choose a

different constant for each ray. We will see later that we can evaluate $k(v)$ for large $v$'s from physical considerations.

The last step is to calculate $u^\alpha$, the four-velocity of the free-falling observer. Again, we will restrict ourselves to radial motion. In order to solve the geodesic equation for $u^\alpha$, we will use the same technique as in section 2.4. The Lagrangian for the motion of our observer is, from eq. (3.17):

$$L = \dot{r}\dot{v} - \tfrac{1}{2} f \dot{v}^2 = -\tfrac{1}{2}, \tag{3.28}$$

where $\dot{x}^\alpha \equiv dx^\alpha/d\tau \equiv u^\alpha$, and where $\tau$ is the proper time of the observer. The Euler-Lagrange equation, eq. (2.99), for the coordinate $v$ yields

$$\frac{\partial L}{\partial \dot{v}} = \dot{r} - f\dot{v} = \text{constant} \equiv -E,$$

which gives

$$\dot{r} = f\dot{v} - E. \tag{3.29}$$

We will have to decide on the sign of $E$ later on. If we substitute eq. (3.29) into eq. (3.28), we get a quadratic equation for $\dot{u}$ in terms of $f$ and $E$. Factorizing this equation yields

$$\dot{v} = \frac{E \pm \sqrt{E^2 - f}}{f},$$

so we, here too, have to choose the correct sign. Our observer falls towards $r_-$; hence $\dot{r}$ must be negative definite. Now, if we evaluate $\dot{r}$ with the help of eq. (3.29) and of our expression for $\dot{v}$, we find that $\dot{r} = \pm\sqrt{E^2 - f}$. Therefore, we have to choose the lower sign:

$$\dot{v} = \frac{E - \sqrt{E^2 - f}}{f}. \tag{3.30}$$

We have now to choose the sign of the constant $E$. A look at Fig. 3.2 informs us that the observer we are interested in crosses the $v = \infty$ sheet of the inner apparent horizon. This means that $\dot{v}$ must go to infinity as we cross $r = r_-$, or $f = 0$. It is easy to see that only an $E$ *negative* will produce this result. Therefore we choose

$$E < 0; \tag{3.31}$$

an observer with positive $E$ would cross the $u = -\infty$ sheet of the inner horizon.

We have now everything in hand to evaluate $\rho_{\text{in}}^{\text{obs}}$. Eqs. (3.25) and (3.30) give

$$u^\alpha l_\alpha = \frac{-E + \sqrt{E^2 - f}}{f}; \tag{3.32}$$

and substituting this and eq. (3.27) into eq. (3.20) yields

$$\rho_{\text{in}}^{\text{obs}} = k \left( \frac{E - \sqrt{E^2 - f}}{rf} \right)^2 . \tag{3.33}$$

This expression, we underline once more, is valid for each given ingoing light ray. But we have to consider a sequence of rays approaching the inner apparent horizon; this means that we have to evaluate eq. (3.33) for each ingoing ray, as we approach the line $v = \infty$, and find the limiting value of $\rho_{\text{in}}^{\text{obs}}$ as $v$ goes to infinity. We can do this by evaluating $\rho_{\text{in}}^{\text{obs}}$ for each $v$ as we go along an outgoing radial line $u =$ constant, on which there is a relation between $r$ and $v$ given by eq. (3.21):

$$2\, dr - f\, dv = 0. \tag{3.34}$$

Once integrated, this equation gives the relationship $r(v)$ on our $u$ = constant line, and eq. (3.33) then gives $\rho_{\rm in}^{\rm obs}$ as a function of $v$:

$$\rho_{\rm in}^{\rm obs} = (\text{finite coefficient})\ k(v) f^{-2}(v). \tag{3.35}$$

Let us now integrate eq. (3.34) in the vicinity of $f = 0$ ($v = \infty$). We can Taylor expand $f$ around $r = r_-$ and get

$$f \simeq -2\kappa_-(r - r_-), \tag{3.36}$$

where

$$\kappa_- \equiv -\frac{1}{2}\left.\frac{df}{dr}\right|_{r=r_-}. \tag{3.37}$$

Substituting eq. (3.36) into eq. (3.34) yields $|r - r_-| = r_- e^{-\kappa_- v}$ and we then get

$$f(v \to \infty) \simeq -2\kappa_- r_- e^{-\kappa_- v}. \tag{3.38}$$

This finally yields

$$\rho_{\rm in}^{\rm obs}(v \to \infty) \simeq (\text{finite coefficient})\ k(v \to \infty)\ e^{2\kappa_- v}, \tag{3.39}$$

and we see that unless $k(v)$ goes exponentially to zero for large $v$, the energy density of the radiation as measured by our free-falling observer will reach infinity on the inner apparent horizon.

It has been mentioned earlier (section 1.1, section 1.4b)) that the amplitude of the backscattered part of the initially outgoing radiation coming from the star and falling towards the black hole decays as a power law in time, for late times.

In particular, if the perturbating field is a multipole of order $l$, its amplitude goes as $v^{-(2l+2)}$. To implement this result in our model, we go back to eq. (3.27) and realize that $k(v)$ precisely represents the time dependence of the amplitude (or the square of it) of the infalling radiation. We therefore have that for realistic external perturbations:

$$k(v \to \infty) \sim v^{-q}, \tag{3.40}$$

where $q$ is a positive number. It is then clear that this inverse power law behavior of $k$ is not sufficient to damp off the exponential factor of eq. (3.39) and we conclude that, as announced:

$$\rho_{\text{in}}^{\text{obs}}(v \to \infty) \to \infty. \tag{3.41}$$

This completes our study of the static model for the Reissner-Nordstrøm black hole. This model, as we pointed out, represents the exterior of a star undergoing a purely spherical gravitational collapse. In the next section, we will consider the effects on the inner apparent horizon of a collapse with small deviations from sphericity. We will see that the outgoing radiation coming from the surface of the star will have an interesting rôle to play on the interior structure of the hole.

### 3.3: The dynamic model

In this section we will consider a model for the Reissner-Nordstrøm spacetime which is an attempt to emulate the effects of a realistic gravitational collapse of a charged spherical star. We will allow the star to emit radiation while collapsing, as would be the case if the collapse possessed (small) departures from sphericity. The outgoing radiation coming from the star will have an effect on the inner apparent horizon; we will see that it produces a separation between the inner apparent horizon and the Cauchy horizon. The question we ask is then the following: in the dynamic model, is there still a singular surface of infinite blueshift, and if there is, where is it? The first thing we will want to verify is whether the situation is regular at the inner horizon. We will find that indeed it is: no infinities occur when light rays cross this horizon. We will look at this problem in subsection b) of this section. Subsection c) will be devoted to the situation at the Cauchy horizon. We expect that we will find the same answer as before: the Cauchy horizon is a singular surface of infinite blueshift. The reason is that there is still an infinite accumulation of light rays on the Cauchy horizon (Fig. 3.3): an observer still receives an infinite amount of information in a finite proper time, as he crosses the Cauchy horizon.

To construct our dynamic model, we will try to follow as closely as possible the physical situation. The basic picture is the following: the collapsing star emits outgoing radiation, part of it will soon be backscattered inwards, part of it will cross the Cauchy and inner horizons to reach the singularity. It is clear that near the surface of the collapsing star, the situation is extremely complicated since both the ingoing and outgoing radiation will have an effect on the background geometry.

But this region of spacetime is irrelevant to our problem. On the other hand, the situation is quite simple at late times since there is very little scattering occurring there. In this region of the black hole interior, it should be sufficient to consider the effect on the background geometry of only the outgoing part of the radiation coming from the star. We should then be able to treat the backscattered part of the radiation as a perturbation. We have seen, and we will see once again, that the response of the spacetime to this perturbation is rather large (infinite!). There is therefore something very unsatisfying about this approach. Let us pursue it anyway for the time being: we will attempt later (and elsewhere) to consider the influence on the geometry of both parts of the radiation coming from the star. Needless to say, this is a much more involved problem!

So, as our idealized model, we will assume that the star emits outgoing radiation, but that no scattering occurs: all the radiation reaches the singularity. In other words, we will neglect the wavelike effects of the radiation, to concentrate on its effect on the inner horizon. This model is expected to give a good description of the physical spacetime at late times ($v$ large) and the hope is that it should be sufficient to emulate the effects of a generic gravitational collapse. What kind of radiation do we want to consider? To make the problem as simple as possible, we have already assumed that the radiation will be composed of lightlike particles following null geodesics. Indeed, this corresponds to the geometric optics approximation [48] in which the wavelength of the radiation is assumed to be much smaller than the characteristic dimensions of the wave front, and also much smaller than the characteristic curvature radius of the spacetime. To show the effects of a charged flux coming from the star, we will also allow our lightlike particles to carry charge.

This further refinement is not necessary, but it does not add any difficulties to the treatment.

Fig. 3.3 shows the spacetime diagram illustrating the model. Our radiation leaves the star and follows outgoing, radial, null geodesics and crosses the inner apparent horizon. The latter responds accordingly, and evolves in a way that we will discover later. The problem is then to consider the propagation of ingoing light rays in this dynamic spacetime and to ask whether we still have a surface of infinite blueshift at the inner horizon (or at the Cauchy horizon). We will find that the situation is regular at the inner horizon, but that there is still a singular surface of infinite blueshift at the Cauchy horizon.

*a) The dynamic spacetime.*

To work out the problem, we need first to find the solution to the Einstein field equations corresponding to the spacetime described above. Since the solution for the interior of the collapsing star is irrelevant to us, what we are looking for is the solution for the spacetime exterior to a spherical charged star, and filled with outgoing radiation that can carry charge. The stress-energy tensor for such a spacetime can be written as

$$T^{\alpha\beta} = \rho_{\rm out} n^\alpha n^\beta + E^{\alpha\beta}, \tag{3.42}$$

where $n^\alpha$ is the four-velocity of an outgoing charged "photon", $\rho_{\rm out}$ plays a rôle similar to that of the $\rho_{\rm in}$ of the last section: it is the "proper" energy density of the photons. Finally, $E^{\alpha\beta}$ is the electromagnetic part of the stress-energy tensor.

The solution of the Maxwell-Einstein equations for this stress-energy tensor was found by Bonnor and Vaidya in 1970 [49]. The simplest form for this solution is found when one uses the $u$, $r$ coordinate system of section 3.1. We find:

$$ds^2 = -du\,[2\,dr + f(r,u)\,du] + r^2 d\Omega^2, \tag{3.43}$$

where

$$f(r,u) \equiv 1 - \frac{2M(u)}{r} + \frac{e^2(u)}{r^2} \equiv \frac{[r - r_+(u)]\,[r - r_-(u)]}{r^2}. \tag{3.44}$$

The interpretation of the solution is obvious: at any time $u$ we have a Reissner-Nordstrøm black hole with mass $M(u)$ and charge $e(u)$. The proper energy density of the outgoing radiation is related to the rate of change of the mass and charge by

$$\rho_{\rm out} = -\frac{1}{4\pi r^2}\,\frac{\partial}{\partial u}\left[M(u) - \frac{e^2(u)}{2r}\right], \tag{3.45}$$

and the interpretation of this too is obvious: in the square bracket is the expression for the mass function, eq. (3.9), at time $u$; $4\pi r^2 \rho_{\rm out}$ is therefore minus the rate of change of the total mass function. This does not mean that the mass of the black hole itself changes, since once the hole is formed, no radiation can escape from it. What we have instead is a redistribution of the matter inside the black hole: some of it leaves the star and goes into the singularity. The electromagnetic part of the stress-energy tensor keeps its original form, for each instant $u$:

$$E^{\alpha}{}_{\beta} = P_{\rm el}\ {\rm diag}(-1,-1,1,1), \tag{3.46}$$

where

$$P_{\rm el} = \frac{1}{8\pi}\left[\frac{e(u)}{r^2}\right]^2. \tag{3.47}$$

Finally, the null vector $n^\alpha$ takes the form

$$\begin{aligned} n^\alpha &= (0,-1,0,0) \\ n_\alpha &= (1,0,0,0), \end{aligned} \tag{3.48}$$

when we use $-r$ as the (non affine) parameter $\lambda$ along the outgoing radiation geodesics.

An important thing to determine is the behavior of the functions $r_\pm(u)$ in this spacetime. A priori, the functions $M(u)$ and $e(u)$ are completely arbitrary, so we could a priori conclude that $r_\pm(u)$ are arbitrary functions. There is however a constraint that we can impose. We will require the stress-energy tensor of our dynamic spacetime to respect the *weak energy condition* [50]. The weak energy condition imposes the following constraint on the stress-energy tensor: the energy density of any reasonable matter distribution as measured by any timelike observer should be non negative. We therefore impose

$$T_{\alpha\beta}v^\alpha v^\beta \geq 0,$$

for any timelike four-velocity $v^\alpha$. If we restrict ourselves to radial four-velocities, we obtain, by using eqs. (3.42), (3.46) and (3.48):

$$\begin{aligned} 0 &\leq \rho_{\rm out}(n_\alpha v^\alpha)^2 + E^\alpha_{\ \beta} v_\alpha v^\beta \\ &\leq \rho_{\rm out}(v^u)^2 + P_{\rm el}(-v_r v^r - v_u v^u) \\ &\leq \rho_{\rm out}\left(\frac{du}{d\tau}\right)^2 + P_{\rm el}, \end{aligned}$$

since $\overline{v^\alpha v_\alpha} = -1$. Now, $P_{\rm el}$ is positive definite, and $du/d\tau$ can be anything from $-\infty$ to $\infty$, depending on the path of the timelike observer. The result is that $\rho_{\rm out}$ must be larger, or equal to zero, in order for the inequality to hold. Using eq. (3.45), we then find a condition on the functions $M(u)$ and $e(u)$ that we write as

$$e\dot{e} - \dot{M}r \geq 0, \tag{3.49}$$

where the dot denotes here a derivation with respect to $u$. This inequality will be most useful when we replace the arbitrary $r$ by the two values of interest: $r_\pm(u)$.

Let us now look at the behavior of the function $r_-(u)$. Eq. (3.44) tells us that $r_- = M - \sqrt{M^2 - e^2}$, and we easily find that

$$\frac{dr_-}{du} = \frac{e\dot{e} - \dot{M}r_-}{\sqrt{M^2 - e^2}}. \tag{3.50}$$

The weak energy condition, eq. (3.49), then implies that $r_-$ increases with $u$:

$$\text{weak energy condition} \Rightarrow \frac{dr_-}{d(-u)} \leq 0. \tag{3.51}$$

On the other hand, a similar demonstration shows that

$$\text{weak energy condition} \Rightarrow \frac{dr_+}{d(-u)} \geq 0. \tag{3.52}$$

We have used $-u$ instead of $u$ to clearly point out that $u$ decreases as we go forward in time, in the interior region $r_- < r < r_+$ of the black hole. We have just found the response of the inner horizon to the presence of the outgoing radiation: its radius decreases as time increases. The situation is represented in Fig. 3.3. We

see that ingoing radiation coming from the singularity can succeed in crossing the inner apparent horizon, while that coming from the exterior region cannot reach it but stays within the right hand sheet of the Cauchy horizon.

The $u$, $r$ coordinate system will be useful for investigating the situation near the inner apparent horizon, described by the equation $r = r_-(u)$. However, to consider the situation at the Cauchy horizon, it will be better to use the $v$, $r$ coordinate system since this horizon is represented by the line $v = \infty$. In the $u$, $r$ system, a radial ingoing null geodesic satisfies the equation $2\,dr + f(r,u)\,du = 0$. In the $v$, $r$ system, it simply satisfies $dv = 0$. We therefore have that $v$, $r$, and $u$ must be related by an equation of the form

$$dv = \frac{e^{-\psi}}{f}\,(2\,dr + f\,du), \tag{3.53}$$

where $e^{-\psi(r,u)}$ plays the rôle of an integrating factor. Since the Cauchy horizon lies somewhere where $r < r_-(u)$, we have that $r$, $u$, and $f$ are all finite there. On the other hand, we know that $v$ is infinite on the Cauchy horizon; in order for eq. (3.53) to hold everywhere, we find that $e^{\psi}$ must go to zero on the Cauchy horizon:

$$e^{\psi}(v \to \infty) \to 0. \tag{3.54}$$

If we substitute now eq. (3.53) into eq. (3.43), we get that in the $v$, $r$ coordinates, our line element becomes

$$ds^2 = e^{\psi} dv(2\,dr - f e^{\psi} dv) + r^2 d\Omega^2, \tag{3.55}$$

where $\psi$ and $f$ are now viewed as functions of $r$ and $v$; in particular, we recall that

$$f(r,v) = 1 - \frac{2M(r,v)}{r} + \frac{e^2(r,v)}{r^2}. \tag{3.56}$$

The field equations for this line element can be found in ref. [51]. To write them down, we decompose the stress-energy tensor as

$$T^{\alpha\beta} = e^{\psi}\rho_{\text{out}} n^{\alpha} n^{\beta} + E^{\alpha\beta}, \tag{3.57}$$

where the first term represents the outgoing radiation, the second term representing the electric field. The four-velocity $n^{\alpha}$ is now written as

$$\begin{aligned} n_{\alpha} &= (-fe^{\psi}, 1, 0, 0), \\ n^{\alpha} &= (2e^{-\psi}, f, 0, 0). \end{aligned} \tag{3.58}$$

The field equations hence read

$$\begin{aligned} \frac{\partial M}{\partial v} &= -4\pi r^2 \rho_{\text{out}} (e^{\psi} f)^2, \\ \frac{\partial M}{\partial r} &= 8\pi r^2 \rho_{\text{out}} e^{\psi} f, \\ \frac{\partial \psi}{\partial r} &= 16\pi r \rho_{\text{out}} e^{\psi}. \end{aligned} \tag{3.59}$$

(We have assumed for simplicity that $e$ is a constant. This has no consequence on the following.)

If we turn off the radiation source, the spacetime becomes static and according to eqs. (3.55), (3.56) and (3.59), the line element becomes

$$ds^2 = e^{\psi(v)} dv \left[ 2\, dr - f(r) e^{\psi(v)} dv \right] + r^2 d\Omega^2, \tag{3.60}$$

with

$$f(r) = 1 - \frac{2M}{r} + \frac{e^2}{r^2}.$$

We recover eq. (3.17) if we define a new variable $v_{\rm NEW} \equiv \int e^{\psi} dv_{\rm OLD}$ and express eq. (3.60) in terms of $v_{\rm NEW}$. We may not always have this liberty, however. As an example, consider the following: let us suppose that before the retarded time $u_0$, the spacetime was static and described by the line element (3.17). At time $u_0$ until time $u_1$, the outgoing radiation source is turned on and the inner apparent horizon evolves accordingly, moving away from the Cauchy horizon. At time $u_1$, the source is turned off and the spacetime becomes static again, and is now described by the more general line element of eq. (3.60). In order to have a continuous labelling of the ingoing lines $v$ = constant, we clearly do not want to redefine $v$ in the way described above. In particular, since $e^{\psi}$ goes to zero at the Cauchy horizon while $dv_{\rm OLD}$ becomes infinite, we would find a finite $dv_{\rm NEW}$ on the Cauchy horizon. In order to avoid such an infinite jump in the labelling of the lines $v$ = constant, we have to leave unchanged the form (3.60) of the line element to describe the second static region. It was worth noting this in such detail because we will make use of the static line element (3.60) in subsection c).

We now have everything in hand to consider the propagation of radiation in the dynamic spacetime. In the next subsection, we will look at the situation where ingoing radiation crosses the inner horizon. In the following subsection, we will consider the situation at the Cauchy horizon.

*b) Infalling radiation crossing the inner horizon.*

We will consider in this subsection the situation where ingoing radiation coming from the singularity crosses the inner apparent horizon (Fig. 3.3). In particular, we want to evaluate, as in section 3.2, the energy density of the radiation as measured by a free-falling observer crossing this horizon. We will therefore follow closely the analysis of section 3.2, this time in the dynamic model and using the $u$, $r$ coordinate system. The object we want to evaluate is then

$$\rho_{\rm in}^{\rm obs} = \rho_{\rm in}(u^\alpha l_\alpha)^2, \tag{3.61}$$

where $l^\alpha$ is the four-velocity of the infalling photons, $u^\alpha$ that of the free-falling observer, and where $\rho_{\rm in}$ is the proper energy density of the radiation. The line element of the dynamic spacetime is given by eq. (3.43) that we rewrite here for convenience:

$$ds^2 = -du\,[2\,dr + f(r,u)\,du] + r^2 d\Omega^2; \tag{3.43}$$

we recall that the term in the square bracket is zero for radial, ingoing null geodesics.

We remember that in the static case, $-r$ was an affine parameter along the ingoing geodesics. It is therefore a good idea to use $-r$ again here, but this time as a non affine parameter. From eq. (3.43) we thus get that $l^\alpha$ takes the form

$$\begin{aligned} l^\alpha &= \left(\frac{2}{f}, -1, 0, 0\right) \\ l_\alpha &= \left(-1, -\frac{2}{f}, 0, 0\right), \end{aligned} \tag{3.62}$$

but does not satisfy eq. (3.26), $l^{\alpha}{}_{|\beta}l^{\beta} = 0$. Instead, it satisfies the more general geodesic equation

$$l^{\alpha}{}_{|\beta}l^{\beta} = \Lambda l^{\alpha}, \tag{3.63}$$

where $\Lambda$ is a function that can be determined by direct calculation. It is straightforward to show that it is given by

$$\Lambda = -\frac{2f_{,u}}{f^2}. \tag{3.64}$$

The expression for $u^{\alpha}$ can be found by writing down the Lagrangian corresponding to the line element (3.43). Since we consider only radial motion, this Lagrangian is

$$2L = -2\dot{u}\dot{r} - f\dot{u}^2 = -1, \tag{3.65}$$

where $\dot{x}^{\alpha} \equiv dx^{\alpha}/d\tau$. This last equation gives a quadratic equation for $\dot{u}$ as a function of $\dot{r}$, which is everywhere finite and well behaved. In solving this equation for $\dot{u}$, we have to make a choice for the sign in front of the square root. Since we assume that in the static limit our observer would cross the $v = \infty$ sheet of the inner apparent horizon, we shall choose the sign that yields a finite $\dot{u}$, as we cross the surface $r = r_{-}(u)$. It is easy to verify that

$$\dot{u} = \frac{-\dot{r} - \sqrt{\dot{r}^2 + f}}{f}, \tag{3.66}$$

is the correct expression for $\dot{u}$. Using eq. (3.62), we can now write down the expression for the inner product $u^{\alpha}l_{\alpha}$. We find:

$$u^\alpha l_\alpha = \frac{-\dot{r} + \sqrt{\dot{r}^2 + f}}{f}, \tag{3.67}$$

which goes to infinity like $-2\dot{r}/f$ when $f$ goes to zero. So unless $\rho_{\rm in}$ goes to zero at least as fast as $f^2$, the value of $\rho_{\rm in}^{\rm obs}$ will go to infinity as the observer crosses the inner horizon.

To find an expression for $\rho_{\rm in}$, we apply the energy conservation equation for the stress-energy tensor $\rho_{\rm in} l^\alpha l^\beta$. We obtain

$$0 = \left(\rho_{{\rm in},\beta} l^\beta + \rho_{\rm in}\Lambda + \rho_{\rm in} l^\beta{}_{|\beta}\right) l^\alpha,$$

if we also use eq. (3.63). A little algebra then gives

$$\frac{1}{\rho_{\rm in}} \frac{d\rho_{\rm in}}{d(-r)} = -\Lambda - \frac{1}{\sqrt{-g}} \left(\sqrt{-g} l^\alpha\right)_{,\alpha},$$

or, if we use eqs. (3.43) and (3.64):

$$\frac{1}{\rho_{\rm in}} \frac{d\rho_{\rm in}}{d(-r)} = \frac{4f_{,u}}{f^2} + \frac{2}{r}. \tag{3.68}$$

We will now show that $\rho_{\rm in}$ goes to zero precisely like $f^2$, when $r$ approaches $r_-$. What we want to do is to evaluate eq. (3.68) in the limit where $r$ goes to $r_-$; to do so, we can first rewrite it as

$$-\frac{f}{2} \frac{d}{dr} \ln \rho_{\rm in} r^2 = \frac{\partial}{\partial u} \ln f^2,$$

and we recall from eq. (3.43) that for our radial, ingoing light ray, the equation $2\,dr + f\,du = 0$ holds. We can therefore replace the total differentiation with respect to $r$ by a total differentiation with respect to $u$, and this yields

$$\frac{d}{du} \ln \rho_{\text{in}} r^2 = \frac{\partial}{\partial u} \ln f^2. \tag{3.69}$$

We now observe that when $f$ goes to zero, the differential element $dr$ must vanish as well, in order for the equation $2\,dr + f\,du = 0$ to remain valid. This means that in the small region of interest, around $f = 0$, on our ingoing geodesic, $r$ is effectively constant. Consequently, the total differentiation of the left hand side of eq. (3.69) can be replaced by a partial differentiation, and we get $\rho_{\text{in}} r^2 / f^2 \simeq$ an arbitrary function of $r$. Again, since $r$ is essentially a constant in the region of interest, the final result, as announced, is

$$\rho_{\text{in}}(f \to 0) \simeq \text{constant } f^2. \tag{3.70}$$

We note that this result is independent of the actual form of the metric element $f$.

Combining eqs. (3.70), (3.67) and (3.61), we find that the energy density of the infalling radiation, measured by a free-falling observer, reaches the finite limit when $r$ goes to $r_-$:

$$\rho_{\text{in}}^{\text{obs}}(r \to r_-) \to \text{constant } \dot{r}^2. \tag{3.71}$$

This result shows that the situation is, as announced, perfectly regular at the inner apparent horizon: an observer crossing it would measure a finite amount of energy density for the radiation coming from the singularity. This result could be expected from the heuristic picture discussed earlier: there is no accumulation of light rays on the inner apparent horizon, as there is on the Cauchy horizon. In the next subsection, we will finally consider the situation at the Cauchy horizon.

*c) Infalling radiation at the Cauchy horizon:*

We will repeat in this subsection the calculations of the previous one, but this time using the $v$, $r$ coordinate system. This will allow us to consider the situation at the Cauchy horizon and we will show that there is a singular surface of infinite blueshift there, as there was in the static model. We will interpret this result in terms of our heuristic argument of section 1.1, according to which there is an infinite accumulation of light rays on the Cauchy horizon. We have introduced at the end of subsection a) the line element for the dynamic spacetime in this coordinate system. We recall that it is

$$ds^2 = e^{\psi} dv(2\, dr - f e^{\psi} dv) + r^2 d\Omega^2, \tag{3.55}$$

where $\psi \equiv \psi(r,v)$, $f \equiv f(r,v)$, and from eq. (3.54) we know that $e^{\psi}$ goes to zero on the Cauchy horizon. Since the latter lies where $r < r_-$, we also know that $f$ is nowhere zero on the Cauchy horizon. Now, the expression that we want to evaluate is, as usual: $\rho_{\rm in}^{\rm obs} = \rho_{\rm in}(u^\alpha l_\alpha)^2$, so we will have to find expressions for the three objects $l^\alpha$, $u^\alpha$, $\rho_{\rm in}$.

Radial, ingoing null geodesics follow lines of constant $v$, so we shall choose the following form for the null four-velocity:

$$\begin{aligned} l_\alpha &= (-1,0,0,0), \\ l^\alpha &= (0,-e^{-\psi},0,0); \end{aligned} \tag{3.72}$$

which guarantees that $l^\alpha$ obeys the geodesic equation $l^\alpha{}_{|\beta} l^\beta = 0$, since $l_\alpha$ is expressed as the gradient of $-v$ (we do not choose $-r$ as a parameter along the ingoing lines, as we did in section 3.2).

From eq. (3.72), it is clear that only the component $\dot{v} \equiv dv/d\tau$ of the four-velocity $u^\alpha$ of the free-falling observer will contribute in the inner product $u^\alpha l_\alpha$. This component can be expressed in terms of $\dot{r}$ (everywhere finite) via the Lagrangian constraint

$$2L = 2e^\psi \dot{v}\dot{r} - e^{2\psi} f \dot{v}^2 = -1,$$

which is a quadratic equation for $\dot{v}$. To choose the correct sign in front of the square root, we once again invoke the fact that in the static limit ($\psi = 0$), our observer would cross the $v = \infty$ sheet of the inner apparent horizon. The answer can be verified to be

$$\dot{v} = \frac{\dot{r} - \sqrt{\dot{r}^2 + f}}{e^\psi f}. \tag{3.73}$$

We see once again that $v$ reaches infinity when $e^\psi$ goes to zero, which occurs at the Cauchy horizon. Combining eqs. (3.72) and (3.73) yields

$$u^\alpha l_\alpha = \frac{-\dot{r} + \sqrt{\dot{r}^2 + f}}{e^\psi f}, \tag{3.74}$$

which goes to infinity on the Cauchy horizon.

We can now find the expression for $\rho_{\rm in}$ by imposing the energy conservation equation:

$$\begin{aligned} 0 &= (\rho_{\rm in} l^\alpha l^\beta)_{|\beta} \\ &= (\ln \rho_{\rm in})_{,\beta} l^\beta + \frac{1}{\sqrt{-g}} (\sqrt{-g} l^\beta)_{,\beta}. \end{aligned}$$

The value of $\sqrt{-g}$ can be easily evaluated from eq. (3.55): $\sqrt{g} = e^{\psi} r^2 \sin\theta$. Use of eq. (3.72) and a little algebra then yields

$$\frac{\partial}{\partial r} \ln \rho_{\rm in} r^2 = 0,$$

which can be integrated to give

$$\rho_{\rm in} = \frac{k(v)}{r^2}, \tag{3.75}$$

where $k(v)$ is an arbitrary function of $v$; it plays the same rôle as in eq. (3.27): it tells how the amplitude of the radiation has to evolve with time. From the discussion of section 3.2, we impose that

$$k(v \to \infty) \sim v^{-q}, \tag{3.40}$$

expressing the fact that the amplitude of the backscattered radiation must die off like a power-law tail.

Combining eqs. (3.74), (3.75) and (3.40), we find that the energy of the ingoing radiation as measured by a free-falling observer in the vicinity of the Cauchy horizon is given by

$$\rho_{\rm in}^{\rm obs}(v \to \infty) = (\text{finite coefficient})\ e^{-2\psi(v\to\infty)} v^{-q}. \tag{3.76}$$

We know that $e^{-\psi}$ goes to infinity on the Cauchy horizon, while the factor $v^{-q}$ goes to zero. We have now to find out which goes faster; we will show that $e^{-\psi}$ goes to infinity exponentially, therefore making $\rho_{\rm in}^{\rm obs}$ infinite on the Cauchy horizon.

To show this, we will simplify our dynamic model a bit further. We will divide our dynamic spacetime into slices (Fig. 3.4). In the region corresponding

to the range $u_0 \to u_0 + \Delta u$, we will assume that the spacetime is static. In the following slice $u_0 + \Delta u \to u_0 + 2\Delta u$, we will assume that the spacetime is dynamic. And so on. We will further assume that the increment $\Delta u$ can be as small as one wishes. We therefore end up with a succession of alternating thin slices. Each static slice can be described by a line element of the form (3.60):

$$ds^2 = e^{\psi(v)} dv \left[2\, dr - f(r) e^{\psi(v)} dv\right] + r^2 d\Omega^2,$$

with $f(r)$ of the usual form

$$f(r) = 1 - \frac{2M}{r} + \frac{e^2}{r^2}.$$

Because two successive static slices are always separated by a dynamic slice, where the mass and charge are allowed to vary, we have that each static slice possesses a different mass, charge and function $\psi$. We will therefore characterize each static slice by a discrete index $n$, and accordingly, the line element for the $n^{\text{th}}$ slice will be written as

$$ds^2 = e^{\psi_n(v)}\, dv \left[2\, dr - f_n(r) e^{\psi_n(v)} dv\right] + r^2 d\Omega^2, \tag{3.77}$$

with

$$f_n(r) = 1 - \frac{2M_n}{r} + \frac{e_n^{\,2}}{r^2}. \tag{3.78}$$

By construction, the $0^{\text{th}}$ static slice is connected to the exterior region of the spacetime; so according to eq. (3.17), we have that

$$\psi_0(v) = 0. \tag{3.79}$$

Our aim is to find out what the function $e^{\psi_n(v)}$ is. To this end, consider the $n^{\text{th}}$ and $(n+1)^{\text{th}}$ static slices. In the limit considered, the dynamic region between those slices is simply a very thin bundle of radial outgoing null geodesics. At the limit, the bundle becomes a single geodesic. As viewed from the $n^{\text{th}}$ static slice, the differential equation describing this geodesic is

$$2\,dr = f_n(r)e^{\psi_n(v)}dv,$$

whereas if viewed from the $(n+1)^{\text{th}}$ slice it is

$$2\,dr = f_{n+1}(r)e^{\psi_{n+1}(v)}dv.$$

The differential elements $dr$ and $dv$ are here the same in both slices since both equations describe the same line. We then can divide the second equation by the first and find

$$e^{\psi_{n+1}} = \frac{f_n}{f_{n+1}}\, e^{\psi_n}; \tag{3.80}$$

where $f_n$ and $f_{n+1}$ can be viewed as functions of $v$ once the differential equations are integrated. Eq. (3.80) can now be iterated to express $e^{\psi_n}$ in terms of $e^{\psi_0}$ ($= 1$, according to eq. (3.79)). We find

$$e^{\psi_n(v)} = \frac{f_0(v)}{f_n(v)}. \tag{3.81}$$

Now the last step. In the $0^{\text{th}}$ static slice, the inner apparent horizon still lies on the Cauchy horizon; in the $n^{\text{th}}$ one, they are completely separated. In other

words, we have that $f_n$ remains non-zero while $f_0$ goes to zero at $v = \infty$. We can therefore write, eliminating the subscript $n$:

$$e^{\psi(v)} = (\text{finite coefficient}) f_0(v).$$

We already have an expression for $f_0(v)$: we have done this calculation at the end of section 3.2. Substituting eq. (3.38) into our last equation yields

$$e^{\psi(v)} = (\text{finite coefficient}) e^{-\kappa_0 v}, \tag{3.82}$$

which shows that, as announced, $e^{-\psi}$ goes exponentially to infinity, when $v$ goes to infinity. Inserting eq. (3.82) in eq. (3.76) finally yields

$$\rho_{\text{in}}^{\text{obs}}(v \to \infty) \to \infty. \tag{3.83}$$

We still find a singular surface of infinite blueshift at the Cauchy horizon, as we expected in view of the infinite accumulation of light rays: an observer crossing the Cauchy horizon receives an infinite amount of information within a finite proper time.

This completes our discussion of the dynamic model. We have shown that the outgoing radiation emitted by the collapsing star (as it happens when the collapse presents small deviations from spherical symmetry) produces a separation between the Cauchy horizon and the inner horizon. We have shown that a free-falling observer crossing the inner horizon would not measure any infinities, but that one crossing the Cauchy horizon would. This establishes on firm grounds the heuristic argument of section 1.1, in terms of which the infinite blueshift is produced by an infinite accumulation of light rays on the Cauchy horizon. Since this

argument is quite general and does not depend on spherical symmetry, it can be expected that singular surfaces of infinite blueshift are a general characteristic of Cauchy horizons and that they should appear in generic situations, in particular, the Kerr black hole.

### 3.4: Conclusion

The reader has been more than patient for long enough, let us now summarize and conclude. The central goal of this thesis was to investigate the effects on the geometry inside non rotating black holes of gravitational collapses presenting small deviations from spherical symmetry. The hope is that this analysis can succeed in showing the qualitative behavior of a non spherical collapse. The same investigation was carried out for the exterior geometry by Richard Price [4]; we were able to extend his results to the interior case.

For the Schwarzschild black hole, we were able to show in section 1.4b) that the asymptotic portion (for late advanced times) of the interior spacetime was essentially unaffected by the aspherical perturbations. Hence, spherical symmetry holds even down to very small radii in this asymptotic portion. This result is remarkable since it could be expected that the perturbations would grow more and more as the star collapses, and that the situation would be very chaotic near the singularity. We have shown that this picture holds only for small advanced times (of order $2M$). For late times, order exists and the singularity is rather "clean".

This result then allowed us to consider quantum effects near the singularity from a spherically symmetric point of view, which eases the investigation considerably. Our analysis has been there very schematic and more detailed work will have to be undertaken in order to verify or contradict our conclusions. But that is Ph.D. material! Our schematic analysis showed that two possibilities can arise, depending on the sign of the stress induced by the quantized fields. The first possibility was that the quantum effects could provoke the infinite rise of the spacetime

curvature *sooner* than in the classical solution: the curvature would reach infinity at a non-vanishing value of $r$. The second possibility, the most aesthetically pleasing one, states that quantum effects could slow down the rise of the curvature, and leave it bounded at Planckian magnitudes in accordance with Markov's "new law of nature" [11]. The curvature is moreover found to be essentially constant for small radii, which is the signature of the de Sitter spacetime describing an exponentially collapsing universe. In fact, we found from the semiclassical Einstein field equations a whole family of de Sitter-like solutions which describe anisotropic collapses. It is clear that this analysis cannot be valid for very small radii where the effects due to the fully quantized gravitational field would become important. It would therefore be very unsafe to assume that the curvature remains finite even at the origin. In fact, there is another term in the curvature function, called the *transverse curvature*, which is the curvature associated with the collapsing 2-spheres. This term goes like $1/r^2$ and will start to dominate around the Planck length. According to this, the curvature would still blow up at $r = 0$, but in a "milder" way than before.

It is too tempting not to dive into wild speculations at this point. Let us imagine for a short while that Markov's law holds and that curvature (even the transverse term) is always subject to an upper limit. In this picture, the spacetime is not singular at $r = 0$ and this brings us to the fascinating question: what happens for negative $r$'s? Since there is no singularity anymore at $r = 0$ there is no reason whatsoever for the spacetime to naturally stop at that instant of time. An observer at $r = 0$ could always wait a little while to see what happens, and while doing that, would automatically pass to the negative $r$ region. The existence of such a region hence appears inevitable. So what happens in this region? A possibility is

that the de Sitter collapsing universe would bounce and start to expand, producing a brand new inflationary universe. According to this picture, universes can be created out of black holes! Although very speculative, this question was addressed in a very recent work by Frolov, Markov and Mukhanov [52]; we did not dare to go that far into speculations in our own paper [53]! Another possibility would be the existence of another de Sitter-Schwarzschild transition in the negative $r$ region. For an observer in this region, however, $r$ (as a spacelike coordinate) would still be perceived as positive; it is the mass of the "white hole" that would be interpreted as being negative. We would then wind up with repulsive gravity in this region of spacetime. This idea is not new, similar things happen in the Kerr spacetime when an observer passes through the ring singularity. The fate of the negative $r$ region is therefore rich in possibilities, and it would be more than prudent to leave the question open for the time being. The level of speculations has indeed become very high! To conclude on this part, it appears that a detailed calculation of the renormalized expectation value of the stress-energy tensor of quantized fields in the Hartle-Hawking vacuum (the vacuum state seen by a free-falling observer) would be of considerable interest in regard to the conclusions of the schematic result presented here. We should attack this problem shortly.

The presence of an inner-Cauchy horizon in the Reissner-Nordstrøm spacetime makes this black hole interior even more interesting to study. Because the Cauchy horizon is the prolongation of future null infinity, we discover that an infinite number of light rays propagate along the Cauchy horizon, hence forming a thin shell of infinite energy density, as measured by an observer crossing it. We have verified this statement explicitly in the static model (section 3.2); and in the dynamic

model (section 3.3), where the star emits outgoing radiation while it collapses, as would be the case if the collapse presented small deviations from sphericity. Furthermore, since this outgoing radiation produces a separation between the Cauchy and inner horizons, we find that the situation becomes perfectly regular at the inner apparent horizon. The final picture is that there exists on the dynamic Cauchy horizon a singular thin shell formed by the accumulation of infalling radiation propagating at very late times. We stress that this analysis was carried out assuming that the response of the spacetime to the ingoing radiation would remain small. This is hardly the case and a direct calculation where both the effects of the ingoing and outgoing radiation are taken into account needs to be performed in order to draw a conclusion. This project presents a natural prolongation of this thesis and we have started to work on it at the time of writing.

It is too tempting not to go, once again, into the area of speculation. Let us imagine once again that Markov's law holds and that in fact, the energy density of the ingoing thin shell is found to be finite. That would mean that the total mass of the shell would also be finite and that our observer could go through it. What could we then say about the nature of the spacetime inside the inner apparent horizon, in particular about the curvature singularity when we consider quantum effects? Let us consider a spacelike slice taken in the future of the Cauchy horizon (see Figs. 3.1 or 3.3). At the extreme left of the slice, we find the centre $r = 0$ of the collapsing star, which is an origin for the slice. At the extreme right, we now find the singularity, a boundary of the spacetime. We hence have that this spacelike slice is a *closed* hypersurface (or volume): the slice has a finite extent. Now, the collapsing star carries a charge, say, of $+e$. Since the slices are closed,

we must have that the singularity carries a charge $-e$. This follows from the fact that the total net charge can be evaluated using a surface integral (Gauss' law) and that the surface of support can be shrunk to a point, hence imposing a zero net charge. We therefore have an infinite concentration of charge at the singularity, hence producing a very intense electric field in its vicinity. It is well known from QED that extreme electric fields produce an abundance of pair creations, so there will be a lot of particle-antiparticle pairs produced in the vicinity of the singularity. The positively charged particles will be attracted towards the singularity, whereas the negatively charged ones will go towards the collapsing star. The end result will be that all the charge inside the black hole will be annihilated and we will end up with a neutral closed universe. Presumably, the pair creations will also succeed in removing the singularity so that our spacetime will be perfectly regular. But once again, we should refrain from going too deeply into speculations and leave this issue open.

To summarize, we have shown that, within our perturbative analysis, the property that the Cauchy horizon is a singular surface of infinite blueshift is preserved when one considers a gravitational collapse with small deviations from sphericity. It is plausible that this property could also be preserved when the deviations are arbitrarily large and that any Cauchy horizon would be a singular surface of infinite blueshift. This conclusion follows from the fact that an infinite accumulation of light rays occurs whenever a Cauchy horizon exists. It is obvious that a direct calculation where the ingoing and outgoing radiation is allowed to play a rôle would be highly interesting and some new phenomena could thus be discovered.

The physics of black hole interiors is a very fascinating topic that has been left almost untouched until now. This thesis is just the beginning of the exploration of what appears to be a very rich and interesting subject of research. It certainly is very bold to give to this thesis the title "Black holes: the inside story" since we are only at the first page of what will probably become a very thick volume. I hope the reader will forgive such an absence of humility!

# BIBLIOGRAPHY


[1] Israel, W. (1987) in *300 Years of Gravitation*,
eds. S.W. Hawking and W. Israel (Cambridge: CUP)
This volume will be referred to as "300 Years of Gravitation".

[2] Wald, R.M. (1984) *General Relativity*
(Chicago: The University of Chicago Press) p. 322–324
Hereafter referred to as "Wald".

[3] Misner, C.W., Thorne, K.S. and Wheeler, J.A. (1973) *Gravitation*
(San Francisco: Freedman) p. 876
Hereafter referred to as "MTW".

[4] Price, R.H. (1972) *Phys. Rev. D*, **5**, 2419.
Price, R.H. (1972) *Phys. Rev. D*, **5**, 2439.
MTW p. 864–866

[5] MTW chapter 33

[6] see for example Blandford, R.D. (1987) in *300 Years of Gravitation*

[7] MTW p. 843–844

[8] MTW chapter 27

[9] Belinskii, V.A., Lifshitz, E.M., Khalatnikov, I.M. (1970)
*Adv. Phys.*, **19**, 525.
Belinskii, V.A., Lifshitz, E.M., Khalatnikov, I.M. (1972)
*Sov. Phys. JETP*, **35**, 838.
Barrow, J.D. and Tipler, F.J. (1979) *Phys. Rep.*, **56C**, 372.
Belinskii, V.A., Khalatnikov, I.M., Lifshitz, E.M. (1980)
*Phys. Lett.*, **77A**, 214.

[10] Wald section 9.5

[11] Markov, M.A. (1982) *JETP Lett.*, **36**, 265.
See also Markov (1984), ref. [29].

[12] Le Châtelier, H. (1884) *Compt. Rend. Acad. Sci.*, **99**, 786.

[13] González-Díaz, P.F. (1981) *Lett. Nuovo Cimento*, **32**, 161.

[14] de la Cruz, V. and Israel, W. (1967) *Nuovo Cimento*, **A48**, 744.
Boulware, D.G. (1973) *Phys. Rev. D*, **8**, 2363.

[15] McNamara, J.M. (1978) *Proc. R. Soc. Lond. A.*, **358**, 499.
McNamara, J.M. (1978) *Proc. R. Soc. Lond. A.*, **364**, 121.
Gürsel, Y., Sandberg, V.D., Novikov, I.D., Starobinsky, A.A. (1979)
*Phys. Rev. D*, **19**, 413.
Matzner, R.A., Zamorano, N., Sandberg, V.D. (1979)
*Phys. Rev. D*, **19**, 2821.
Chandrasekhar, S. and Hartle, J.B. (1982)
*Proc. Roy. Soc. Lond.*, **A284**, 301.

[16] MTW p. 595
Wald p. 121

[17] MTW p. 598

[18] MTW chapter 31

[19] MTW section 32.6

[20] Graves, J.C. and Brill, D.R. (1960) *Phys. Rev.*, **120**, 1507.
Waugh, B. and Lake, K. (1986) *Phys. Rev. D*, **34**, 2978.

[21] Wald p. 330–332

[22] Synge, J.L. (1960) *Relativity: The General Theory*
(Amsterdam: North-Holland) p. 39–41

[23] Israel, W. (1966) *Nuovo Cimento*, **44B**, 1.
Taub, A.H. (1980) *J. Math. Phys.*, **21**, 1423.
Clarke, C.J.S. and Dray, T. (1987) *Class. Quantum Grav.*, **4**, 265.
Barrabès, C. (1988) *Singular Hypersurfaces in General Relativity: A Unified Description*
Preprint, Laboratoire de Modèles de Physique Mathématique, Tours, France.

[24] Grøn, Ø. (1985) *Lett. Nuovo Cimento*, **44**, 177.

[25] Shen, W. and Zhu, S. (1988) *Phys. Lett.*, **126A**, 229.

[26] Blau, S.K. and Guth, A.H. (1987) in *300 Years of Gravitation*

[27] Hartle, J.B. and Hawking, S.W. (1983) *Phys. Rev. D*, **28**, 2960.
Halliwell, J.J. and Hawking, S.W. (1985) *Phys. Rev. D*, **31**, 1777.
Vilenkin, A. (1985) *Phys. Rev. D*, **32**, 2511.
Laflamme, R. and Shellard, E.P.S. (1987) *Phys. Rev. D*, **35**, 2315.
Nambu, N. and Sasaki, M. (1988) *Prog. Theor. Phys.*, **79**, 96.
Vilenkin, A. (1988) *Phys. Rev. D*, **37**, 888.

[28] MTW section 21.2
Wald appendix E

[29] Birrell, N.D. and Davies, P.C.W. (1982) *Quantum Fields in Curved Space* (Cambridge: CUP) chapter 1, chapter 6
Hereafter referred to as "Birrell & Davies".
Wald chapter 14
Sakharov, A.D. (1968) *Sov. Phys. Dok.*, **12**, 1040.
Ginzburg, V.L., Kirzhnits, D.A., Lyubushin, A.A. (1971) *Sov. Phys. JETP*, **33**, 242.
Starobinsky, A.A. (1980) *Phys. Lett.*, **91B**, 99.
Mamaev, S.G. and Mastepanenko, V.M. (1980) *Sov. Phys. JETP*, **51**, 9.
Markov, M.A. (1984) *Ann. Phys.* (NY), **155**, 333.

[30] Doroshkevich, A.G. and Novikov, I.D. (1978) *Sov. Phys. JETP*, **47**, 1.

[31] Wald section 7.2

[32] Wald chapter 5
MTW chapter 27

[33] See Birrell & Davies for a brief review.

[34] Wald appendix D

[35] Birrell & Davies p. 181

[36] Birrell & Davies p. 183–185

[37] Birrell & Davies p. 119–121

[38] Birrell & Davies p. 180

[39] Zel'dovich, Y.B. and Starobinskii, A.A. (1972)
*Sov. Phys. JETP*, **34**, 1159.
Fulling, S.A., Parker, L., Hu, B.L. (1974) *Phys. Rev. D*, **10**, 3905.
Hu, B.L. and Parker, L. (1978) *Phys. Rev. D*, **17**, 933.
Hu, B.L. (1978) *Phys. Rev. D*, **18**, 4460.
Berger, B.K. (1981) *Phys. Rev. D*, **23**, 1250.

[40] Wald p. 70

[41] Kamke, E. (1948) *Differentialgleichungen: Lösungsmethoden Und Lösungen*
(New York: Chelsea Publishing Company) p. 440
Arfken, G. (1985) *Mathematical Methods For Physicists*
(Orlando: Academic Press) chapter 11

[42] MTW box 13.3

[43] MTW p. 840–841
Wald p. 157–158

[44] MTW section 22.4
Wald p. 70

[45] MTW p. 921

[46] Wald section 8.3

[47] Wald p. 41

[48] MTW section 22.5

[49] Bonnor, W.B. and Vaidya, P.C. (1970) *Gen. Rel. Grav.*, **1**, 127.

[50] Wald p. 218–219

[51] Israel, W. (1986) *Can. J. Phys.*, **64**, 120.

[52] Frolov, V.P., Markov, M.A., Mukhanov, V.F. (1989)
*Phys. Lett.*, **216B**, 272.

[53] Poisson, E. and Israel, W. (1988) *Class. Quantum Grav.*, **5**, L201.

# APPENDIX

## FIGURES AND TABLES

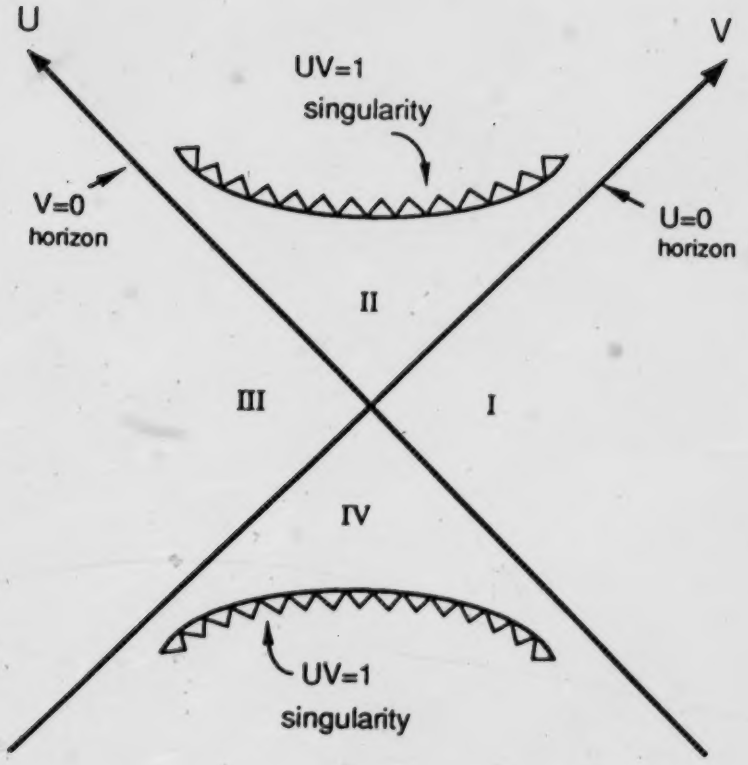


**Figure 1.1:** The Schwarzschild spacetime in Kruskal coordinates. The null coordinates $U$ and $V$ are related to the Schwarzschild radial coordinate by eq. (1.24). Region I is the exterior of the black hole, Region II the interior. Regions III and IV are exact replicas of those two regions, belonging to another universe. Only the first two regions are realized when the black hole corresponds to the endpoint of a gravitational collapse.

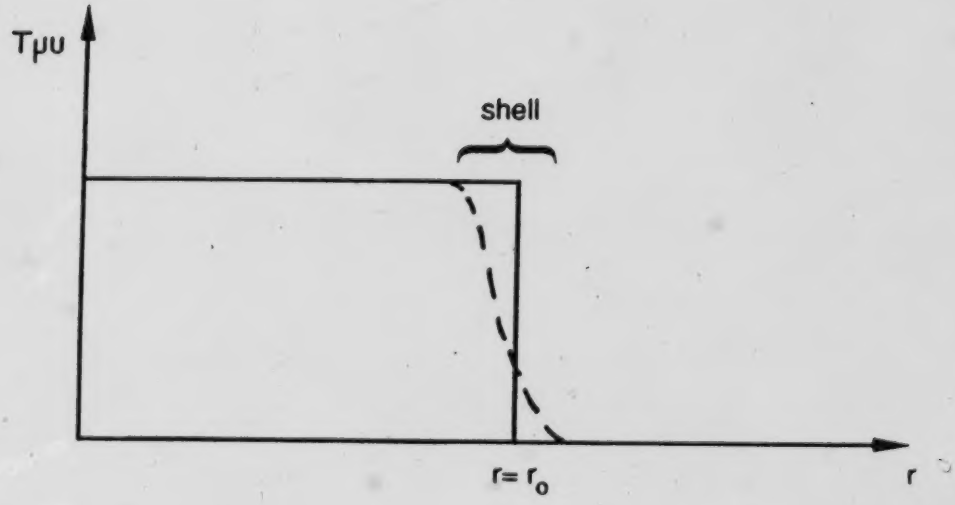


**Figure 1.2:** The González-Díaz model where $T_{\mu\nu}$ is constant inside the black hole horizon, and zero outside. A shell of matter is substituted for the sharp jump in order to obtain a smooth join. The thickness of the shell is formally taken to be zero.

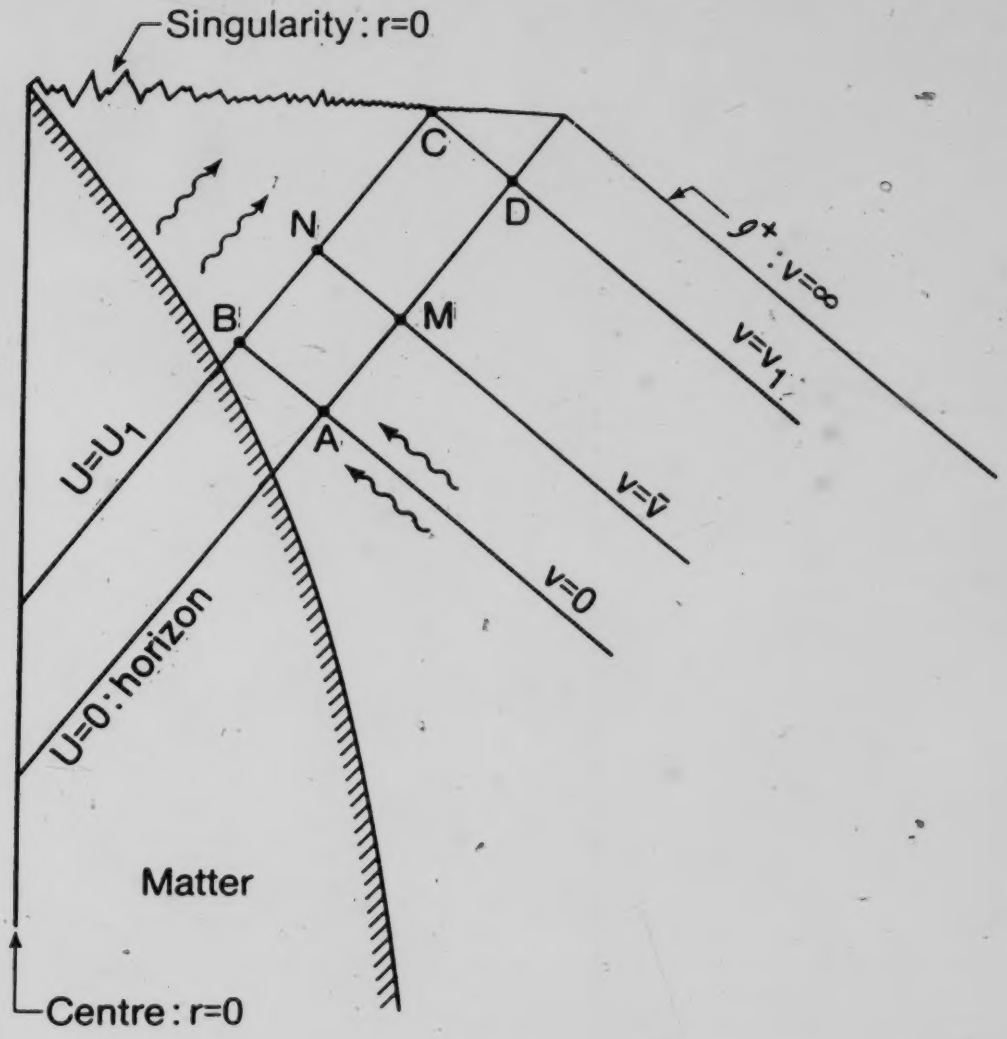


**Figure 1.3:** The conformal diagram of a gravitational collapse presenting small departures from spherical symmetry. The coordinates are defined in section 1.2b) and are the same as in Fig. 1.1. The wavy lines represent infalling and outgoing radiation.

| Case | Semiclassical equation |
|---|---|
| $m \neq 2,\ m \neq 0$ | cannot be solved<br>see eqs. (2.26) and (2.30) |
| $m = 0$ | cannot be solved<br>see eqs. (2.34) and (2.35) |
| $m = 2$ | can be solved<br>see eqs. (2.37), (2.38) and (2.40) |

**Table 2.1:** Solving the semiclassical equation in the power-law spacetimes, for the isotropic case $n = 2$. This table summarizes section 2.2a).

| Case | Semiclassical equation |
|---|---|
| $m \neq 2,\ n + 3m \neq 2$ | cannot be solved<br>see eq. (2.54) |
| $m \neq 2,\ n + 3m = 2$ | cannot be solved<br>see eq. (2.56) |
| $m = 2,\ n \neq -4$ | can be solved<br>see eqs. (2.59)–(2.62) |
| $m = 2,\ n = -4$ | can be solved<br>see eqs. (2.63) and (2.64) |

**Table 2.2:** Solving the semiclassical equation in the power-law spacetimes in the general case. This table summarizes section 2.2b).

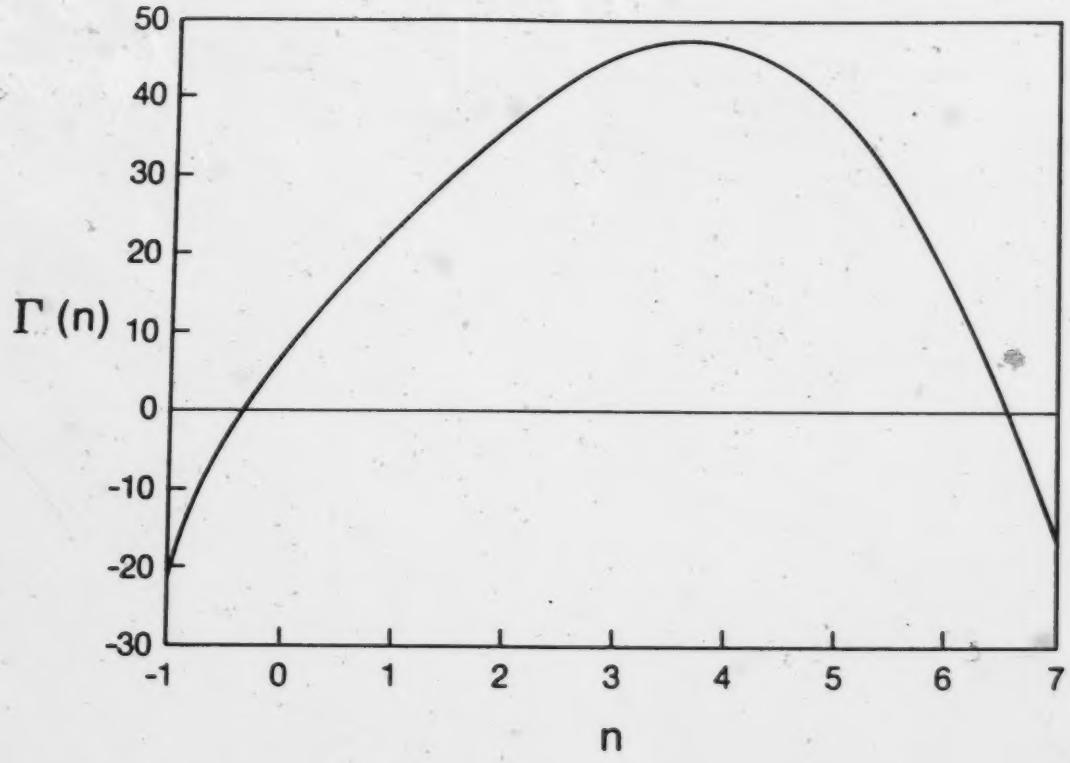


**Figure 2.1:** The graph of $\Gamma(n)$. The function is defined in eq. (2.62). Only the integer values of $n$, and the corresponding values of $\Gamma$ are of interest.

| Case | | $Q$ |
|---|---|---|
| $m = 0$ | $n \leq -2$ | $0$ |
| | $-2 \leq n \leq 2$ | $-\frac{1}{2}(2+n)$ |
| | $n > 2$ | $-1$ |
| $m + n = 2$ | $m \leq 0$ | $0$ |
| | $m > 0$ | $\frac{1}{4}(m-4)$ |
| $n = 2$ | $m \leq -4$ | $0$ |
| | $-4 \leq m \leq 0$ | $-\frac{1}{2}(m+4)$ |
| | $m > 0$ | $-1$ |
| $n > 2$ | $m + n \leq -2$ | $0$ |
| | $-2 \leq m + n \leq 2$ | $-\frac{1}{2}(2+m+n)$ |
| | $m + n > 2$ | $-1$ |
| $n < 2$ | $m \leq 0,\ m + n \leq -2$ | $0$ |
| | $m \leq 0,\ m + n \geq -2$ | $-\frac{1}{2}(2+m+n)$ |
| | $m > 0$ | $-\frac{1}{4}(2+n)$ |

**Table 2.3:** The asymptotic behavior $x^Q$ for $x \ll 1$ of a massless scalar field propagating in the power-law spacetimes of eq. (2.1). This table is the summary of section 2.3b).

| Case | | Condition on $Q$ |
|---|---|---|
| $m \geq 0$ | $n \geq 2$ | $\geq \frac{1}{2}(n-2)$ |
| | $n \leq 2$ | $\geq 0$ |
| $m \leq 0$ | $m+n \geq 2$ | $\geq \frac{1}{2}(m+n-2)$ |
| | $m+n \leq 2$ | $\geq 0$ |

**Table 2.4:** The stability test. This table gives the conditions that the actual values of $Q$ must satisfy, in order for the geometry $(m, n)$ to be stable.

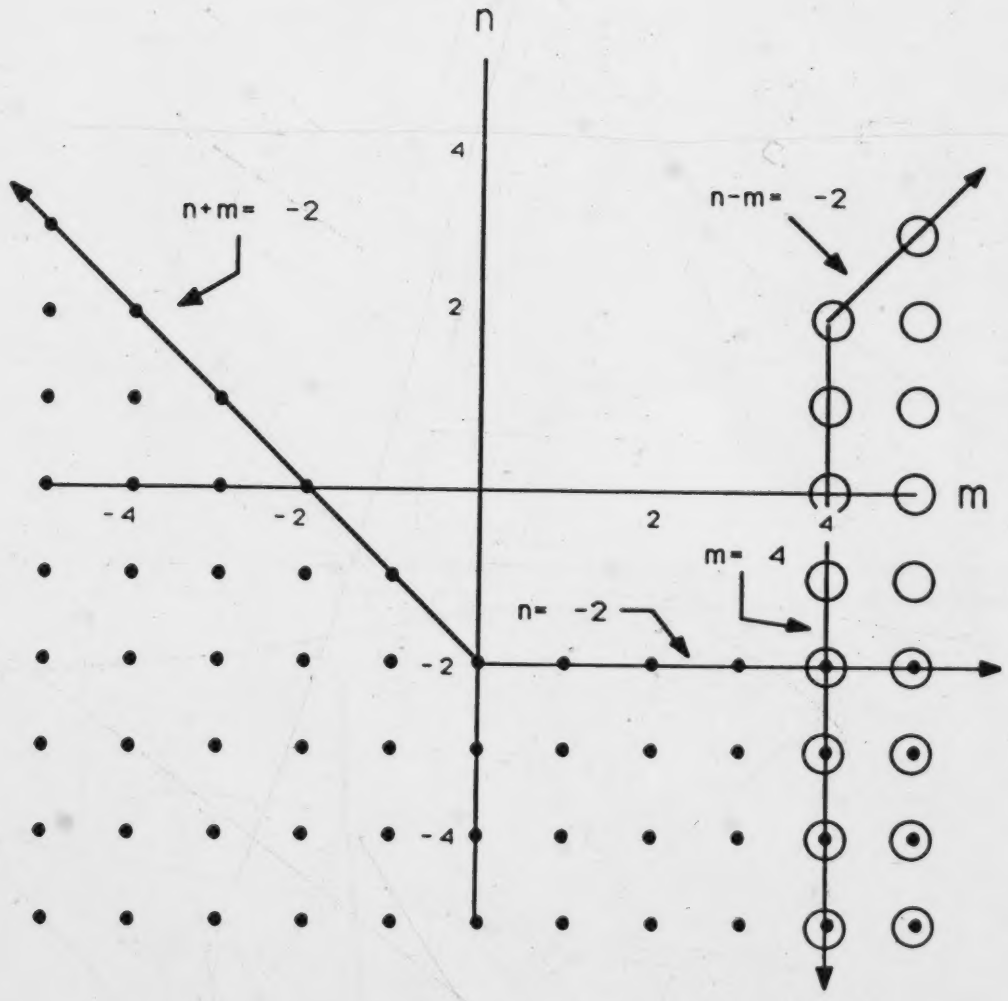


**Figure 2.2:** The plane $(m, n)$ represents all the possible spacetimes of eq. (2.1). The points of the plane corresponding to stable geometries are represented by dots. Those corresponding to spacetimes with inaccessible origin are represented by circles. This figure summarizes the work of the sections 2.3 and 2.4.

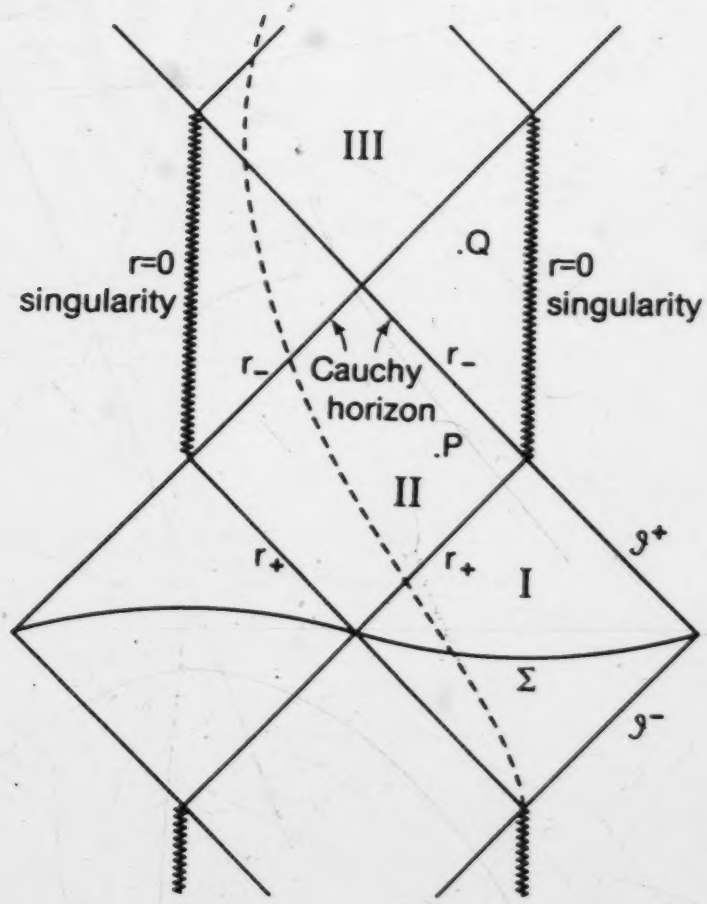


**Figure 3.1:** The Reissner-Nordstrøm spacetime. Region I is the exterior region of the black hole, belonging to "our" universe. Region II is the interior of the hole, and region III is another universe. If the black hole is the result of the gravitational collapse of a charged star, only the part of the diagram at the right of the dashed line is realized. The part at the left is then replaced by the interior of the collapsing star. More details are given in the text of section 3.2a).

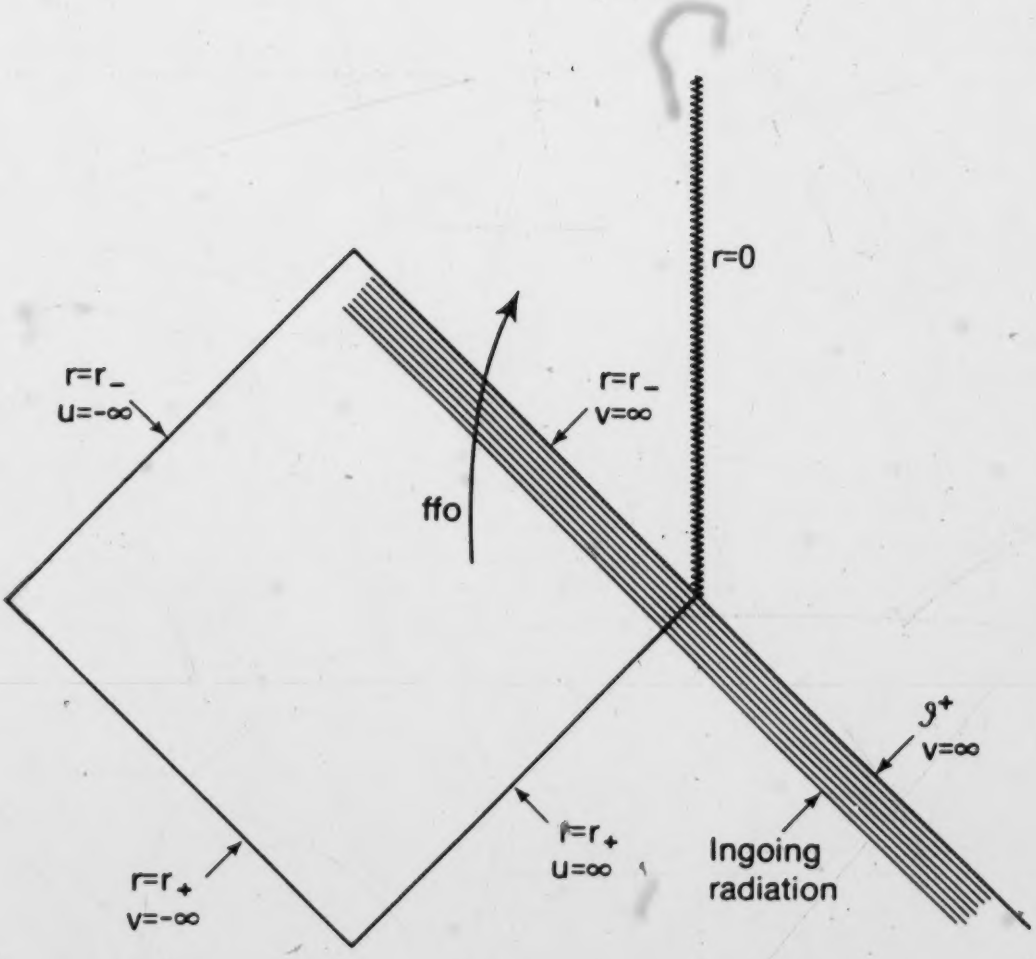


**Figure 3.2:** Infalling radiation near the inner apparent horizon. This picture shows the free falling observer crossing the inner horizon, where there is a flow of ingoing radiation coming from the exterior region.

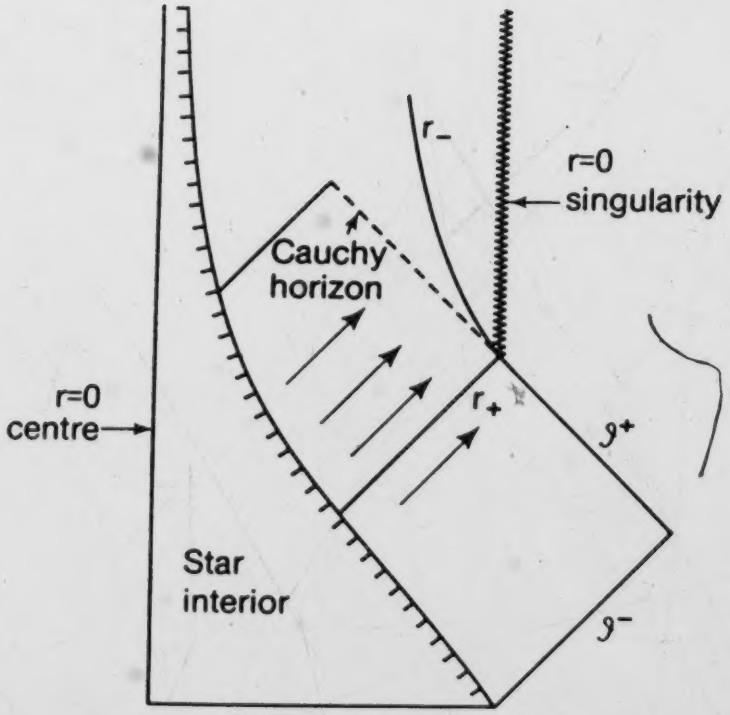


**Figure 3.3:** The dynamic model. The collapsing star emits outgoing radiation which disturbs the inner apparent horizon. Infalling radiation that comes from the exterior region cannot reach the surface $r = r_-$, but stays within the Cauchy horizon. However, ingoing radiation coming from the singularity succeeds in crossing it.

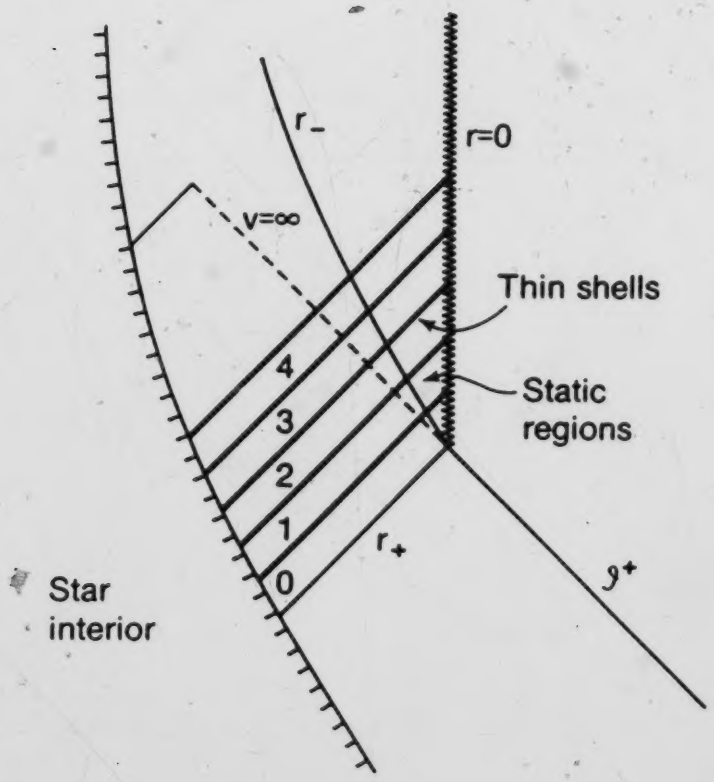


**Figure 3.4:** The "sliced" dynamic model. The dynamic spacetime is here replaced by alternating static and dynamic slices; each static slice being represented by a discrete index $n$. We take the limit where each slice becomes an infinitesimally thin shell.